Titre: Title:	Computer-assisted knee surgery system planning of prosthetic ligament insertion
Auteur: Author:	Marwan Sati
Date:	1995
Type:	Mémoire ou thèse / Dissertation or Thesis
Référence: Citation:	Sati, M. (1995). Computer-assisted knee surgery system planning of prosthetic ligament insertion [Ph.D. thesis, École Polytechnique de Montréal]. PolyPublie. https://publications.polymtl.ca/31749/

Document en libre accès dans PolyPublie
Open Access document in PolyPublie

URL de PolyPublie: PolyPublie URL:	https://publications.polymtl.ca/31749/
Directeurs de recherche: Advisors:	Gilbert Drouin
Programme: Program:	Unspecified

UNIVERSITÉ DE MONTÉAL

COMPUTER-ASSISTED KNEE SURGERY SYSTEM:
PLANNING OF PROSTHETIC LIGAMENT INSERTION

MARWAN SATI
INSTITUT DE GÉNIE BIOMÉDICAL
ÉCOLE POLYTECHNIQUE DE MONTRÉAL

THÈSE PRÉSENTÉE EN VUE DE L'OBTENTION
DU DIPLÔME DE PHILOSOPHIAE DOCTOR (Ph.D.)
(GÉNIE BIOMÉDICAL)
NOVEMBRE 1995

Canada

Nom MARWAN SATI

Dissertation Abstracts International est organisé en catégories de sujets. Veuillez s.v.p. choisir le sujet qui décrit le mieux votre thèse et inscrivez le code numérique approprié dans l'espace réservé ci-dessous.

BIOMEDICALE

| 0 | 5 | 4 | 1 | U·M·I

SUJET   CODE DE SUJET

Catégories par sujets

HUMANITÉS ET SCIENCES SOCIALES

COMMUNICATIONS ET LES ARTS
Architecture 0729
Beaux-arts 0357
Bibliothéconomie 0399
Cinéma 0900
Communication verbale 0459
Communications 0708
Danse 0378
Histoire de l'art 0377
Journalisme 0391
Musique 0413
Sciences de l'information 0723
Théâtre 0465

ÉDUCATION
Généralités 515
Administration 0514
Art 0273
Collèges communautaires 0275
Commerce 0688
Économie domestique 0278
Éducation permanente 0516
Éducation préscolaire 0518
Éducation sanitaire 0680
Enseignement agricole 0517
Enseignement bilingue et
  multiculturel 0282
Enseignement industriel 0521
Enseignement primaire. 0524
Enseignement professionnel 0747
Enseignement religieux 0527
Enseignement secondaire 0533
Enseignement spécial 0529
Enseignement supérieur 0745
Évaluation 0288
Finances 0277
Formation des enseignants 0530
Histoire de l'éducation 0520
Langues et littérature 0279

Lecture 0535
Mathématiques 0280
Musique 0522
Orientation et consultation 0519
Philosophie de l'éducation 0998
Physique 0523
Programmes d'études et
  enseignement 0727
Psychologie 0525
Sciences 0714
Sciences sociales 0534
Sociologie de l'éducation 0340
Technologie 0710

LANGUE, LITTÉRATURE ET LINGUISTIQUE
Langues
  Généralités 0679
  Anciennes 0289
  Linguistique 0290
  Modernes 0291
Littérature
  Généralités 0401
  Anciennes 0294
  Comparée 0295
  Médiévale 0297
  Moderne 0298
  Africaine 0316
  Américaine 0591
  Anglaise 0593
  Asiatique 0305
  Canadienne (Anglaise) 0352
  Canadienne (Française) 0355
  Germanique 0311
  Latino-américaine 0312
  Moyen-orientale 0315
  Romane 0313
  Slave et est-européenne 0314

PHILOSOPHIE, RELIGION ET THÉOLOGIE
Philosophie 0422
Religion
  Généralités 0318
  Clergé 0319
  Études bibliques 0321
  Histoire des religions 0320
  Philosophie de la religion 0322
Théologie 0469

SCIENCES SOCIALES
Anthropologie
  Archéologie 0324
  Culturelle 0326
  Physique 0327
Droit 0398
Économie
  Généralités 0501
  Commerce-Affaires 0505
  Économie agricole 0503
  Économie du travail 0510
  Finances 0508
  Histoire 0509
  Théorie 0511
Études américaines 0323
Études canadiennes 0385
Études féministes 0453
Folklore 0358
Géographie 0366
Gérontologie 0351
Gestion des affaires
  Généralités 0310
  Administration 0454
  Banques 0770
  Comptabilité 0272
  Marketing 0338
Histoire
  Histoire générale 0578

Ancienne 0579
Médiévale 0581
Moderne 0582
Histoire des noirs 0328
Africaine 0331
Canadienne 0334
États-Unis 0337
Européenne 0335
Moyen-orientale 0333
Latino-américaine 0336
Asie, Australie et Océanie 0332
Histoire des sciences 0585
Loisirs 0814
Planification urbaine et
  régionale 0999
Science politique
  Généralités 0615
  Administration publique 0617
  Droit et relations
    internationales 0616
Sociologie
  Généralités 0626
  Aide et bien-être social 0630
  Criminologie et
    établissements
    pénitentiaires 0627
  Démographie 0938
  Études de l'individu et
    de la famille 0628
  Études des relations
    interethniques et
    des relations raciales 0631
  Structure et développement
    social 0700
  Théorie et méthodes. 0344
  Travail et relations
    industrielles 0629
Transports 0709
Travail social 0452

SCIENCES ET INGÉNIERIE

SCIENCES BIOLOGIQUES
Agriculture
  Généralités 0473
  Agronomie. 0285
  Alimentation et technologie
    alimentaire 0359
  Culture 0479
  Élevage et alimentation 0475
  Exploitation des péturages ... 0777
  Pathologie animale 0476
  Pathologie végétale 0480
  Physiologie végétale 0817
  Sylviculture et faune 0478
  Technologie du bois 0746
Biologie
  Généralités 0306
  Anatomie 0287
  Biologie (Statistiques) 0308
  Biologie moléculaire 0307
  Botanique 0309
  Cellule 0379
  Écologie 0329
  Entomologie 0353
  Génétique 0369
  Limnologie 0793
  Microbiologie 0410
  Neurologie 0317
  Océanographie 0416
  Physiologie 0433
  Radiation 0821
  Science vétérinaire 0778
  Zoologie 0472
Biophysique
  Généralités 0786
  Medicale 0760

SCIENCES DE LA TERRE
Biogéochimie 0425
Géochimie 0996
Géodésie 0370
Géographie physique 0368

Géologie 0372
Géophysique 0373
Hydrologie 0388
Minéralogie 0411
Océanographie physique 0415
Paléobotanique 0345
Paléoécologie 0426
Paléontologie 0418
Paléozoologie 0985
Palynologie 0427

SCIENCES DE LA SANTÉ ET DE L'ENVIRONNEMENT
Économie domestique 0386
Sciences de l'environnement 0768
Sciences de la santé
  Généralités 0566
  Administration des hipitaux .. 0769
  Alimentation et nutrition 0570
  Audiologie 0300
  Chimiothérapie 0992
  Dentisterie 0567
  Développement humain 0758
  Enseignement 0350
  Immunologie 0982
  Loisirs 0575
  Médecine du travail et
    thérapie 0354
  Médecine et chirurgie 0564
  Obstétrique et gynécologie ... 0380
  Ophtalmologie 0381
  Orthophonie 0460
  Pathologie 0571
  Pharmacie 0572
  Pharmacologie 0419
  Physiothérapie 0382
  Radiologie 0574
  Santé mentale 0347
  Santé publique 0573
  Soins infirmiers 0569
  Toxicologie 0383

SCIENCES PHYSIQUES

Sciences Pures
Chimie
  Generalités 0485
  Biochimie 487
  Chimie agricole 0749
  Chimie analytique 0486
  Chimie minérale 0488
  Chimie nucléaire 0738
  Chimie organique 0490
  Chimie pharmaceutique 0491
  Physique 0494
  PolymÇres 0495
  Radiation 0754
Mathématiques 0405
Physique
  Généralités 0605
  Acoustique 0986
  Astronomie et
    astrophysique 0606
  Electronique et électricité 0607
  Fluides et plasma 0759
  Météorologie 0608
  Optique 0752
  Particules (Physique
    nucléaire) 0798
  Physique atomique 0748
  Physique de l'état solide 0611
  Physique moléculaire 0609
  Physique nucléaire 0610
  Radiation 0756
Statistiques 0463

Sciences Appliqués Et Technologie
Informatique 0984
Ingénierie
  Généralités 0537
  Agricole 0539
  Automobile 0540

Biomédicale 0541
Chaleur et ther
  modynamique 0348
Conditionnement
  (Emballage) 0549
Génie aérospatial 0538
Génie chimique 0542
Génie civil 0543
Génie électronique et
  électrique 0544
Génie industriel 0546
Génie mécanique 0548
Génie nucléaire 0552
Ingénierie des systàmes 0790
Mécanique navale 0547
Métallurgie 0743
Science des matériaux 0794
Technique du pétrole 0765
Technique minière 0551
Techniques sanitaires et
  municipales 0554
Technologie hydraulique 0545
Mécanique appliquée 0346
Géotechnologie 0428
Matières plastiques
  (Technologie) 0795
Recherche opérationnelle 0796
Textiles et tissus (Technologie) 0794

PSYCHOLOGIE
Généralités 0621
Personnalité 0625
Psychobiologie 0349
Psychologie clinique 0622
Psychologie du comportement 0384
Psychologie du développement .. 0620
Psychologie expérimentale 0623
Psychologie industrielle 0624
Psychologie physiologique 0989
Psychologie sociale 0451
Psychométrie 0632

Name _____

Dissertation Abstracts International is arranged by broad, general subject categories. Please select the one subject which most nearly describes the content of your dissertation. Enter the corresponding four-digit code in the spaces provided.

SUBJECT TERM

☐☐☐☐ U·M·I

SUBJECT CODE

Subject Categories

THE HUMANITIES AND SOCIAL SCIENCES

COMMUNICATIONS AND THE ARTS
Architecture 0729
Art History 0377
Cinema 0900
Dance 0378
Fine Arts 0357
Information Science 0723
Journalism 0391
Library Science 0399
Mass Communications 0708
Music 0413
Speech Communication 0459
Theater 0465

EDUCATION
General 0515
Administration 0514
Adult and Continuing 0516
Agricultural 0517
Art 0273
Bilingual and Multicultural 0282
Business 0688
Community College 0275
Curriculum and Instruction 0727
Early Childhood 0518
Elementary 0524
Finance 0277
Guidance and Counseling 0519
Health 0680
Higher 0745
History of 0520
Home Economics 0278
Industrial 0521
Language and Literature 0279
Mathematics 0280
Music 0522
Philosophy of 0998
Physical 0523

Psychology 0525
Reading 0535
Religious 0527
Sciences 0714
Secondary 0533
Social Sciences 0534
Sociology of 0340
Special 0529
Teacher Training 0530
Technology 0710
Tests and Measurements 0288
Vocational 0747

LANGUAGE, LITERATURE AND LINGUISTICS
Language
General 0679
Ancient 0289
Linguistics 0290
Modern 0291
Literature
General 0401
Classical 0294
Comparative 0295
Medieval 0297
Modern 0298
African 0316
American 0591
Asian 0305
Canadian (English) 0352
Canadian (French) 0355
English 0593
Germanic 0311
Latin American 0312
Middle Eastern 0315
Romance 0313
Slavic and East European 0314

PHILOSOPHY, RELIGION AND THEOLOGY
Philosophy 0422
Religion
General 0318
Biblical Studies 0321
Clergy 0319
History of 0320
Philosophy of 0322
Theology 0469

SOCIAL SCIENCES
American Studies 0323
Anthropology
Archaeology 0324
Cultural 0326
Physical 0327
Business Administration
General 0310
Accounting 0272
Banking 0770
Management 0454
Marketing 0338
Canadian Studies 0385
Economics
General 0501
Agricultural 0503
Commerce-Business 0505
Finance 0508
History 0509
Labor 0510
Theory 0511
Folklore 0358
Geography 0366
Gerontology 0351
History
General 0578

Ancient 0579
Medieval 0581
Modern 0582
Black 0328
African 0331
Asia, Australia and Oceania 0332
Canadian 0334
European 0335
Latin American 0336
Middle Eastern 0333
United States 0337
History of Science 0585
Law 0398
Political Science
General 0615
International Law and
Relations 0616
Public Administration 0617
Recreation 0814
Social Work 0452
Sociology
General 0626
Criminology and Penology ... 0627
Demography 0938
Ethnic and Racial Studies 0631
Individual and Family
Studies 0628
Industrial and Labor
Relations 0629
Public and Social Welfare 0630
Social Structure and
Development 0700
Theory and Methods 0344
Transportation 0709
Urban and Regional Planning 0999
Women's Studies 0453

THE SCIENCES AND ENGINEERING

BIOLOGICAL SCIENCES
Agriculture
General 0473
Agronomy 0285
Animal Culture and
Nutrition 0475
Animal Pathology 0476
Food Science and
Technology 0359
Forestry and Wildlife 0478
Plant Culture 0479
Plant Pathology 0480
Plant Physiology 0817
Range Management 0777
Wood Technology 0746
Biology
General 0306
Anatomy 0287
Biostatistics 0308
Botany 0309
Cell 0379
Ecology 0329
Entomology 0353
Genetics 0369
Limnology 0793
Microbiology 0410
Molecular 0307
Neuroscience 0317
Oceanography 0416
Physiology 0433
Radiation 0821
Veterinary Science 0778
Zoology 0472
Biophysics
General 0786
Medical 0760

EARTH SCIENCES
Biogeochemistry 0425
Geochemistry 0996

Geodesy 0370
Geology 0372
Geophysics 0373
Hydrology 0388
Mineralogy 0411
Paleobotany 0345
Paleoecology 0426
Paleontology 0418
Paleozoology 0985
Palynology 0427
Physical Geography 0368
Physical Oceanography 0415

HEALTH AND ENVIRONMENTAL SCIENCES
Environmental Sciences 0768
Health Sciences
General 0566
Audiology 0300
Chemotherapy 0992
Dentistry 0567
Education 0350
Hospital Management 0769
Human Development 0758
Immunology 0982
Medicine and Surgery 0564
Mental Health 0347
Nursing 0569
Nutrition 0570
Obstetrics and Gynecology .. 0380
Occupational Health and
Therapy 0354
Ophthalmology 0381
Pathology 0571
Pharmacology 0419
Pharmacy 0572
Physical Therapy 0382
Public Health 0573
Radiology 0574
Recreation 0575

Speech Pathology 0460
Toxicology 0383
Home Economics 0386

PHYSICAL SCIENCES
Pure Sciences
Chemistry
General 0485
Agricultural 0749
Analytical 0486
Biochemistry 0487
Inorganic 0488
Nuclear 0738
Organic 0490
Pharmaceutical 0491
Physical 0494
Polymer 0495
Radiation 0754
Mathematics 0405
Physics
General 0605
Acoustics 0986
Astronomy and
Astrophysics 0606
Atmospheric Science 0608
Atomic 0748
Electronics and Electricity 0607
Elementary Particles and
High Energy 0798
Fluid and Plasma 0759
Molecular 0609
Nuclear 0610
Optics 0752
Radiation 0756
Solid State 0611
Statistics 0463

Applied Sciences
Applied Mechanics 0346
Computer Science 0984

Engineering
General 0537
Aerospace 0538
Agricultural 0539
Automotive 0540
Biomedical 0541
Chemical 0542
Civil 0543
Electronics and Electrical 0544
Heat and Thermodynamics ... 0348
Hydraulic 0545
Industrial 0546
Marine 0547
Materials Science 0794
Mechanical 0548
Metallurgy 0743
Mining 0551
Nuclear 0552
Packaging 0549
Petroleum 0765
Sanitary and Municipal 0554
System Science 0790
Geotechnology 0428
Operations Research 0796
Plastics Technology 0795
Textile Technology 0994

PSYCHOLOGY
General 0621
Behavioral 0384
Clinical 0622
Developmental 0620
Experimental 0623
Industrial 0624
Personality 0625
Physiological 0989
Psychobiology 0349
Psychometrics 0632
Social 0451

♲

UNIVERSITÉ DE MONTRÉAL

ÉCOLE POLYTECHNIQUE DE MONTRÉAL

Cette thèse intitulée:

COMPUTER-ASSISTED KNEE SURGERY SYSTEM:

PLANNING OF PROSTHETIC LIGAMENT INSERTION

présentée par: SATI Marwan

en vue de l'obtention du diplôme de: Philosophiae Doctor

a été dûment acceptée par le jury d'examen consitué de:

M. SAVARD Pierre, Ph. D., président

M. DROUIN Gilbert, Ph.D., membre et directeur de recherche

M. DE GUISE Jacques, Ph.D., membre et codirecteur de recherche

M. PARR Jack E., Ph.D., examinateur externe

M. NEWMAN Nicholas N., M.D., membre

À mes parents qui sont les piliers de mon mérite,

et à ma copine pour sa tolérance et son appui.

Remerciements

Je désire remercier tout d'abord celui qui m'a ouvert la porte dans le domaine de la biomédical, Gilbert Drouin. J'aimerais le remercier pour ses précieux conseils ainsi que pour la disponibilité dont il a fait preuve malgré son horaire très chargé. Sa vision globale sur les aspects biomécaniques m'a guidé dans le bon chemin et ce jusqu'à la fin de mon doctorat.

J'aimerais aussi remercier Jacques de Guise, mon codirecteur, dont j'admire les qualités de communicateur, les connaissances en imagerie médicale et la rigueur scientifique, pour son assistance et ses conseils. Jacques m'a aussi donné l'opportunité de rencontrer plusieurs stagiaires, qui ont collaboré de près ou de loin à mon travail. J'aimerais particulièrement remercier parmi ces stagiaires Benoît Allard, Armelle Clech, Alain Richard, Louis-Philippe Amiot, et Francis Baeriswil. Je tiens aussi à remercier Jacques pour son assistance tout au long de mon travail et surtout lors de la rédaction finale de ma thèse. J'ai eu l'occasion de présenter le sujet de ma recherche lors de nombreux congrès internationaux grâce au support de mes deux directeurs.

Mon projet n'aurait pas été possible sans le support financier de la compagnie Howmedica, du FCAR et du CRSNG, que je tiens à remercier. Merci aussi à L'Hocine Yahia pour la gestion de ces fonds, les contacts avec le milieu et le support technique qu'il m'a accordé pour m'aider à terminer mon travail. Merci aussi à Dr. Nicolas Duval pour son aide sur les aspects cliniques du projet.

Je tiens aussi à exprimer ma gratitude envers Yves Martel, un génie dans l'art de la programmation, qui a été responsable en très grande partie de la création des interfaces informatiques qui mettent mon travail en valeur.

vii

«Word» et à Sophie Alain pour son aide en traduction, sans laquelle je n'aurais pu remettre le document final dans les délais prescrits.

Je tiens à remercier mes parents pour leurs bons conseils et leur support durant les moments difficiles. Je tiens aussi à remercier mes amis pour leurs encouragements.

En terminant, je remercie beaucoup mon amie Paule Dion pour sa patience, son support affectif et technique et pour m'avoir maintenu en contact avec mes amis et avec la réalité lorsque j'étais en plein voyage astral au monde de la recherche.

Résumé

Le genou est une articulation tridimensionnelle dont le mouvement peut être décrit par une cinématique très complexe. L'évaluation précise de cette cinématique peut jouer un rôle important dans le diagnostic, la planification et l'évaluation des méthodes chirurgicales associées aux problèmes des pathologies du genou. Par exemple, la rupture du ligament croisé antérieur (LCA) ou du ligament croisé postérieur (LCP) est un traumatisme qui peut déstabiliser le genou et initier un processus dégénératif précoce au niveau de l'articulation (arthrite). Pour stabiliser le genou après de telles ruptures, des prothèses ligamentaires artificielles ont été développées. Cependant, celles-ci n'ont pas connu le succès escompté. En effet, le chargement extensif cyclique imposé aux ligaments synthétiques cause une rupture prématurée de ceux-ci. Une des causes de rupture prématurée de ces prothèses serait reliée à la technique chirurgicale et plus spécifiquement au choix de l'emplacement des insertions sur l'articulation.

Une meilleure connaissance de la cinématique du genou permettra de mieux comprendre le chargement de la structure ligamentaire ainsi que l'amélioration des techniques chirurgicales. Cependant, l'évaluation *in vivo* précise de la cinématique est rendue très difficile par la présence des différents tissus mous entourant le genou et empêchant un accès direct aux structures osseuses. En particulier, le mouvement relatif des masses molles comme la peau et les muscles nuit considérablement à l'acquisition non invasive des données cinématiques du mouvement des os du genou.

Ces considérations ont inspiré le présent travail de doctorat portant sur l'évaluation *in vivo* de la cinématique de l'articulation du genou.

Traditionnellement, l'analyse *in vivo* de la cinématique est rendue possible par l'utilisation de capteurs de mouvement attachés directement sur la peau. Le déplacement

relatif de la peau et des muscles entraîne une imprécision importante lors de la mesure des mouvements du genou. Afin de développer un système d'analyse tridimensionnel (3D) précis, la première étape consiste à étudier de façon quantitative ce phénomène. Une méthode fluoroscopique incluant une technique de correction informatique 3D de l'agrandissement et de l'orientation des images radiographiques nous a d'abord permis de quantifier avec une précision sous millimétrique le mouvement relatif de la peau par rapport aux os de l'articulation du genou. Des mouvements relatifs présentent des erreurs quadratiques moyennes variant entre 2 à 17 mm rms ont été mesurés pour des marqueurs radio-opaques placés à différents endroits sur les côtés médiaux et latéraux du genou. On a aussi remarqué des différences significatives en fonction de l'emplacement des différents marqueurs.

Cette source d'erreur étant très importante, la seconde étape a porté sur la conception et la réalisation d'un système d'attache fémoral et tibial des capteurs de position permettant la réduction du mouvement relatif de la peau par rapport aux os. Une étude précise et détaillée de l'anatomie du genou humain, combinée aux données issues de l'étude des mouvements de la peau, nous a permis de concevoir un système d'attache semi-flexible assurant à la fois le confort du patient et une grande précision dans les mesures. La méthode fluoroscopique mentionnée ci-dessus nous a permis d'observer une réduction du mouvement de la peau au-dessus du condyle latéral de 11,0 mm rms à 1,7 mm rms et une réduction de 8,5 mm rms à 2,9 mm rms au dessus du condyle médial. Ceci représente une réduction importante de la plus grande source d'erreur dans l'acquisition de la cinématique du genou. Le système d'attache permet ainsi la mesure de la cinématique du genou sur 65 degrés de flexion avec une précision de 0,4 degrés pour la rotation ab-adduction, 2,3 degrés pour la rotation axiale, 2,4 mm pour le déplacement antéro-postérieur et 1,1 mm pour le déplacement axial.

La troisième étape consiste à concevoir et à réaliser un système d'acquisition de la cinématique du genou. Ce système associe plusieurs technologies dans un environnement informatique. Des capteurs magnétiques fixés au système d'attache permettent l'acquisition en temps réel des mouvements 3D des os de l'articulation du genou, soit le tibia et le fémur. Ces renseignements sont associés, par une méthode de calibrage, à une représentation géométrique 3D des os du genou, permettant une visualisation sur écran graphique de leurs mouvements en temps réel. Les modèles géométriques des os d'un patient donné sont obtenus par une technique d'imagerie 3D qui utilise des coupes tomodensitométriques.

Le logiciel permet l'enregistrement des mouvements en trois dimensions, la représentation graphique de la cinématique, la simulation interactive de l'insertion de prothèses ligamentaires et le calcul des déplacements et rotations aux extrémités des ligaments. Un nouvel indice cinématique, l'axe de flexion-extension (FE) moyen est aussi calculé par le système.

L'erreur quadratique moyenne totale du système, incluant les erreurs associées au système d'attache, à l'imprécision des capteurs magnétiques, à la représentation 3D du genou et à la méthode de calibrage a été évaluée à environ 3 mm pour les déplacements et 2,5 degrés pour les rotations.

Une analyse de sensibilité sur le calcul des déformations ligamentaires en fonction de cette erreur a aussi été effectuée. Les erreurs maximales de flexion, de torsion et d'élongation sont évaluées respectivement à 6,5 degrés, 5,0 degrés et 3,8 mm.

Le système a permis d'obtenir les premières données de flexion, de torsion et d'élongation ligamentaires calculées à partir de données cinématiques enregistrées *in vivo*. Les résultats correspondant aux élongations ligamentaires se comparent bien aux

études cadavériques rapportées dans la littérature. Ces données ont aussi permis la simulation de la chirurgie ligamentaire et l'illustration de l'utilisation du nouvel indice cinématique, l'axe FE, comme guide permettant l'installation des insertions ligamentaires dans des sites minimisant ou maximisant les déformations ligamentaires. Il a ainsi été suggéré que les tunnels ligamentaires orientés de façon parallèle à l'axe FE, surtout pour l'insertion fémorale, causaient une grande déformation en torsion dans le ligament. Inversement, les tunnels orientés de façon perpendiculaire subissaient très peu de torsion mais un grand changement dans l'angle de flexion entre le tunnel et la portion intra-articulaire du ligament. Donc, un emplacement chirurgical pouvant minimiser toutes les déformations ligamentaires n'existe pas. Les emplacements suggérés par un manufacturier de prothèses ligamentaires LCA et LCP ont été simulés et analysés. Les résultats de l'analyse de la prothèse LCA suggèrent un changement dans son design. Malheureusement, la simulation de l'emplacement chirurgical du LCP ne pouvait pas être reproduit assez précisément pour en tirer des conclusions de l'analyse.

Le système d'analyse du genou présenté dans cette thèse est le premier, à notre connaissance, qui permet à l'utilisateur d'interagir avec une représentation directe et personnalisée des mouvements et de la géométrie *in vivo* des os du genou. L'environnement informatique interactif permet la manipulation et l'analyse d'un « genou virtuel » qui pourra éventuellement servir au diagnostic des pathologies du genou de même qu'à la planification et à l'évaluation des interventions chirurgicales. Cette technologie a été conçue pour être pratique, peu encombrante et assez précise pour être utilisée en clinique.

Abstract

The knee is a sensitive mechanism that exhibits both complex three-dimensional (3D) movement and geometry. Once injured, kinematic analysis plays an essential role in the diagnosis and choice of surgical intervention.

Rupture of the anterior cruciate ligament (ACL) and rupture of the posterior cruciate ligament (PCL) are pathologies that can destabilize the knee and lead to premature degenerative arthritis of the joint. Prosthetic cruciate ligaments have been developed to stabilize the knee following such disruption. These devices are generally no longer used since extensive *in vivo* cyclic loading causes material fatigue that often leads to their failure. There is evidence that improved surgical placement could reduce fatigue wear making prosthetic replacement feasible.

Better knowledge of the knee's kinematics would help understand the ligament loading and improvement of surgical methods. However, analysis of the knee's movement is hindered by large amounts of soft tissue surrounding the articulation. The difficulty in examining *in vivo* knee movement has inspired the development of the 3D knee analyzer presented in this thesis. The use of this system to investigate prosthetic ligament deformation for surgical planning purposes is demonstrated as its first clinical application.

Movement tracking sensors are traditionally taped onto the surface of the skin to track limb movement for kinematic analysis. However, soft tissue surrounding the knee moves during knee flexion causing an artifact in the measurement of underlying bone motion. To understand and record this phenomenon, an X-ray based method was developed to quantify relative sensor-bone movement. Real time X-ray (fluoroscopic) images of knee flexion with radio-opaque markers individually taped onto the surface of the subjects' skin were digitized onto computer. A 3D computer model was developed to correct for

magnification and bone orientation which allowed sub-millimeter tracking of skin-bone movement. Skin movement measured during flexion over several regions of both medial and lateral sides of the knee ranged from 2 to 17 mm root mean square (rms) and varied significantly with marker placement. Data obtained in this study is the most detailed description to date. It identifies skin-bone movement as the largest source of error in knee movement analysis. This affirmation stresses the need for improved methods.

Since the source of error was so significant, a new mechanical non-invasive device was designed. Based on this quantitative skin movement data and a detailed study of knee anatomy, the system was to physically reduce movement between motion sensors and underlying bone. The semi-flexible design of the system provided subject comfort without compromising precision. Radio-opaque markers were placed at the attachment sites of this system and the aforementioned X-ray method used to evaluate the device's accuracy in tracking bone movement. Skin movement over the lateral condyle was reduced from 11 to 1.7 mm rms and over the medial condyle from 8.5 to 2.9 mm rms. This allowed measurement of joint kinematics over 65 degrees knee flexion with an error of 0.4 degrees for ab-adduction rotation, 2.3 degrees for axial rotation, 2.4 mm for AP translation and 1.1 mm for axial translation. Medial attachment movement was mostly responsible for these small inaccuracies. Use of this system reduces skin movement artifacts by one order of magnitude making more detailed analyses possible.

The third step was to create an acquisition system to record the knee's movement. The mechanical apparatus was equipped with magnetic sensors to non-invasively track underlying bone movement and provide kinematic input to the 3D knee analyzer. Three-dimensional imagery techniques, based on computed tomography (CT scan) have been developed to accurately obtain 3D reconstruction of knee geometry. A mathematical calibration method allows real-time correspondence between the spatial position of the patient's femur and tibia and the "virtual" 3D medical image of the corresponding

personalized geometry. Software allows recording of 3D kinematics, interactive simulation of prosthetic ligament insertion and calculation of the displacements and rotations at the ligament extremities. The average flexion-extension (FE) axis is also calculated by the system to serve as a 3D reference landmark for surgical planning.

Errors from all the components were combined through the root of the sum of their squares. The system's total error in measuring knee movement was an average of 3 mm in displacement and 2.5 degrees in rotation and a maximum of 6.1 mm in displacement and 5.3 degrees in rotation. A sensitivity analysis showed that movement data from this system could be used to simulate prosthetic ligament deformation calculations to below 6.5 degrees bending, 5 degrees torsion and 3.8 mm elongation. Ligament elongation data compared well to cadaver studies reported in the literature, especially for knee flexion below 65 degrees. This represents the first *in vivo* prosthetic ligament bending, torsion and elongation data obtained from non-invasive measurement that can be used for surgical planning.

Changes in femoral insertion orientation were found to have much greater effect on ligament torsion and bending deformations than the tibial insertion. Femoral insertion regions creating maximal and minimal deformations were explained by the ligament's insertion orientation with respect to the knee's flexion-extension (FE) axis. Ligaments placed parallel to the FE axis underwent maximal torsion deformation and minimal changes in bending deformation. The inverse was true for ligaments placed perpendicular to the FE axis indicating that a tradeoff exists between minimizing bending and torsion. The surgical placements suggested by a manufacturer of prosthetic ACL and PCL ligaments were simulated and analyzed. Results of this analysis suggest changes in the design of the ACL ligament are required to reduce its fatigue wear. Analysis of the PCL ligament was not possible because of the inability to consistently simulate its surgical placement.

The technology developed in this work represents the first knee analyzer providing direct representation of personalized *in vivo* 3D bone movement and geometry with which the user can interact. The interactive computer environment defines a "virtual knee" in which diagnoses may eventually be performed and surgical procedures planned. This technology has been conceived to be compact and practical for clinical use, providing the user with accurate 3D knee movement data.

Condensé

Introduction

Le genou est une articulation 3D dont le mouvement peut être décrit par une cinématique très complexe. L'évaluation précise de cette cinématique peut jouer un rôle important dans le diagnostic, la planification et l'évaluation des méthodes chirurgicales associées aux problèmes des pathologies du genou. Par exemple, la rupture du ligament croisé antérieur (LCA) ou du ligament croisé postérieur (LCP) est un traumatisme qui peut déstabiliser le genou et initier un processus dégénératif précoce de l'articulation (arthrite). Pour stabiliser le genou après de telles ruptures, des prothèses ligamentaires artificielles ont été développées. Cependant, celles-ci n'ont pas connu le succès escompté. En effet, le chargement sévère cyclique imposé aux ligaments synthétiques cause une rupture prématurée de ceux-ci (Drouin et al., 1991) et les particules d'usure peuvent entraîner une réaction immunitaire (Claes et al., 1995). Une des causes de rupture prématurée de ces prothèses serait reliée au choix de l'emplacement des insertions sur l'articulation (Gely et al., 1984) (Drouin et al., 1991) et à l'inaptitude des matériaux à répondre au chargement.

L'évaluation de la cinématique du genou et de son effet sur les ligaments permettrait de mieux comprendre ce phénomène et d'améliorer les techniques chirurgicales. Cependant, l'évaluation précise *in vivo* de la cinématique est très difficile car la présence des différents tissus mous entourant le genou empêche l'accès direct aux structures osseuses et ligamentaires. En particulier, le mouvement relatif des masses molles comme la peau et les muscles nuit considérablement à l'acquisition non invasive des données cinématiques du mouvement des os du genou (Cappozzo et al., in press).

Ces considérations ont inspiré le présent travail de doctorat portant sur l'évaluation *in vivo* de la cinématique de l'articulation du genou. Ce condensé présente le projet selon l'ordre de ses objectifs spécifiques:

1. quantifier et comprendre le mouvement de la peau dans la région du genou afin d'améliorer les techniques d'acquisition

2. développer une méthode pour augmenter la précision de mesure du mouvement du genou

3. intégrer cette méthode dans un système d'analyse du genou assistée par ordinateur

4. avec cette technologie, analyser les déformations des prothèses en fonction de leur insertion afin d'aider la planification chirurgicale

Méthodologie

Étude du mouvement de la peau

Traditionnellement, des capteurs de mouvement étaient attachés sur la surface de la peau pour enregistrer les mouvements des segments du corps en vue d'une analyse cinématique. Cependant, les tissus mous qui entourent le genou bougent lors de la flexion et entraînent des artifacts dans la mesure des mouvements des os. Pour comprendre et évaluer ce phénomène, une méthode utilisant les rayons-X a été développée qui quantifie le mouvement relatif des capteurs par rapport aux os. Des images du genou en mouvement sont ainsi obtenues par radiographie en temps réel (fluoroscopie). Un suivi du mouvement de l'os et de marqueurs radio-opaques, placés à la surface de la peau du sujet, est enregistré et numérisé sur ordinateur (voir Figure 2-1, p. 31).

Un modèle informatique 3D a été développé pour corriger l'agrandissement et l'orientation des os afin de permettre un suivi sous-millimétrique des mouvements de la

peau et des os. Des paramètres géométriques personnalisés du modèle sont extraits de deux clichés radiographiques, un antéro-postérieure (AP) et un médio-latérale (ML). Ensuite, des projections sagittales prises durant une flexion du genou servent au calcul du mouvement cinématique. La projection des condyles médial et latéral, les paramètres géométriques et les principes de vision artificielle (Ullman, 1986) permettent le suivi des marqueurs par rapport à l'os. Le mouvement de la peau sur les zones médiales et latérales du genou a ainsi été quantifié chez trois sujets (Figure 2-8; Figure 2-9, p. 52).

Méthode de réduction de l'erreur

Un système mécanique pour l'attache non invasive sur le genou des capteurs de mouvement a été conçu en fonction des données quantitatives du mouvement de la peau et d'une étude détaillée de l'anatomie du genou. Ce système permet de réduire physiquement le déplacement entre les capteurs de mouvement sur la peau et l'os sous-jacent (voir Figure 3-3; Figure 3-4, p. 84).

Sur le coté médial, le dispositif s'appuie sur le tubercule de l'adducteur et derrière le magnus adducteur. Sur le coté latéral, l'appui se trouve entre la bande ilio-tibiale et le biceps femoris et se dépose sur la partie supérieur du condyle postérieur. Un élément flexible joint ces appuis, exerçant une pression intérieure qui solidifie l'attache, sans toutefois provoquer de douleur au sujet. Afin de stabiliser le système par rapport à l'orientation du fémur, une tige verticale est fixée à la cuisse avec une bande élastique et du "velcro". Le système est équipé de capteurs magnétiques permettant de mesurer de façon non invasive le mouvement des os sous-jacents. Des marqueurs radio-opaques ont été placés aux sites d'attache du système. La méthode de radiographie mentionnée ci-dessus a été utilisée pour évaluer la précision du système dans la mesure du mouvement des os chez trois sujets.

L'analyseur 3D du genou

Les données cinématiques obtenues de ce dispositif ont été intégrées dans une interface informatique. Cet ensemble s'appelle l'analyseur 3D du genou (Figure 4-1, p.112). La technique d'imagerie (de Guise & Martel, 1988), basée sur la tomographie axiale (CT scan), a été développée pour obtenir une reconstruction précise, en trois dimensions, de la géométrie du genou. Une méthode mathématique de calibrage permet une correspondance en temps réel entre la position dans l'espace du fémur et du tibia du patient et l'image médicale virtuelle en trois dimensions de la géométrie personnelle correspondante. Ceci est réalisé en localisant les coordonnées de trois objets de calibrage (non illustré sur la figure) apparaissant dans les référentiels de l'image et celui du capteur magnétique. La racine carré de la sommation des composantes d'erreur au carré définit l'erreur maximale du système.

Le logiciel permet l'enregistrement de mouvements en trois dimensions, la simulation interactive de l'insertion de prothèses ligamentaires et le calcul des déplacements et des rotations aux extrémités des ligaments qui peuvent en résulter (Figure 4-4, p. 121). Les calculs de déformations ligamentaires sont basés sur le *principe de déformation inverse* décrit par Gely et al. (1984). L'erreur totale du système a été simulée comme une perturbation des calculs de déformation pour établir la sensibilité du système. Les données d'élongation générées par l'analyseur ont été comparées avec des données issues de la littérature et portant sur des spécimens cadavériques.

Déformation des prothèses ligamentaires

Un nouvel axe de flexion-extension (FE) moyen est aussi calculé (Richard, 1995). Cet axe peut servir de référence 3D lors de la planification chirurgicale. Les régions

d'insertion qui engendrent des déformations ligamentaires minimales et maximales ont été examinées et localisées par rapport à cet axe chez trois sujets. Le placement chirurgical d'une prothèse ligamentaire commerciale tel que suggéré par le manufacturier a été analysé et expliqué en fonction de son orientation par rapport à l'axe FE, pour démontrer l'utilisation du système et aider la planification chirurgicale. L'élongation ne varie pas avec les changements d'orientation, car les mêmes insertions intra-articulaires ont été choisies pour tous les essais. Ceci permet d'isoler l'effet de l'orientation sur les déformations ligamentaires.

Résultats

Le mouvement relatif de la peau par rapport aux os du genou a été estimé comme variant de 2 à 17 mm *root mean square* (rms) dépendant de la position des marqueurs situés des deux côtés du genou (Figure 2-8, p. 52; Figure 2-9, p. 52).

Avec le dispositif mécanique installé sur des sujets, le mouvement de la peau au-dessus du condyle latéral a été réduit de 11 à 1,7 mm rms et celui au-dessus du condyle médial a été réduit de 8,5 à 2,9 mm rms. Avec cette amélioration, le mouvement de l'articulation du genou sur une flexion de 65 degrés peut être mesuré avec une précision de 0,4 degrés pour la rotation ab-adduction, 2,3 degrés pour la rotation axiale, 2,4 mm pour le déplacement AP et 1,1 mm pour le déplacement axial. Le mouvement du point d'attache médial était en grande partie responsable de ces imprécisions (Figure 3-6, p. 95).

Avec le dispositif d'attache intégré dans le système d'analyse du genou, l'erreur totale sur les mesures cinématiques est en moyenne en dessous de 3 mm pour le déplacement et en dessous de 2,5 degrés pour la rotation et au maximum 6,1 mm pour le déplacement et 5,3 degrés pour la rotation. L'analyse de sensibilité a montré que les données de mouvement provenant de ce système donnaient des erreurs de calcul des déformations des prothèses

ligamentaires de moins de 6,5 degrés en flexion, 5 degrés en torsion et 3,8 mm en élongation. Les donnés sur l'élongation ligamentaire obtenues se comparent bien à celles rapportées dans la littérature lors d'études faites sur des cadavres, particulièrement pour les flexions du genou au-dessous de 65 degrés (Figure 4-7, p. 130; Figure 4-8, p. 131).

Les déformations étaient plus sensibles à l'emplacement chirurgical du côté fémoral (Figure 5-1, p. 139: lig1, lig2, lig3). Les insertions ligamentaires placées parallèlement à l'axe FE subissaient une grande sollicitation en torsion et une flexion élevée mais constante (Figure 5-1: lig1). Inversement, placés perpendiculairement à cet axe, les ligaments subissaient une torsion relativement constante et une sollicitation importante en flexion (Figure 5-1: lig2, lig3). L'insertion fémorale de la prothèse ligamentaire commerciale était orienté perpendiculairement à l'axe FE du genou. Elle subissait donc une grande variation en flexion et une petite variation en torsion. La flexion du côté fémoral du ligament passait par un minimum proche de zéro degrés à la mi-flexion du genou.

Discussion et conclusions

Les données sur le mouvement de la peau obtenues dans cette étude sont, à notre connaissance, les plus détaillées à ce jour. Elles identifient le mouvement de la peau par rapport aux os comme étant la plus grande source d'erreur dans l'analyse des mouvements du genou et soulignent l'importance d'améliorer la précision des méthodes d'acquisition.

Le dispositif d'attache a répondu à ce besoin en réduisant de façon significative le mouvement de la peau permettant d'obtenir des données cinématiques utiles lors de l'analyse détaillée du genou. Éventuellement, l'utilisation de ce dispositif en clinique fournirait des données précises au praticien sans compromettre le confort du patient.

L'analyse de sensibilité de la méthode de calcul des déformations ligamentaires a démontré que la flexion, la torsion et l'élongation pourraient être calculées avec des erreurs maximales de respectivement 6,5 degrés, 5 degrés et 3,8 mm. Ceci représente les premières mesures *in vivo* de flexion, d'élongation et de torsion des prothèses ligamentaires obtenues à partir d'un système non invasif.

Les analyses de simulation de l'emplacement chirurgical des prothèses ligamentaires ont démontré que le placement chirurgical du tunnel d'insertion parallèle à l'axe FE maximise la torsion et minimise la flexion dans le ligament et inversement pour les placements perpendiculaires au FE. Les déformations sont ainsi associées à l'orientation relative entre le tunnel d'insertion et l'axe de flexion-extension du genou.

L'orientation de l'insertion du ligament commercial réduisait l'effet de fatigue car la flexion fémorale était minimale et proche de zéro degrés à une position fréquente du genou. Ce ligament est fabriqué avec une pré-torsion de 90 degrés pour minimiser la fatigue en torsion lors de la flexion du genou. La torsion prédite par l'analyseur du genou est seulement de 25 degrés ce qui indiquerait que la pré-torsion du ligament est beaucoup trop élevée.

Le système d'analyse du genou développé dans cette thèse est le premier qui permet à l'utilisateur d'interagir avec une représentation directe et personnalisée des mouvements et de la géométrie *in vivo* des os du genou. L'environnement informatique interactif définit un «genou virtuel» qui pourra éventuellement servir à diagnostiquer les pathologies du genou et à planifier les interventions chirurgicales. Cette technologie a été conçue pour être compacte et pratique dans le cadre d'une utilisation en clinique où elle permettra au chirurgien d'acquérir des données précises, en trois dimensions, sur les mouvements du genou.

Table of Contents

List of Tables

List of Figures

List of Symbols and Abbreviations

X, Y, Z	axes defined on image of bone
Blumensaat	projection of the roof of the intercondylar notch
$slope_{mag}$	slope of the fluoroscopic magnification
$magAP_{ruler}$	reference AP ruler magnification
$magML_{ruler}$	reference ML ruler magnification
DAPm(i)	distance between AP ruler and marker "i"
DAPc	distance between the AP ruler and the average distal condyle
DYm(i)	distance along the bone's Y axis to marker i
DYc_M, DYc_L	distance along the bone's Y axis to the medial and lateral condyles respectively
$DMLc_M$, $DMLc_L$	distance between the ML ruler and the medial and lateral condyles respectively
Pmx, Pmz	x and z components of uncorrected marker position
Tib	axis defining the tibial flexion angle
Dx, Dz	the distance between the posterior and distal condyles respectively the ML view
$magAP_m(i)$	the AP magnification of marker i
$magAP_{dc}$	the AP magnification of the distal condyles
$magML_{avgc}$	the average ML magnification of the medial and lateral condyles
Rx, Rz	rotation of the bone about its X and Z axes respectively
dc	distance between the distal condyles (mm)
dz'(f)	difference in distal condyle distance between frame f and the reference image frame f (pixels) (dz(f) in mm)

dx'(f) difference in posterior condyle distance between frame f and the reference image frame (pixels) (dx(f) in mm)

corrz(f,i), corrx(f,i) marker position corrections in the Z and X axes respectively for frame f, marker i

px(f,i), pz(f,i) x and z componenets of corrected marker positions for frame f, marker i

RMSd, rms, PASE error in marker position expressed as the root mean square distance from its mean position

PROLIGS
(or ProLIGS) Prosthetic Ligament Information Generating System

ACL Anterior cruciate ligament of the knee

PCL Posterior cruciate ligament of the knee

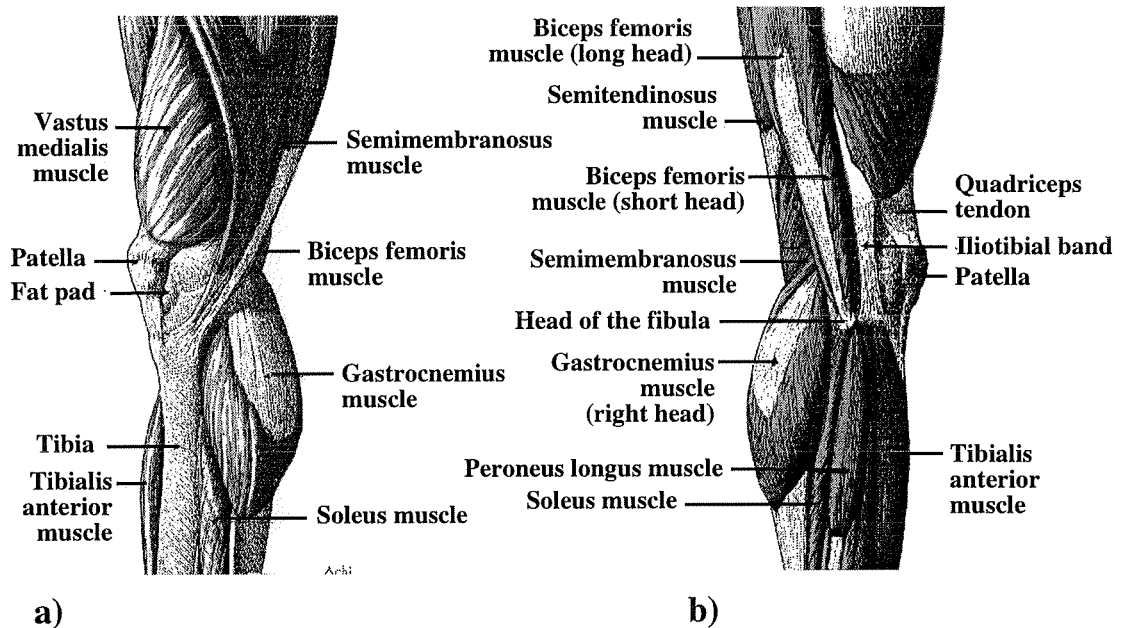FE Flexion-extension axis of the knee

CHAPTER I

## 1. INTRODUCTION

1.1 Background and situation of work

The human knee was once believed to be a simple hinge-like mechanism. This incorrect supposition is not surprising since the knee joint articulation is hidden beneath layers of skin and soft tissue involved in its function (Figure 1-1)

Figure 1–1 Soft tissue surrounding the a) lateral and b) medial aspects of the knee (Schider, 1957).

Unseen beneath these structures is a complex and sensitive mechanism, injury of which can lead to loss of mobility and premature degeneration of its structures. Movement of the joint is guided by a complex interaction among bones, ligaments and muscles. The presence of thick soft tissue enveloping the knee renders diagnosis and correction of pathologies difficult. One example of these difficulties is the surgical replacement of a ruptured anterior cruciate ligament (ACL) via a prosthesis (see Figure 1–2). Optical fiber technology (arthroscopy) has been developed to help the surgeon see internal structures hidden beneath the skin and between the femoral condyles. Even with this technology, it is difficult to know where and how to properly position the ACL prosthesis replacement (Gely et al., 1984).
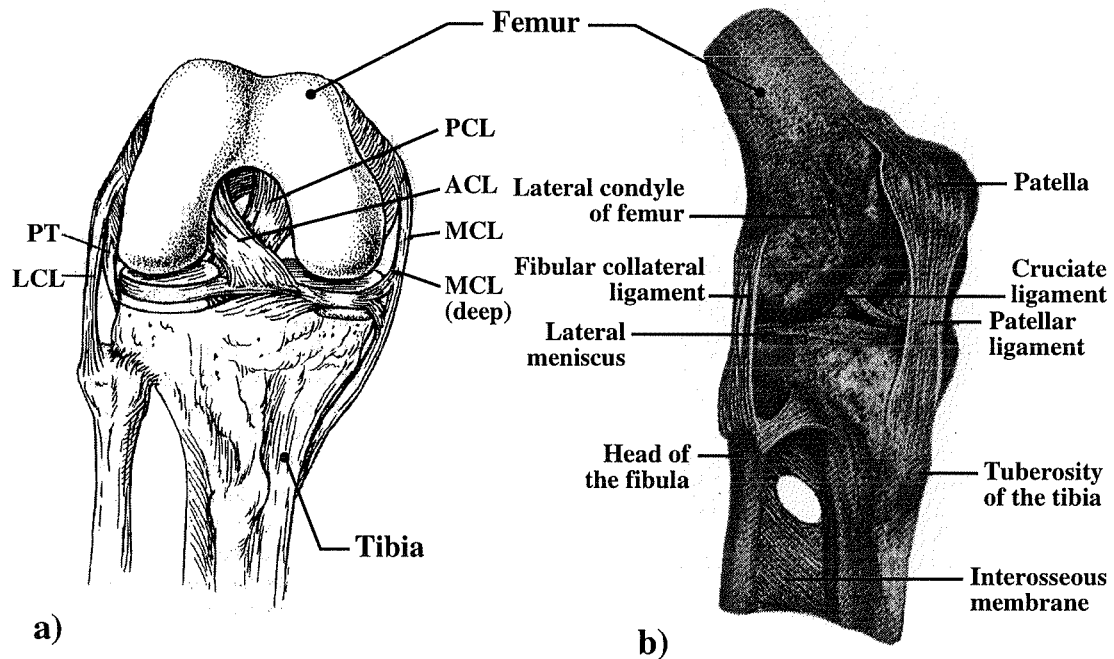
Figure 1–2 Knee geometry of bones (femur, tibia, fibula) and main ligamentous structures a) Anterior cruciate ligament (ACL), posterior cruciate ligament (PCL), medial collateral ligament (MCL), lateral collateral ligament (LCL), popliteus tendon (PT). Antero–posterior (AP) view. (Griffin, 1995) b) antero–lateral view (Schider, 1957).

In 1991, 3700 ligament surgeries were performed in Canada, 733 in Quebec alone (CCP, 1986). Each surgery corresponds to an average 7.5 day hospital stay with very significant costs.

Knee ligaments are loaded by the displacement of their extremities which are anchored into bone. Therefore, accurate kinematics of bone movement are the basis for the diagnosis of the pathology and, if possible, the planning of the corrective measure. However, non–invasive measurement of knee movement is impeded by large amounts of soft tissue which surround the knee.

Presently, technologies for kinematic analysis of knee movement are only available in specialized centers and detailed kinematic analyses are performed only on an experimental basis. This is largely due to the cost of these systems, impracticality of their use in a spatially restricted clinical environment and the complexity of the data they generate. The accuracy of these methods is sufficient for to general movement analysis but is inadequate for specific clinical applications such as knee ligament analysis.

There is, therefore, a need for an affordable technology which provides accurate knee movement data on a routine basis in a format that both the biomechanist and clinician can understand.

The heart of this work is the development of a new technology which improves both the accuracy of existing knee measurement instrumentation and the communication of the resulting data between research and clinical specialists.

Problems of existing methods to acquire and represent knee movement data put into context the specific design criteria of the proposed knee analysis system. The required system should improve knee movement measurement and help interpret the data to assist in analysis and surgical planning. Planning of surgical insertion of prosthetic ligaments in the knee is an important application that can directly benefit from this technology.

This chapter presents the background, the context of the work and a review of the pertinent literature which is divided into three sections: 1) kinematic measurement 2) interpretation of human movement data and 3) application to prosthetic ligament analysis. The objectives of this thesis are then put into context and presented in reference to the current state of knowledge.

1.2 Literature Review

1.2.1 Kinematic measurement

Modern movement analysis can be traced back to the 19th century when Muybridge (1882, 1887) used sequentially fired cameras to investigate the gait of race horses, other animals and humans (Paul, 1995). Human walking was investigated by Marey (1887) and Carlet (1872) using pneumatic devices to measure limb movement. Comprehensive three dimensional (3D) human body movement was first performed by Braune and Fischer (1895) using four plate cameras to track 11 incandescent tube markers strapped onto segments of the subject dressed in black. Images of the tubes' movements resulted in stick figure animations of the subject's movement from which various kinematic and dynamic parameters were derived.

Although moving about in the dark with glowing markers is a thing of the past in biomechanics, most human movement analyses are still performed using optical tracking of markers mounted on the surface of the skin. For biomechanical quantification of joint movement, the implicit assumption of such methods is that measurement of the markers' movements reflect the movement of the underlying bone. However, soft tissue motion about the bones introduces an experimental artifact which can be an order of magnitude higher than the error from the instrumentation used to track marker position (Cappozzo et al., in press). This artifact is acceptable for certain studies requiring low levels of kinematic accuracy. However, it is not adequate for detailed articular movement required for prosthetic biomechanical analysis.

The first step towards improving the accuracy of a measurement system is to study the sources of error. It is known that the main contributor to the total measurement error is the

error due to the movement between the position sensor mounted on the skin and the underlying bone.

Macleod and Morris (1987) were the first to study the relative movement between skin and bone during movement analysis. To investigate this experimental artifact, they compared the relative distance between several skin-mounted markers during brisk walking. Lafortune et al. (1992) later used video X-ray fluoroscopy to obtain qualitative data on skin movement over the lateral condyle of the knee and the same approach was applied by Cappozzo et al. (1993, 1995) to study the same phenomenon. Several authors have since employed invasive bone pins (Murphy, 1990;Karlsson & Lundberg, 1994;Cappozzo et al., in press) or "halo rings" (Holden et al., 1994) to evaluate skin-bone movement about the knee.

To improve the accuracy of knee movement measurement techniques, correction of the error via mathematical procedures (Cappello et al., 1994;Wang et al., 1993;Veldpaus et al., 1988;Spoor & Veldpaus, 1980;Cheeze, 1993) and improved marker placement (Söderkvist & Wedin, 1993;Crisco III et al., 1994) have been proposed. Others approached the problem by attempting to improve the link between motion sensors and underlying bone (Cappozzo et al., 1993;Ladin & Wu, 1991;Wu & Ladin Z., 1993;Mills & Hull, 1991;Quinn & Mote Jr., 1990;Murphy, 1990).

Ironically until today, movement analysis sensors are often purchased based on their tracking accuracy. Considering the magnitude of skin movement artifacts, very accurate and correspondingly expensive systems are excessive for many biomechanical analyses. Quotation of the instrument's accuracy as that of the kinematic accuracy of the experiment is a pitfall related to the confusion between the precision and accuracy of a system. In biomechanics of movement, a measurement of a limb segment movement is very accurate when it is close to the "true" value of position and orientation, or that

obtained by a perfect measurement method. An instrument can be very precise in locating the position of a sensor in space, but when the sensor moves with respect to the underlying bone, we can obtain very precise measurement yet inaccurate bone movement evaluation. On this subject, professor David Winter, recently retired from biomechanics, said jokingly during a keynote speech at the 1995 International Society of Biomechanics conference "... with the new instrumentation, we are now able to measure our skin movement with sub-millimeter precision ".

Since the discovery of cine film, several technologies capable of tracking human movement have emerged. These technologies are referred to as "navigation systems" and are based on different physical principles, which we use to define four different categories namely: Instrumented Space Linkages (ISL or otherwise referred to as position and orientation goniometers), magnetic, acoustic and optic systems. The advantages and disadvantages of these systems are summarized in Table 1-1.

Instrumented space linkages (ISL) are non-motorized robot-like linkages which use interlink potentiometers to measure joint angles. The position and orientation of the end effector is calculated using standard Denavitt-Hartenburg mathematics from robotics. Several authors have used these systems in the field of biomechanics (Kinzel et al., 1972;Townsend et al., 1977;Isacson et al., 1986;Lewis et al., 1988;Suntay et al., 1983;Marans et al., 1989) and discussed their resolution (Chao, 1980;Suntay et al., 1983;Lewis et al., 1988;Kettelkamp, 1976;Shiavi et al., 1987). ISL systems can be very accurate (of the order of 0.1 mm) and do not suffer from either metallic or atmospheric interference as do some of the following systems. A disadvantage of the use of a robot-like linkage is the slight awkwardness of its use during complex movements and the limit in the number of segments which can be analyzed simultaneously. Some of these systems suffer from "sticktion", which is a mechanical blocking due to friction between links.

Table 1-1 Navigation systems

Navigation System	Advantages	Disadvantages
Instrumented Space Linkage (ISL)	High accuracy Not sensitive to metallic or atmospheric interference.	Cumbersome Physically difficult to attach onto several limb segments.
Magnetic	No physical link between sensor and emitter. No problem with "shadowing" Not sensitive to atmospheric conditions.	Sensitive to magnetically permeable metals.
Acoustic	No mechanical attachment between sensor and emitter. Not sensitive to metallic interference.	Must be calibrated for atmospheric conditions. Problem with shadowing and sometimes echoes. Presently, limited number of segments can be analyzed simultaneously
Optic	No mechanical attachment. Not sensitive to metallic or atmospheric environment. Good range.	Problem with shadowing.

Magnetic systems emit either an AC or a DC magnetic field about three orthogonal base coils. The projection of these fields onto three smaller orthogonal coils found in the receiver give nine elements of information. Subtracting for the earth's ambient magnetic field, in the case of the DC systems, the position and orientation of the sensor can be found with respect to the base emitter without a physical connection between the two. Accuracy of magnetic systems is of the order of 2.5 mm rms in position and 0.5 degrees in rotation, however, these systems can be calibrated to increase their position accuracy to 1 mm rms. One disadvantage is the system's sensitivity to certain metals which can perturb magnetic fields. Magnetic systems are very flexible since they have no

mechanical emitter-receiver linkage, other than a small cable connected to the sensor, and the magnetic field can pass through most solid objects, including humans, thus eliminating the problem of shadowing. Several sensors can be used per emitter to track several limb segments simultaneously.

For 3D analysis, sonic systems require the placement of at least 3 ultrasound emitters on each limb segment and at least 3 receivers fixed in the laboratory frame. It is possible to calculate position of the emitter and therefore compute the orientation of the limb with respect to the receivers based on time of arrival of the sonic signals. Acoustic systems have been used for human movement analysis (Andrews & Youm, 1979;Siegler et al., 1988) of the shoulder (Engin et al., 1984), elbow (Engin & Peindl, 1987) and hip (Engin & Chen, 1988). Resolution of these systems has been found to be of the order of 1mm in position and orientation error depends on the distance between the emitters. One problem with such ultrasound systems is that their signal frequency does not pass through tissue or dense objects. Therefore, neither the subject nor other objects must be placed between the transmitter and receiver. These systems are also sensitive to humidity and air currents, so they must be calibrated before each use and air currents must be controlled. However, some self calibrating systems have recently become available.

Optic (or "camera") systems are either passive-marker or active-marker based and can use several different light sources. Active optic systems have markers which emit light on the moving body which are tracked by cameras. Passive systems use markers placed on the moving body which reflect light from either ambient or source illumination. Optical systems offer the same freedom of movement as magnetic and ultrasound systems. The accuracy of cheaper optical systems is comparable to their magnetic and acoustic counterparts yet more expensive optical systems offering very high accuracy and resolution are available. However, as with ultrasound systems, they rely on a direct line of sight between the marker and camera. These systems can suffer from artifacts due to

reflections and their setup can in some cases be time consuming, requiring on-site calibration and proper camera placement. Optical distortion must be corrected for accurate measurements.

Error due to skin movement artifacts can be of the order of 10-20 mm (Cappozzo et al., in press) whereas navigation system errors are of the order of millimeters. This affirms the fact that skin movement is the largest obstacle to detailed non-invasive analysis of human movement. Consequently, the accuracy specification should not be a predominant factor in the choice of a navigation system technology for an analysis where sensors are mounted on the surface of the skin, since all the sensors mentioned above have error at least one order of magnitude smaller than the error arising from marker-bone displacement.

1.2.2 Interpretation of human movement data

Detailed biomechanical analysis is based on sound kinematic data, but this data must be presented in an appropriate format to be useful. Several practical mathematical descriptors exist to describe rigid body movement namely: Euler rotations, direction cosines, screw (or helical) axes and quartemions. In biomechanics, two functional approaches to describe human movement have evolved from these descriptors:

1) A bone axis-based approach describing movement as a Eulerian-type three-parameter set consistent with clinical definitions.

2) A centrode or Helical-based approach describing movement via instantaneous or finite rotations about and translations along a moving centrode or Helical axis.

The first of these approaches is used mostly in clinical situations due the facility with which its data format is compatible with the medical terminology of joint rotations. The

second approach has been limited to experimental and biomechanic research contexts since the relationship between anatomical movements and the mathematical descriptors is less intuitive.

1.2.2.1 2D Methods

Helical axis methods in biomechanics have evolved from two dimensional (2D) centrode methods. The earliest kinematic interpretation methods in biomechanics determined the centrodes of knee rotation via the method of Reuleaux (1900). Frankel et al. (1971) estimated instant center of rotation displacements of the knee during walking to determine a correlation between pathomechanics and traumatic degenerative disease. Freudenstein and Woo (1969) fitted experimental centrode data to a logarithmic spiral for use in the design of polycentric knee prostheses. Walker (1972) related clinical findings using full knee flexion for both normal and pathological knee motions. His data was later used in the design of fixed-axis prosthetic knees and was a basis for his work on polycentric knee designs. Soudan et al. (1979) traced curves formed by two points on the moving tibia and calculated the intersection of their normals to find the pathway of instant centers during knee flexion. These studies were later criticized by Panjabi et al. (1982) for improper experimental design which could lead, for example in the studies of Frankel et al., to errors of 6.3 cm in the calculation of the centers of rotation.

Moreover, observations made of 3D rotations along 2D projections give elliptical centrode paths. Some early center of rotation curves measured from lateral views and often cited in many texts suggest that the knee has a variable elliptic-like flexion axis, even for passive knee flexion. However, recent studies using both mechanical and optical methods show that there may exist 2D plane orientations from which the centrodes are coincident during passive knee flexion (Hollister et al., 1986). This implies that for passive knee flexion the femur may rotate about a single fixed flexion-extension (FE)

axis. It is ironic that early data taken from simple 2D views suggested complex 3D knee motion and that this recent data from 3D movement analysis suggests the contrary. Several authors, in an attempt to find an "optimal axis" (Lewis & Lew, 1978) or the degrees of freedom of passive knee flexion (Murphy, 1990), have generated single flexion axes for the knee, without claiming this axis to be stationary during knee flexion.

We must therefore be careful when referring to knee movement information generated by 2D methods. Soudan et al. (1979) suggested that for 2D techniques to be used, verification of the plane of motion must be performed and analyses conducted perpendicular to this plane.

1.2.2.2 3D Helical Methods

Three dimensional studies of knee movement started with work by Blacharski et al. (1974), who used stroboscope lights and time lapse photography to plot reference points. In a simple extension of the 2D Reuleaux method, they projected segment motion onto two parallel planes to calculate finite centrodes which they connected to estimate a finite helical axis. Soudan et al. (1979), showed that extending the 2D method to a 3D method in this way was incorrect. Furthermore, it was found that these extended 2D methods have much greater inaccuracies than the original 2D methods.

Mozzi was the first to propos that general 3D spatial motion was equivalent to an infinitesimal twist about a screw. Later, Chastle (Hunt, 1978) proved that the instantaneous screw axis is the most general representation of spatial motion of a rigid body. To understand the concept of an instant axis, Soudan et al. (1979) stated "after a translation, all points of the body instantaneously describe circular paths around that axis.

The points lying on it only translate. The instant axis of a joint changes both in place and direction during joint movement, forming the instant axis pathway".

The first exact 3D method based on spatial kinematics was introduced into biomechanics by Kinzel et al. (1972). We must note that Kinzel's method described finite helical axes (or finite "screw axes") which are an estimation of the instantaneous helical axes. Finite helical axes are calculated from subsequent position data whereas instantaneous helical axes are determined from segment velocities. Because of the difficulty in calculating velocities due to noise, most biomechanical studies have employed finite helical axes. The finite helical axis can be calculated from subsequent position and orientation data by solving a system of equations (Kinzel et al., 1972) requiring the inversion of a non-orthogonal 4x4 matrix (Spoor & Veldpaus, 1980). Another way to determine these axes is by a simple vectorial method based on Rodrigues' formula, repopularized by Bisshop (1969) and applied to biomechanics by Dimnet and Guinguand (1984). Peterson and Erdman (1986) showed the conditions under which the finite helical axis was a good estimator of the instantaneous axis. Finite helical axes based on tibial and femoral position data have been used by several authors (Blankevoort et al., 1990;Huiskes et al., 1985;Shiavi et al., 1987;Quinn & Mote Jr., 1990;Hart et al., 1991).

Murphy (1990) showed the derivation of instantaneous helical axes from velocity data which he used to calculate *in vivo* knee movement of one subject using both invasive pins and skin-mounted markers. Good references on helical axis mathematics are Ball's original treatise (1900), Beggs (1966), Hunt (1978) and McCarthy (1990).

Finite helical axes (and instantaneous helical axes) of knee movement have been reported in the literature to changed their position and orientation during flexion. This data has implicitly supported the assumption that the knee possesses a variable flexion axis.

However, the relationship between the helical description and the fixed flexion-extension (FE) rotation axis found by Hollister et al. remains to be determined.

1.2.2.3 From Euler Rotations to Bone-based Description Methods In Biomechanics

Traditional Euler rotations (ex. Yaw, Pitch and Roll as in aircraft orientation description) are still sometimes utilized in biomechanics to describe relative segment orientations although care must be taken to respect the sequence of rotations and to interpret what these values mean physically. Chao (1980) was the first to employ a gyroscopic system which could allow independent rotations, for example for knee movement analysis, about a femoral-fixed mediolateral axis, a tibial-fixed longitudinal axis and a floating axis. Knee flexion/extension was defined by the rotation about the femoral axis, tibial internal/external rotation about the tibial axis and abduction/adduction about the floating axis. Grood and Suntay (1983) used an identical axis system with emphasis on the possibility of defining clinical displacements along these three independent "anatomical" axes.

Pennock and Clark (1990) have argued that, anatomically speaking, rotations do not occur about the same axes as translations. Furthermore, they noted that there are no commonly accepted location or orientations for the three rotation axes. They reviewed three commonly used axis systems by Grood and Suntay (1983), Lafortune (1984) and the Genucom (Registered by Faro[TM], 1986) seen in Figure 1-3 and proposed improved definitions based on a complete review of the literature on functional rotation axes of the knee (Morrison, 1970;Frankel et al., 1971;Walker et al., 1972;Wang et al., 1973;Shaw & Murray, 1974;Crowninshield et al., 1976;Goodfellow & O'Connor, 1978;Lewis & Lew, 1978;Chao, 1980).
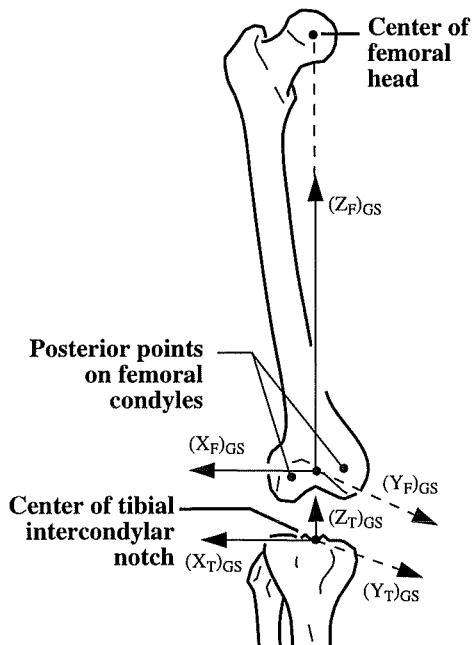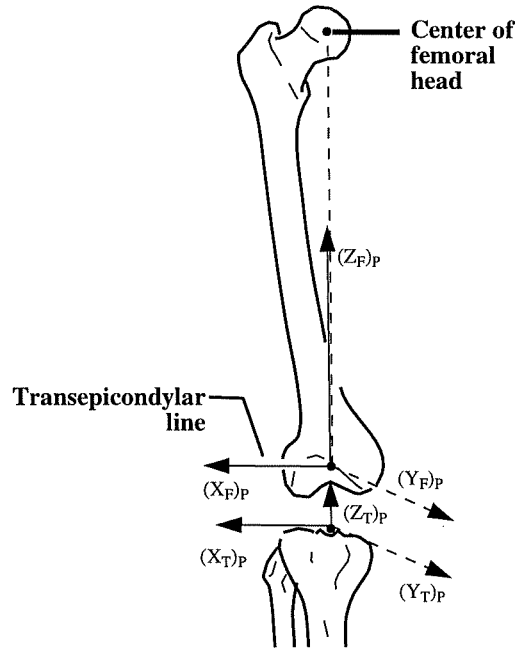
a) Grood and Suntay (1983)
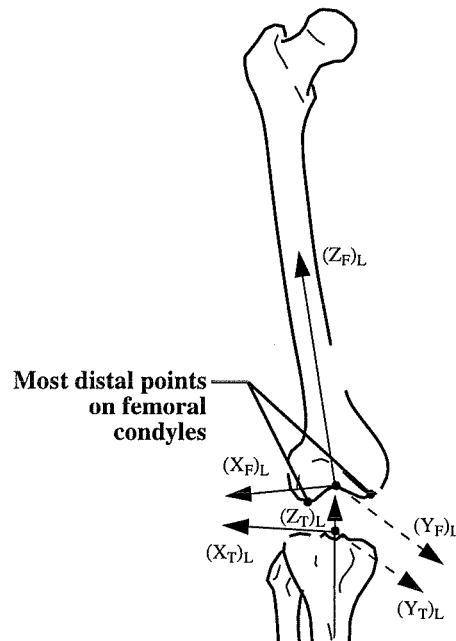
b) Lafortune (1984)
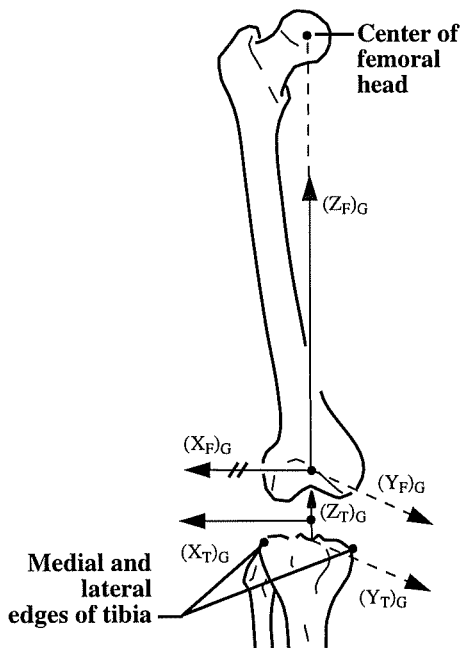
c) Genucom

d) Pennock and Clark (1990)

Figure 1–3 Four bone reference axis systems from antero–posterior view (Pennock and Clark, 1990).

They also commented that systems used by Grood and Suntay (1983), Lafortune (1984) and Genucom assumed that rotation axes not only intersect, but intersect at right angles. They claimed that this oversimplification represented the knee as a kinematically simple three-cylinder open chain, which is anatomically incorrect.

Despite their call for translation axes to be independent of rotation axes, their proposed system continued to assume that the translations occur along their improved rotation axes due to the numerical complexity of a 6 link open-chain system. However, by utilizing experimentally determined rotation axes which are not restricted to intersect or be orthogonal, their method is more general than most of the open chains found in the literature.

From this review, it can be seen how existing methods to describe human movement are relatively complex and controversial. This makes interpretation of human movement for clinical analysis difficult especially since clinicians do not have a mathematical background. For example, relating 3D knee kinematics in the form of helical axes to the surgical placement of prosthetic ligaments in the knee is very difficult. It would also be difficult to relate knee rotations and displacements to prosthetic knee placement. Therefore, a simple 3D parameter is required to help relate measured kinematics to surgical interventions.

1.2.3 Application to prosthetic ligament analysis

The first prosthetic materials used for surgical repair of a ligament appeared as early as 1906 and was made of silk. Since then a variety of materials have been used for ligament replacement. In 1959, Gort and Rostrup used a polytetrafluoroethylene (PFFE) structure to replace the ACL in a canine model. Later, fine braided structures of Nylon®

(polyamide) and Dacron® were tested on dogs (Johnson, 1960;Vaughn, 1963;Gupta & Brinker, 1969). Research conducted by several groups since the early sixties lead to many prosthetic ligament trademarks of which some of the most studied are: Gore-Tex® ACL ligaments (W.L. Gore & Ass. Ince, USA); PHP® ligaments (Cendis medical); Kennedy L.A.D.® ligament augmentation device (3M company, USA); Stryker® ligament (Stryker Corp., USA); Leeds Keio® ligament; LARS ligament (LARS, France); Proflex® prostheses (Protek AG, Bern, Switzerland); Lafil (B. Braun-Dexon GmbH, D-3509 Spangenberg).

The development and commercialization of many of these synthetic ligaments was initially met with great enthusiasm by the orthopedic community. However, it was not long before clinical studies showed disappointing and sometimes catastrophic results. For example, the ProCol bioprosthesis (Xenotech Laboratories Inc, U.S.A.) which was used in both Europe and USA showed poor clinical results just after 22 months (13/14 ruptures) (Good et al., 1989). The Stryker® prosthesis showed satisfactory early results, but after a few years, 34% of the ligaments were found to have lost their mechanical function (Gillquist, 1990). Carbon fibers showed good bone ingrowth and cellular adhesion (Claes et al., 1995) but later clinical studies revealed that sharp wandering fiber particles penetrated living tissue causing sometimes serious complications. As a result of these poor clinical results, research on the mechanisms of prosthetic ligament failure was undertaken.

The concept of prosthetic ligament loading has evolved over the past decades to understand the mechanisms of their rupture. Since natural ligaments fail due to impacts or excessive loads, it is not surprising that the earliest prostheses were designed to possess a high ultimate breaking strength. After the failure of prostheses based on this concept, detailed biomechanical studies lead to designs which more closely reproduced the elastic non-linear force deformation curve of the natural ligament (Dorlot et al., 1980). However,

the plastic deformations in the material were found to lead to permanent elongation (Gillquist, 1990) and rupture by fatigue. To minimize fatigue due to tension, the concept of "isometric" attachment of the ligament, i.e. finding two points on the femur and tibia respectively between which no elongation occurs during knee flexion, was introduced into the surgical procedure (Flemming et al., 1992). Although this concept has been, and still is, the subject of active debate (Hefzy et al., 1989;Grood et al., 1989;Blankevoort & Huiskes, 1991;Covey et al., 1992), it has highlighted the importance of adequate surgical procedure for good long-term clinical results. To help avoid the catastrophic failures experienced in earlier replacement, *in vitro* fatigue testing by cyclic elongation was introduced to predict *in vivo* performance. Cyclic loading on a not perfectly elastic material can cause premature elongation resulting in loss of its prescribed function. Unlike the natural ligament, the prosthesis cannot regenerate its material. Even low rates of fatigue wear can, over time, result in catastrophic failure since the ligament is exposed to 1×10^6 cycles per year *in vivo* (Drouin, 1986;Seedhom, 1992). This makes surgical placement which minimizes fatigue wear essential. Even failures due to immune response can be related to the fatigue of the ligament under *in vivo* conditions. Fatigue wear on a prosthetic ligament, due to both inter-fiber and ligament-bone abrasion, produces small particles which can evoke an immune response even if the material is biocompatible in its intact form (Claes et al., 1995).

A biomechanical study by Gely et al. (1984) revealed that simple elongation fatigue testing did not tell the whole story about *in vivo* conditions. In fact, the ligament is subjected to combined elongation, flexion and torsion deformation. Unlike the natural ligament, prosthetic ligaments are anchored via tunnels in the femur and tibia. The angle formed between the tunnels and the ligament body create combined elongation, flexion and torsion deformations in the ligament as the knee is flexed. Elongation of the ligament depends on the sites where the ligament body enters the femur and tibia and knee kinematics. Keeping these entry sites constant for a given knee kinematic movement, it is

possible to change flexion and torsion in the ligament by varying the angle between the tunnel and the ligament body. Ligament torsion is defined as the twisting of the functional part of the ligament about its long axis. Bending of the ligament is defined as the angle between the ligament functional body with respect to either the femoral insertion tunnel (femoral bending) or the tibial insertion tunnel (tibial bending) (see Figure 1-4).
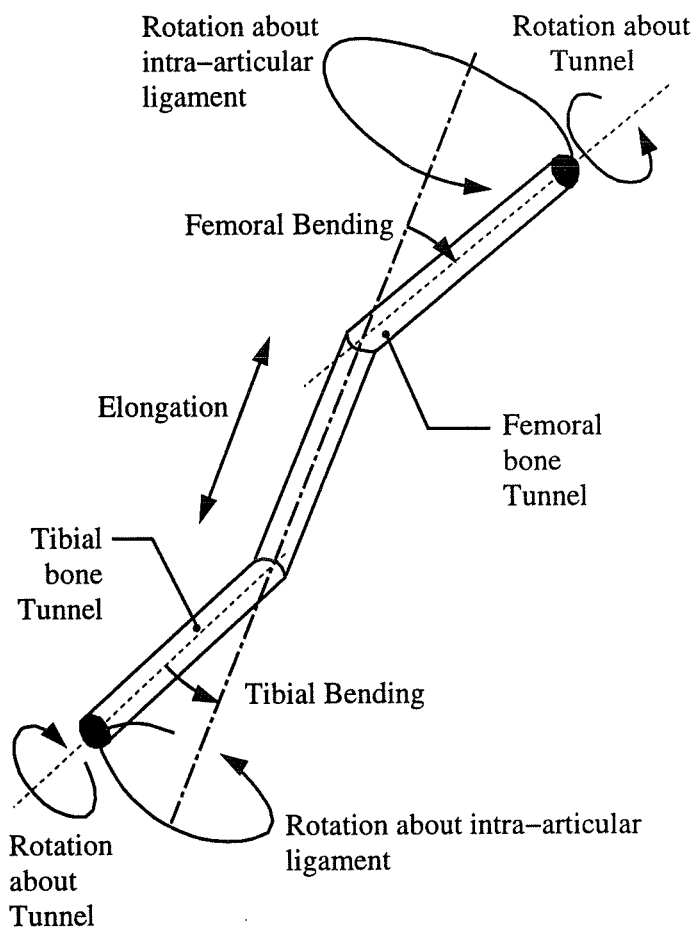
Figure 1-4 Combined deformations of elongation, bending and torsion which occur in prosthetic ligaments

Most *in vitro* ligament testing has involved simple elongation or combined flexion-tension cyclic deformations (Claes et al., 1995). For example, Dürselen and Claes have performed bending fatigue tests which showed poor fatigue life: 14 077 and 1.4×10^6 bending cycles until failure for the Lafil® and Gore Tex® prostheses respectively. The importance of combined elongation, flexion, and torsion has been recently shown through mechanical tests. Combining cyclic 110 N tensile load, 45 degrees bending and 40 degrees torsion resulted in ligament failure after 5×10^6 cycles (Drouin et al., 1991) with significant decrease in fatigue life with increased tensile loads.

The effect of bending and torsion on the fatigue of the ligament is best understood though a physical example. If one was given a section of rope and asked to break it with one's bare hands, one would probably grab it with two hands and simultaneously bend and twist it about a some small region along its length. Applying a tension in the rope would also help the cause. If one were to cheat a bit, a strategically placed bite in this region, applied when nobody is looking, could fray the rope's material and improve chances of success.

Kinematics of dynamic *in vivo* knee movement are a result of the interaction between active structures (muscles) and passive structures (connective tissue). Tendon loading, for example, depends on forces generated by the associated muscle. Unlike tendons, ligaments are loaded by bone movement since their function is to maintain the knee's movement within a safe "envelope" unless a large impact requires their sacrifice to save other structures. Therefore by accurately tracking the kinematics of the femur and tibia during dynamic movements, we can fully describe the displacements the ligament is subjected to (Gely et al., 1984).

1.3 Objectives

The immediate clinical aim of this work is the understanding of the relationship between surgical placement and deformations on prosthetic ligaments.

Since the ligament displacements can be fully described by accurately tracking the kinematics of the femur and tibia during dynamic movements, the overall objective of this work is to develop a new clinical and non-invasive methodology to obtain and analyze detailed and sufficiently accurate knee motion using external movement sensors.

In order to meet this main objective, the specific objectives of this work are:

1) Understand and quantify errors arising from the use of skin mounted external markers to illustrate the problems with existing knee measurement methods.

2) Develop, based on the above information, a non-invasive method that will be practical for routine use in a clinical setting, to reduce the aforementioned errors.

3) Develop a computer interface to help visualize and analyze knee movement, simulate prosthetic ligaments and calculate their deformations.

4) Relate ligament deformations to their surgical insertion orientation with respect to the knee's flexion-extension axis.

The fulfillment of these objectives will provide a non-invasive three-dimensional knee analyzer which is to generate quantitative data in a clinical environment with accuracy superior to conventional laboratory acquisition techniques. The accuracy and usefulness of this system will be illustrated through its use to help analyze and explain prosthetic ligament deformations as a function of their surgical insertion.

1.4 Presentation of thesis

This thesis is composed of 7 chapters, three of which are articles, one in press and the other two submitted for publication. The first chapter has presented the background and the pertinent literature to put into context the objectives of the work. The second chapter is an article which describes a new medical imagery based technique to accurately quantify relative marker-bone movement artifacts *in vivo*. The technique is employed to illustrate and understand errors arising from conventional knee movement measurement techniques. In response to this problem and based on this information, the third chapter is an article which proposes a method to improve knee attachment of external knee movement sensors. Accuracy of the proposed method is evaluated by the aforementioned medical imagery technique. The integration of this instrumentation into a computer-assisted knee analyzer is described through an article which is presented in chapter four. Both the knee movement measurement error of the system and the sensitivity of its prosthetic ligament deformations to these errors are reported. In the fifth chapter, prosthetic ligament deformations are analyzed as a function of their surgical insertion. Chapter 6 is the general discussion of movement data acquisition, prosthetic ligament deformations and the computer information presented in the thesis. Accuracy of the proposed technology and results of the analyses are discussed with respect to the literature. Finally, improvement of surgical insertion of prosthetic ligaments using data generated by the proposed technology is explained and discussed.

CHAPTER II

2. ARTICLE # 1: QUANTITATIVE ASSESSMENT OF SKIN-BONE MOVEMENT AT THE KNEE

2.1 Situation of article in thesis

It is evident from the literature that movement of skin relative to bone is a large source of error which must be reduced to improve non-invasive knee measurement. There is however a lack of detailed knowledge on how skin moves over bone during knee flexion. This phenomenon must be described and understood before a solution can be proposed. To obtain this data, invasive fixation of sensors to the underlying bone is impractical because of the possibility of associated complications. Therefore, medical imagery is a desirable option since it allows non-intrusive measurement of bone movement and external sensor movement.

This article presents an X-ray based technique to quantify movement between external markers and underlying bone. The method is first described and then validated on an

isolated cadaveric bone specimen with respect to known values to quantify its accuracy. Once validated, the method is employed to measure the unrestricted movement of the skin over the knee during flexion. This constitutes the basis for detailed understanding of relative skin-bone movement and the development of the improved acquisition method presented in Chapter III.

QUANTITATIVE ASSESSMENT OF SKIN-BONE MOVEMENT
AT THE KNEE

Sati M.[o], de Guise J.A.[*], Larouche S.[o] and Drouin G.[o]

[o] Biomedical Engineering Department, École Polytechnique, Montréal, Canada; and

[*] Automated Production Department, École de Technologie Supérieure, Montréal, Canada.

Correspondence and Reprint Requests:

Marwan Sati, Biomedical Engineering Department, École Polytechnique, P.O. Box 6079 Station "Downtown", Montréal Québec, Canada H3C 3A7;

tel: (514) 340-4198 ; fax: (514) 340-4611; e-mail: sati@grbb.polymtl.ca

2.2 Abstract

Thick soft tissue and structures involved in the knee's function surround the knee thus hiding the underlying kinematics. This makes diagnosis of pathologies and analysis of biomechanics difficult. This study accurately quantifies the relative movement between skin and the underlying bone, via X-ray fluoroscopy and a mathematical model, in the interest of improving non-invasive knee movement analysis methods. It was found that skin-bone movement varies significantly over both medial and lateral femoral condyles (from 2 to 17 mm rms) and is therefore the greatest obstacle by far to obtaining accurate movement data non-intrusively. Data from the proposed method is fundamental to improving acquisition methods for knee biomechanics and prosthetic analysis and can help in understanding soft tissue movement for orthotic analysis.

2.3 Nomenclature

The variables used in this paper are composed of several descriptive components, which are described in annex A.

X, Y, Z	axes defined on image of bone
Blumensaat	projection of the roof of the intercondylar notch
$slope_{mag}$	slope of the fluoroscopic magnification
$magAP_{ruler}$	reference AP ruler magnification
$magML_{ruler}$	reference ML ruler magnification
DAPm(i)	distance between AP ruler and marker "i"
DAPc	distance between the AP ruler and the average distal condyle
DYm(i)	distance along the bone's Y axis to marker i
DYc_M, DYc_L	distance along the bone's Y axis to the medial and lateral condyles respectively
$DMLc_M, DMLc_L$	distance between the ML ruler and the medial and lateral condyles respectively
Pmx, Pmz	x and z components of uncorrected marker position
Tib	axis defining the tibial flexion angle
Dx, Dz	the distance between the posterior and distal condyles respectively the ML view
$magAP_m(i)$	the AP magnification of marker i
$magAP_{dc}$	the AP magnification of the distal condyles
$magML_{avgc}$	the average ML magnification of the medial and lateral condyles
Rx, Rz	rotation of the bone about its X and Z axes respectively
dc	distance between the distal condyles (mm)
dz'(f)	difference in distal condyle distance between frame f and the reference image frame f (pixels) (dz(f) in mm)

dx'(f)   difference in posterior condyle distance between frame f and the reference image frame (pixels) (dx(f) in mm)

corrz(f,i), corrx(f,i)   marker position corrections in the Z and X axes respectively for frame f, marker i

px(f,i), pz(f,i)   x and z componenets of corrected marker positions for frame f, marker i

Other Definitions:

RMSd or rms or PASE:

error in marker position expressed as the root mean square distance from its mean position

2.4 Introduction

A good understanding of knee behavior starts with sound kinematic data. The accuracy requirements of the kinematics may, however, vary with the studied application. For instance, the level of accuracy required in the study of knee prostheses for an amputee has been met by gait lab apparatus which tracks skin mounted markers via optic tracking equipment.

However, the accuracy required to evaluate the loading of a ligament prosthesis cannot be achieved with the above techniques (Gely et al., 1984). Knee kinematics obtained via surface mounted markers have a large error component due to skin movement relative to the underlying bone. To avoid this error component, kinematic data has been obtained via serial radiography (Frankel et al., 1971;Feudenstein & Woo, 1969;Hallen & Lindahl, 1966;Smidt, 1973), roentgen stereophotogrammetry (Blankevoort et al., 1985;Huiskes et al., 1985;Kärrholm, 1989) or by attaching markers onto the bone by some invasive technique (Lafortune, 1984;Levens et al., 1948).

Recent *in vivo* studies used invasive techniques such as fracture fixation devices (Cappozzo et al., 1993), cortical pin (Lafortune & Lake, 1991;Murphy, 1990;Karlsson & Lundberg, 1994) and minimally invasive "halo ring" pin attachments (Holden et al., 1994) to quantify the movement of markers mounted on the skin.

Most of the recent intrusive techniques were used in order to assess the accuracy of marker attachment methods such as skin mounted markers (Cappozzo et al., 1993;Lafortune & Lake, 1991;Murphy, 1990;Holden et al., 1994) or plate mounted markers attached via a velcro strap onto the leg (Cappozzo et al., 1993).

From this recent literature, the error arising from skin movement has been observed to be of the order of 10 to 20 mm during active movements which is ten to twenty times higher than the error due to video motion analysis equipment. Murphy (1990) found that measuring kinematics through skin mounted markers could underestimate real knee rotations by fifty percent, make underlying smooth kinematics look noisy and complex and degrade the repeatability of results. Therefore, to improve the accuracy, simplicity and repeatability of biomechanical analysis of the knee, efforts should be concentrated on the skin movement problem.

Research is required to understand and quantify skin movement so that the error due to the acquisition methods in measuring real bone movement can be assessed. Only once this error is accurately quantified can steps be taken towards correcting the data and acquisition methods.

Intrusive methods could be used to evaluate skin movement, however, they are not practical for extensive use and care must be taken to avoid complications. For further study of skin movement, there is an interest to develop a minimally invasive method to quantify skin movement error *in vivo*. A medical imagery approach is proposed to quantify skin movement relative to the underlying bone movement at the knee.

2.5 Methodology

A non intrusive method has been developed to measure skin movement with respect to underlying bone movement *in vivo*. To track the skin movement, 3 mm diameter stainless steel ball bearings, referred to as "skin markers", are individually taped onto the skin using small pieces of duct tape between the marker and the skin to ensure that normal skin movement is unhindered. These markers are placed over both the medial and lateral

condyles and on the lateral aspect of the thigh (see Figure 2–1). Several markers are placed on the skin in each of these regions in order to find regions of minimal skin movement.
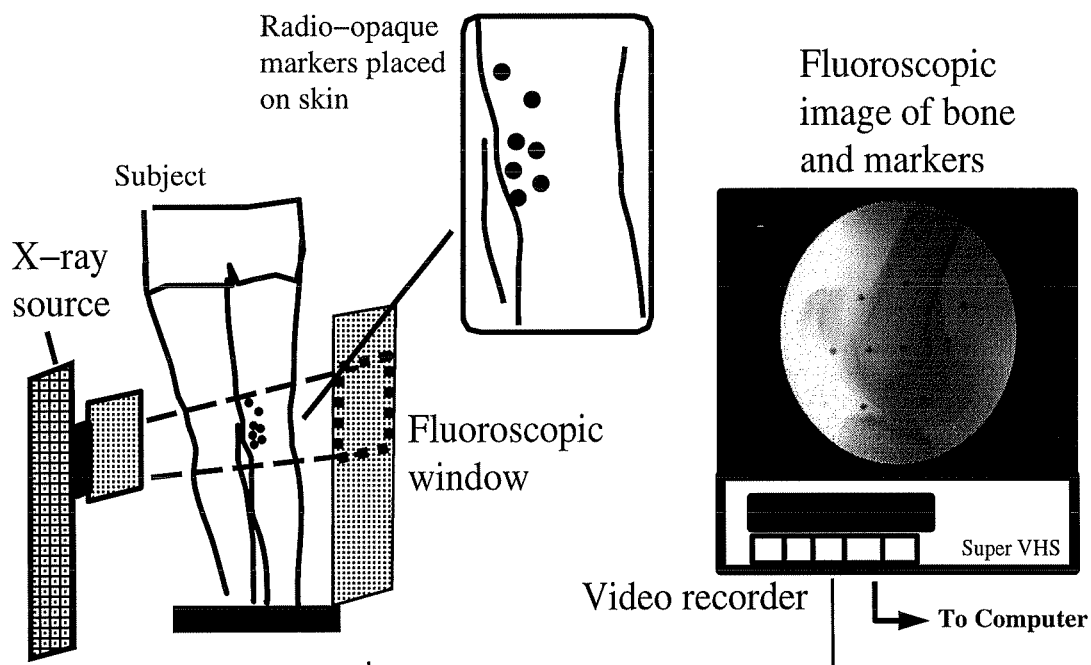
Figure 2–1 Fluoroscopic evaluation setup. Radio–opaque markers (top center) are individually taped onto the medial or lateral aspect of the knee. The subject (left) performs dynamic knee flexions within the fluoroscopic field and data is recorded in real–time (right) then transferred to computer.

Using X–ray medical imagery, the objective is to measure the relative movement between these markers placed on the skin and the underlying bone. A video fluoroscopy system (Philipps Diagnostic 100) was employed to register X–rays in real–time onto a super VHS recorder (Panasonic Industrial 7300). This allowed us to simultaneously visualize the X–ray projection of both the radio–opaque metallic markers placed on the surface of the skin and the underlying bone (see Figure 2–1). Since the markers are individually taped onto the skin as described above, the X–ray projection of

their movement with respect to the X-ray projection of the underlying bone reflects the movement between the skin and the bone. Fluoroscopy has been previously used to obtain a qualitative idea of radio-opaque marker movement on the lateral aspect of the knee (Lafortune et al., 1992;Cappozzo et al., in press), yet the technique has not been elaborated to obtain accurate quantitative data on both the lateral and medial aspects of the knee.

2.5.1 Fluoroscopic image acquisition

A fluoroscope equipped with a super VHS videorecorder was used to register the data (Figure 2-1). Human subjects were made fully aware of the procedure and their consent was obtained before acquisition of the data. Subjects used in this study were of average height and weight and had no previously reported knee problems. The subjects, or cadaveric bone specimen for the validation of the method, were placed such that a lateral profile of both condyles and the superior aspect of the tibia were within the fluoroscopic window. Both an anteroposterior (AP) and mediolateral (ML) fluoroscopic images were first taken to measure several geometric parameters used in later image correction calculations. Once these images were obtained, active knee flexion in the sagittal plane were performed by the live subjects within the fluoroscopic window and data recorded in real time.

The study was limited to marker movement at the femur for low acceleration movements. Femoral marker movement was studied since it is significantly larger than that at the tibia. Low accelerations were investigated since the eventual goal of the research is to obtain accurate low acceleration knee kinematics to predict mechanical loading of prosthetic ligaments.

Fluoroscopic images were later digitized via a frame grabber on an IRIS Indigo Elan on which a MATLAB program was developed to calculate the relative movements between marker and bone.

Dynamic knee flexions were performed over two to three seconds per flexion and the data registered at 30 frames per second. Therefore, this method allows skin movement to be recorded during desired active movements since acquisition frequency is well over three times that of the measured movement.

To obtain accurate quantitative skin movement data from fluoroscopy, rigorous reference axes must be defined in the knee image and both the effects of magnification and the three-dimensional (3D) nature of knee movement must be taken into account.

2.5.2 Definition of reference axes

The first step in obtaining accurate quantitative data of the movement of the markers is the definition of reliable reference axes in the medical image. Marker positions are defined with respect to an orthogonal set of axes fixed with respect to the bone. These axes are defined from a preliminary ML view of the femur, based on two anatomical landmarks: 1) the long axis of the femur, which defines the Z axis and 2) the "Blumensaat line" (Figure 2-2 a). The long axis of an imaged object has long been recognized as a very reliable reference and is often used in artificial vision for object orientation detection (Ullman, 1986;Ullman, 1989). The "Blumensaat" line is the projection of the intercondylar notch. Often used in X-ray radiographic measurements by clinicians, the "Blumensaat" line has been found to be a reliable reference for anatomical measurements in the knee (de Guise et al., 1993).
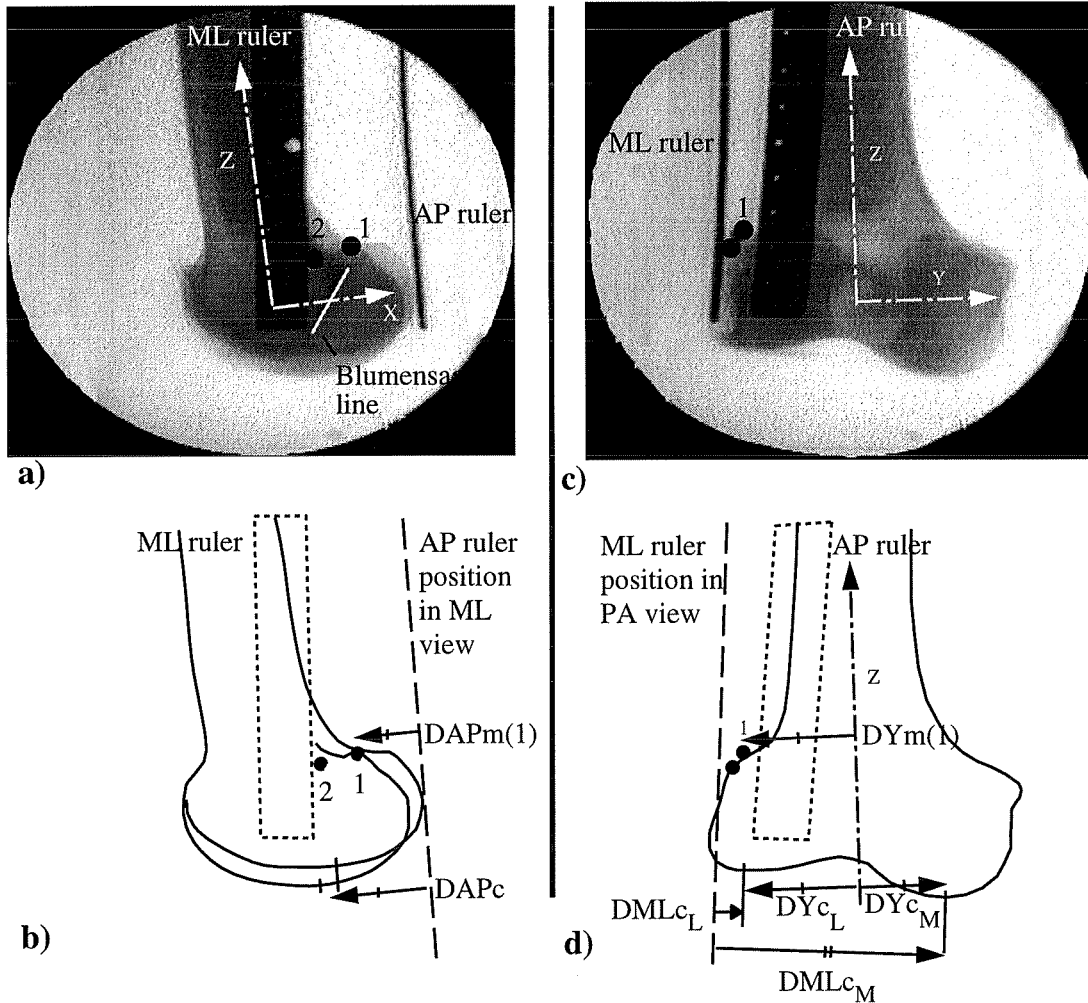
Figure 2–2 (left knee) Geometric parameters of knee and markers for model. X–ray projection of a femur, radio–opaque markers and calibration rulers taken from an a) ML and c) AP view. (b.d.) Distances measured from refererence rulers and from bone axes are used in the model to take into account magnification and 3D geometry respectively.

The center of the "Blumensaat" line is used to define a point on the **X** axis, which is perpendicular to the **Z**-axis, and the intersection of the **X** and **Z** axes defines the origin. The **Y** axis is defined as the cross product of the **Z** and **X** axes. In the AP view, the **Z** axis is again defined as the long axis of the femur (Figure 2-2 c,d) and the **Y** axis is perpendicular to the **Z** axis with the origin at the center of the AP projection of the intercondylar notch.

For the reference axes **X** and **Z** to be accurate, their position should be reproducible regardless of the three dimensional viewpoint of the bone. The **Z** axis corresponds to the midline of the femoral shaft projection. Viewed from different angles, this line always physically corresponds approximately to the projection of the three-dimensional (3D) midline of the femoral shaft. The "Blumensaat" line, used to define the axes' origin and the orientation of the **X** axis, corresponds to the midline of the projection of the roof of the intercondylar notch. Since a part of the roof is approximately a slanted two dimensional (2D) plane, the angle between the Blumensaat line and the **Z** axis changes with femoral axial rotation and ab-adduction. Choosing either end of this line as a reference would cause the reference position to change with different viewpoints since the length of the Blumensaat line would appear to change. For this reason, only the center of the Blumensaat line is used to define the origin and orientation of the **X** axis.

Since both axes are formed from projections of anatomical landmarks physically located in the sagittal plane of the knee, rotation about these **Z** and **X** axes corresponds to femoral and axial rotation and ab-adduction respectively.

These reference axes are defined for each assumed position of the knee. Radio-opaque skin marker position, recorded during active knee flexions, is measured with respect to these axes.

2.5.3 Correction of the image for magnification and perspective error

Fluoroscopic images are the 2D projections of the X-ray attenuation of a 3D geometry. During the X-ray projection, the 3D geometry undergoes magnification and perspective transformations. As a result, the X-ray projection of marker position relative to bone position is a function of both bone position (due to X-ray magnification) and bone orientation (due to the two dimensional X-ray projection of a three dimensional structure). A model was developed to consider both magnification and orientation of the bone when performing marker movement measurements.

Without orientation corrections, a marker's position which is fixed with respect to the bone, would appear to move with respect to the defined **Z** and **X** axes of the bone if the bone's orientation were changed. Three-dimensional bone orientation changes during active knee flexion due to both femoral axial rotation and ab-adduction rotations. It is therefore necessary to correct 2D measurements of marker movement for 3D bone orientation so that pure bone rotations do not cause marker translations in the measurements.

Magnification of the image occurs since X-rays forming the fluoroscopic image originate from a point source. Therefore, magnification of the knee's image increases as the knee approaches the X-ray source. A calibration device, consisting of two radio-opaque rulers placed at different distances from the X-ray source and at a known fixed distance from one another was used to calculate the slope of the magnification which is termed **slope$_{mag}$**.

To correct measurements for magnification, radio-opaque rulers were placed in both AP and ML views to find respective reference magnifications, **magAP$_{ruler}$** and **magML$_{ruler}$** (Figure 2-2). Magnification of each ruler was calculated by digitizing the distance

between the ruler gratings (in pixels) and dividing this value by the real grating spacing. These rulers were placed perpendicular to one another, corresponding to the AP and ML planes respectively, so that the magnification at any depth and viewpoint from the X-ray source could be calculated. In the AP view, since the rulers are perpendicular to one another, only the gratings of the AP ruler are visible to define a reference AP magnification. The projection of the ML ruler, seen from its side, defines a reference *position* in the AP view. Similarly, in the ML view, the gratings of the ML ruler are visible allowing definition of a reference ML magnification, and the position of the AP ruler in the ML view serves as a reference *position*. The reference magnifications and positions from each of the AP and ML views are combined in the model to correct images for magnification.

2.5.4 Geometric parameters

Several model parameters, reflecting the geometrical relationships between the bone and marker positions, were obtained from a single static ML view (Figure 2-2a) and a single static AP view (Figure 2-2c). These geometric parameters adjust the model for different subjects and marker configurations. Measurements of these parameters are detailed in Annex B.

2.5.5 Movement parameters

Once the geometric relationships were defined from both AP and ML views, raw marker position was digitized during active knee flexions with respect to the defined bone axes. With respect to these axes, marker position x and y components **Pmx, Pmz** respectively, were digitized at approximately every 10 to 15 degrees over 0 to 65 degrees of knee
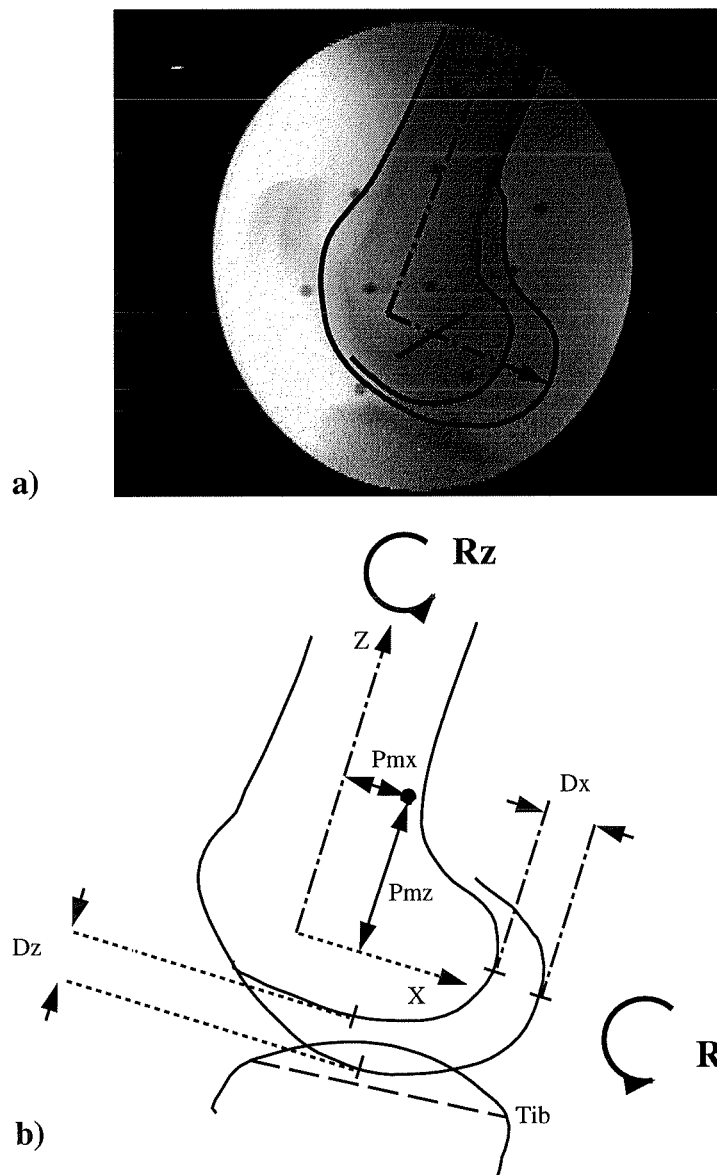
Figure 2–3 Fluoroscopic digitization of marker position (Pmx, Pmz), rotation correction parameters (Dx, Dz) and flexion angle during active knee flexion for one movement frame. Marker position (Pmx, Pmz) is tracked with respect to the Z and X bone axes. Distance between posterior and distal condyles, Dx and Dz (below), are used by the model to take into account the three–dimensional (3D) rotations of the knee (Rx and Rz).

flexion (Figure 2-3). Knee flexion angles were defined by the angle between the **Z** axis and the tibial axis **Tib.** The **Tib** axis is defined by tracing the average projection of the medial and lateral tibial plateau. The distance between posterior condyles **Dx** and distal condyles **Dz** were digitized on these images to correct for both femoral axial rotation and ab-adduction rotation respectively (Figure 2-3).

2.5.6 Correction for magnification

The aforementioned parameters employ a capital first character, for example "**Pmx, Pmz, Dx, Dz**", to indicate that they are digitized values in pixels, not real distances in mm. These pixel values are converted into mm via a magnification correction procedure. Once converted into mm, a lowercase first character is employed in the variable name, for example "**dx**". The nomenclature of other variables is composed of descriptive components which are detailed in Annex A.

The magnification correction procedure, detailed in Annex C, calculates **pmx** and **pmz**, the displacement in mm of the markers with respect to the bone-fixed axes during knee flexion. Once corrected for magnification, these raw position values must then be corrected for the bone's orientation in space.

2.5.7 Correction for bone orientation

When an ab-adduction in the knee occurs, the projected distance between the distal condyles **dz** changes (Figure 2-3). Figure 2-4 shows an AP view of the bone during knee flexion. This viewpoint is not acquired in the protocol during active knee flexion, but serves here simply for illustrative purposes. In this figure, it can be seen how the projected

distance between the distal condyles is used to estimate the ab-adduction rotation of the bone from a ML viewpoint.
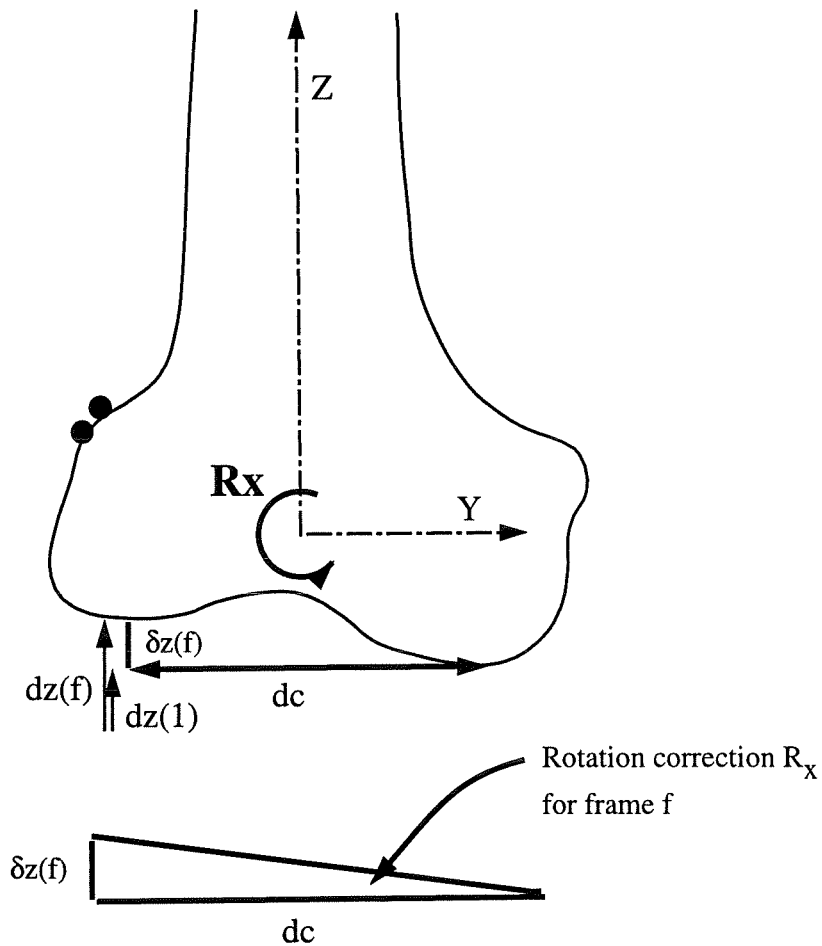
Figure 2-4 Correction for bone orientation. $\delta z(f)$ is the change in projected distance between the distal condyles between the reference ML projection and some image frame f. The triangle formed by this distance and the inter-condylar distance dc (below) allows calculation of bone rotation about the X-axis (Rx).

The first ML image frame of the active movement serves as a reference position, with **dz(1)** serving as a reference distance between the ML projection of the distal condyles. For an image frame **f**, the distance between the distal condyles is **dz(f)**. In Figure 2-4, one can see that the rotation angle **Rx** about the X-axis on an image frame **f** can be found through the triangle formed by the distance between the distal condyles, **dc,** and the difference between **dz(1)**, and **dz(f)** termed **dz(f)**. The rotation about the X-axis at frame f, **Rx(f)**, is therefore calculated by:

$$dc = dYc_M + dYc_L \tag{1}$$

$$\delta z'(f) = Dz(1) - Dz(f) \tag{2}$$

$$\delta z(f) = \frac{\delta z'(f)}{magML_{avgc}} \tag{3}$$

$$Rx(f) = \arctan\left(\frac{\delta z(f)}{dc}\right) \tag{4}$$

where **dYc$_M$**, **dYc$_L$** are the distances between the Z-axis and the medial and lateral condyles respectively (see Annex B), **dc** is the total distance between the distal condyles, **magML$_{avgc}$** is the magnification correction factor (see Annex C) and **dz'(f)** is the change in distal condyle projection for frame **f** measured in pixels. For a left knee, the signs of the right hand side of 2 are changed.

Similarly, when a femoral axial rotation occurs, the projected distance between the posterior condyles **dx** changes. The rotation of the bone at frame **f**, **Rz(f)**, can therefore be found by:

$$\delta x'(f) = Dx(1) - Dx(f) \tag{5}$$

$$\delta x(f) = \frac{\delta x'(f)}{magML_{avgc}} \tag{6}$$

$$Rz(f) = -\arctan\left(\frac{\delta x(f)}{dc}\right) \tag{7}$$

where **dx'** is the change in posterior condyle distance at frame **f** measured in pixels. For a left knee, the signs of the right hand side of 5 are changed.

These rotations are then applied to the marker positions to take into account the three dimensional orientation of the bone in the measurement. The corrections in the **Z** and **X** directions are respectively:

$$corrz(f, i) = dYm(i) \times \left(\frac{\delta Z(f)}{dc}\right) \tag{8}$$

$$corrx(f, i) = dYm(i) \times \left(-\frac{\delta x(f)}{dc}\right) \tag{9}$$

These correction factors become less accurate the further the markers are placed proximally on the femur. The markers in this study are, however, at most placed about 10cm proximally to the femoral condyles.

The fully corrected (for both magnification and bone orientation) positions **px** and **pz** are then defined as:

$$px(1, i) = pmx(1, i) \tag{10}$$

$$pz(1, i) = pmz(1, i) \tag{11}$$

$$px(f, i) = pmx(f, i) - corrx(f, i) \qquad (12)$$

Equations 12 and 12 consider that the subject faces the X-ray source during the reference AP images. For reference AP images taken with the subjects facing away from the source, **corrx** is added and **corrz** subtracted to **pmx** and **pmz** in these respective equations.

$$pz(f, i) = pmz(f, i) + corrz(f, i) \qquad (13)$$

2.5.8 Experimental verification of the model

To test the validity of the method to accurately track 3D bone movement from 2D projections, a cadaveric bone was used. A mechanism was constructed to accurately rotate the bone through various known values of axial rotation and ab-adduction while the fluoroscopic projection of the bone was registered. Since an important assumption of the model was that the parameters **dx** and **dz** reflected femoral axial rotation and ab-adduction, it was first verified that the parameters **dx** and **dz** had a linear relationship with these respective rotations. Unrealistically large rotations were applied to the bone in order to investigate the range of rotation over which the parameters **dx** and **dz** varied linearly with bone rotation.

Once this linearity was verified, the accuracy of the method to track marker movement was evaluated. Two radiopaque markers were fixed on the surface of the lateral condyle of the cadaveric bone which was rotated through various known angles. The registered data was then digitized and corrected, according to the model, for both bone magnification and orientation. Since the markers were physically fixed with respect to the bone, the marker positions corrected by the model were to remain stationary with respect to the defined axes for any bone position or orientation. Therefore, the error in the correction method could be estimated by the error in reproducing a stationary marker

position for several bone positions and orientations. Once again, large rotation values were applied to investigate the limits of the correction method as well as its behaviour near these limits.

Errors in marker position measurement are expressed in terms of a standard error definition which estimates error as the displacement of a marker with respect to its mean position. This error has been termed the "Position Artifact Standard Error" (or PASE), however we will refer to this quantity as RMSd, as previously notated (Cappozzo et al., 1993). Letting x_i and y_i be the components of marker position 'i', the RMSd error of this set of n marker positions is defined as:

$$RMSd = \frac{\left[\sum_{1}^{n}(x_i - \bar{x})^2 + (y_i - \bar{y})^2\right]^{1/2}}{(n-1)^{1/2}}$$

(14)

where the measurement error is estimated as the difference between the position x_i and the mean position of x:

$$\bar{x} = \frac{1}{n}\sum_{i=1}^{n} x_i$$

(15)

The mean position of y is calculated in a similar fashion.

The RMSd definition was also employed in this study to quantify movement of markers with respect to bone. Marker movement is expressed as the rms distance between the positions of a skin marker over several flexion angles and the mean position of that marker during this movement. Therefore skin movement data of this study can be expressed in RMSd with and error of the measurement method also expressed in RMSd. Throughout this article, values expressed in mm rms imply that these values have been calculated via the above RMSd definition.

Although the RMSd displacement is a compact way of representing a three dimensional displacement, the physical interpretation of the RMSd movement is difficult. For this reason, the maximum range of displacement of each marker, Dx along the X-axis and Dz along the Z-axis, is also reported.

2.5.9 Application of the method

Three healthy male subjects were tested. Markers were first placed over several regions of the lateral condyle. The reference static AP and ML images were first obtained to define the geometric parameters required by the model. The subject was then asked to lift the heal of the marked leg off the ground towards the buttock, repeatedly flexing the knee over a range of approximately 65 degrees over 3 cycles. Although this movement did not accurately reproduce the loaded cycle of walking or running, it was similar to the swing phase of gait. Furthermore, this movement was easy to produce while keeping the knee within the fluoroscopic window. Data was digitized onto computer then corrected for both magnification and bone orientation according to the model and the skin movement data analyzed. Each data set was digitized and treated according to the model three times to investigate the repeatability of the results and to reduce the rms error of the method. The skin movement data was then projected onto the initial flexion image of the knee in extension (reference position), to help in the physical interpretation of the skin movement results. This procedure was then repeated on the medial aspect of the knee.

2.6 Results

2.6.1 Model verification

In Figure 2-5a one can see the relationship between axial bone rotation (about the **Z** axis) and both the model parameters **dx** and **dz**. Figure 2-5b shows the relationship between ab-adduction bone rotation (about the **X** axis) and the model parameters **dx** and **dz**. From these experiments, it was seen that the parameter **dx** varies quite linearly (correlation > 0.98) with axial bone rotation, over **Rz** ± 15 degrees, with a small linear change in **dz** over the same range (Figure 2-5a). Similarly, the parameter **dz** varies quite linearly with ab-adduction, -9 <**Rx**<+15 degrees, with a small change in **dx** over this range (Figure 2-5b). The linearity of these parameters with bone rotation suggested that they could be used in a model to accurately reflect the bone's orientation.

Correction of the marker positions via the model for rotations of the specimen about its Z-axis -15<**Rz**<15 deg., can be seen in Figure 2-6a. Similarly corrected marker position can be seen for ad-abduction -9 <**Rx**<+15 degrees (Figure 2-6b), and a combined rotations, **Rz**=5, **Rx**=5 (Figure 2-6c) and **Rz**=10, **Rx**=10 (Figure 2-6d). Non corrected data, connected via a dashed line, indicates the "apparent marker movement", which would be observed without the bone orientation corrections.
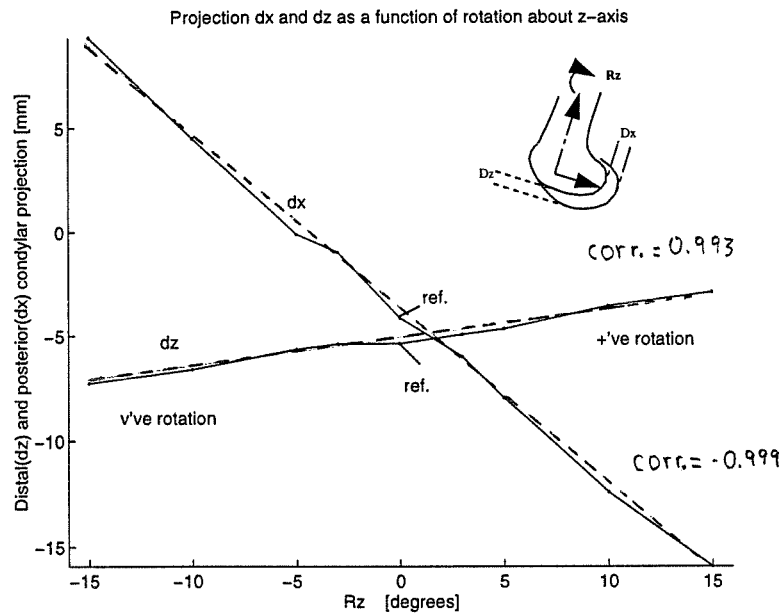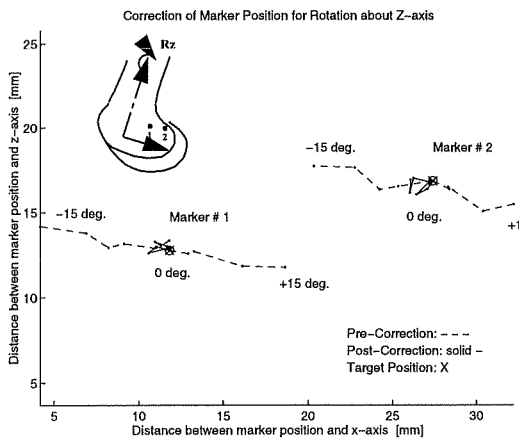
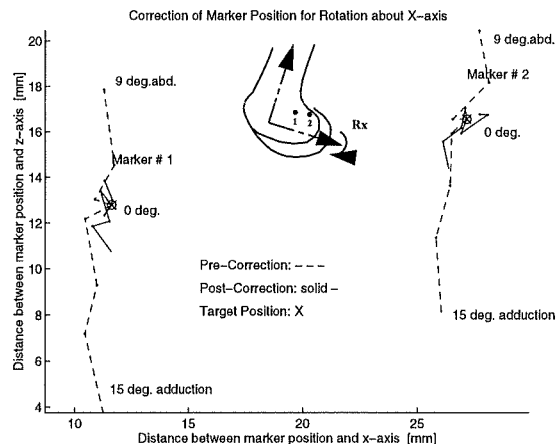a) **Model parameters vs rotation about the Z–axis**
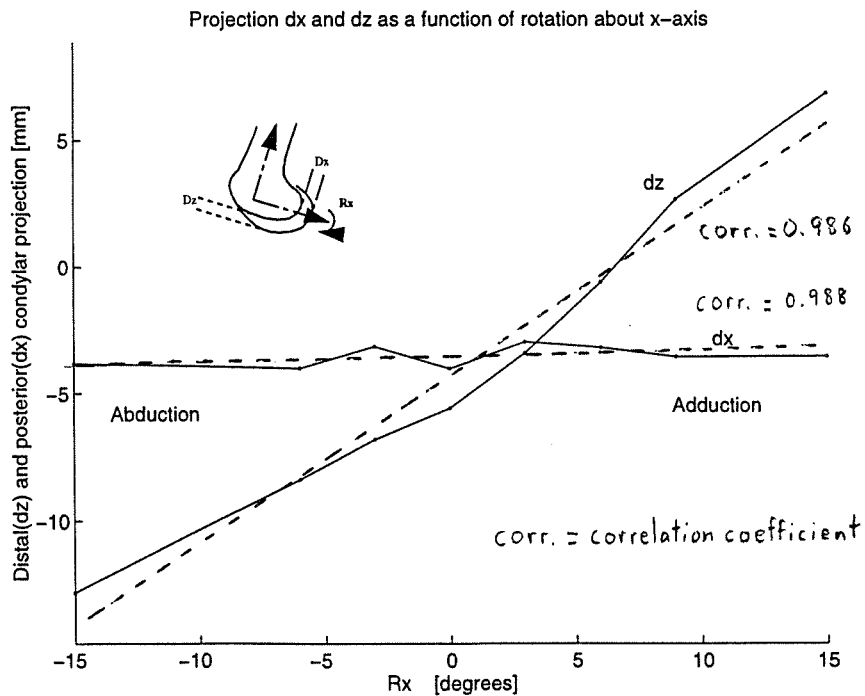
b) **Model parameters vs rotation about the X–axis**

Figure 2-5 a) Model parameters vs rotation about the Z-axis. b) Model parameters vs rotation about the X-axis.
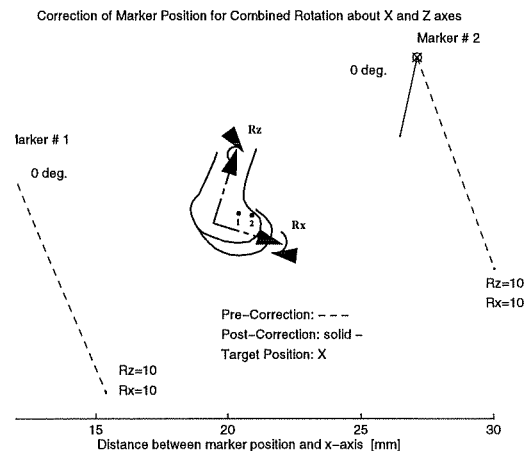
a) Correction for rotation about Z–axis

b) Correction for rotation about X–axis
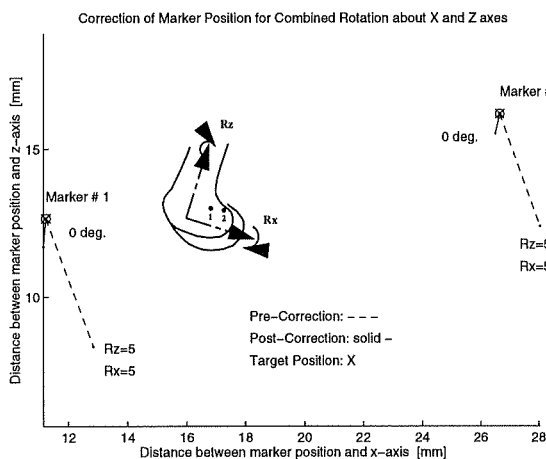
c) Correction for combined rotation

d) Correction for combined rotation

Figure 2–6 a) Correction for rotation about the Z–axis. b) Correction for rotation about the X–axis. c) Correction for combined (typical) rotation. d) Correction for combined (large) rotation.

Data points corrected by the model for bone position and magnification are interconnected via a solid line. The distance between these corrected points, and the original marker positions, which are indicated by "0 deg.", is the error in this method since a perfect correction would map all these points onto the same point.

Table 2-1 Error of model as function of different bone orientations

Rotation	Range of rotation (degrees)	RMSd (mm RMS)	Dx (mm)	Dz (mm)
Rotation about Z axis	-15 < Rz < +15 (maximum error)	0.79	2.12	1.29
	-5 < Rz < 5 (typical error)	0.64	1.75	0.99
Rotation about X axis	-8< Rx < +8 (maximum error)	0.78	0.90	2.66
	-3 < Rx < +3 (typical error)	0.30	0.22	0.84
Combined Rotation	Rx=10, Rz=10 (maximum error)	1.08	0.40	3.14
	Rx= 5, Rz= 5 (typical error)	0.28	0.12	0.81

Table 2-1 summarizes the RMSd values for both maximal rotation values and typical rotation values for rotation about the Z-axis, X-axis and a combined rotation. It can be seen that for large rotation values about the Z axis,-15 <Rz<+15 deg., maximal error of the method is of the order of 0.8 mm rms (Dx = 2.1 mm and Dz = 1.3 mm). For femoral axial rotations -5 <Rz<+5 commonly seen during knee flexion, the correction error is of the order of 0.6 mm rms (Dx = 1.8 mm and Dz = 1.0 mm). Similarly, for large ab-adduction rotations about the X axis, -8 <Rx<+8 deg., maximal error is of the order of 0.8

mm rms and typical error, for -3 <Rx<+3 deg., is of the order of 0.3 mm rms. For the large combined rotation, **Rx**=10, **Rz**=10 degrees, the error in the correction is of the order of 1.1 mm rms (Dx = 0.4 mm and Dz = 3.1 mm). For the typical combined rotation, **Rx**=5, **Rz**=5 degrees, the error in the correction is of the order of 0.3 mm rms (Dx = 0.1 mm and Dz = 0.8 mm). It was found that the rms errors of the method was reduced by averaging data over three trials.

To quantify model performance over large knee rotation values, RMSd values of marker position error are plotted vs. applied rotations about the X, Z axes (Figure 2-7). For adduction rotation about the X-axis, rms error increased quite linearly with applied rotation (Figure 2-7a). For abduction rotation about the X-axis, rms error increased quickly over the first 3 degrees, then increased slowly from 3 to 9 degrees (Figure 2-7b). For rotation about the Z-axis, rms error increased quickly over the first 5 degrees, then increasing slowly from 5 to 15 degrees (Figure 2-7c).

2.6.2 Measurement of skin movement relative to bone

Lateral and medial marker movement for active "heel raised to buttock" knee flexions can be seen for all subjects in Figure 2-8 and Figure 2-9 respectively. Subsequent marker positions are projected onto the 1st image of the knee at 0 degrees knee flexion and interconnected by lines to show the path of their movement. Averaging data over three digitizations resulted in smoother movement curves. There appeared, however, several small irregularities in the movement data which did not disappear when the data over three trials was averaged.
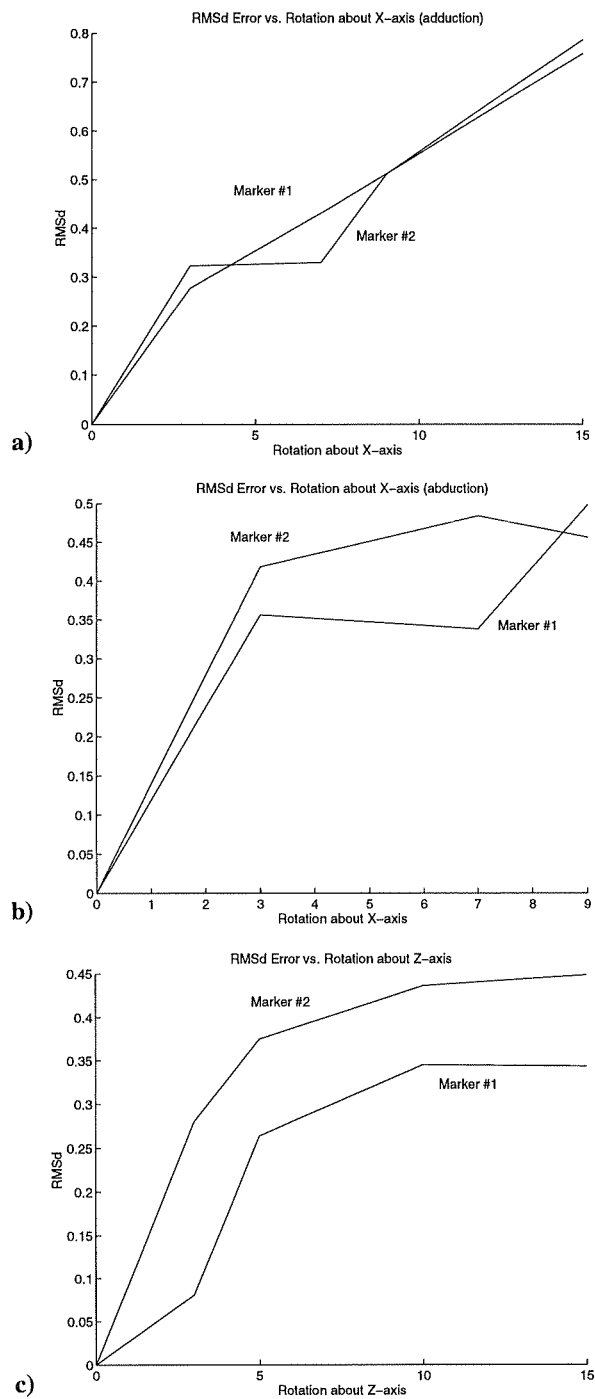
Figure 2–7 a) Error in model as a function of rotation about the X–axis. b) Error in model as a function of rotation about the Y–axis. c) Error in model as a function of rotation about the Z–axis.

a)   subjet #1

b)   subjet #2

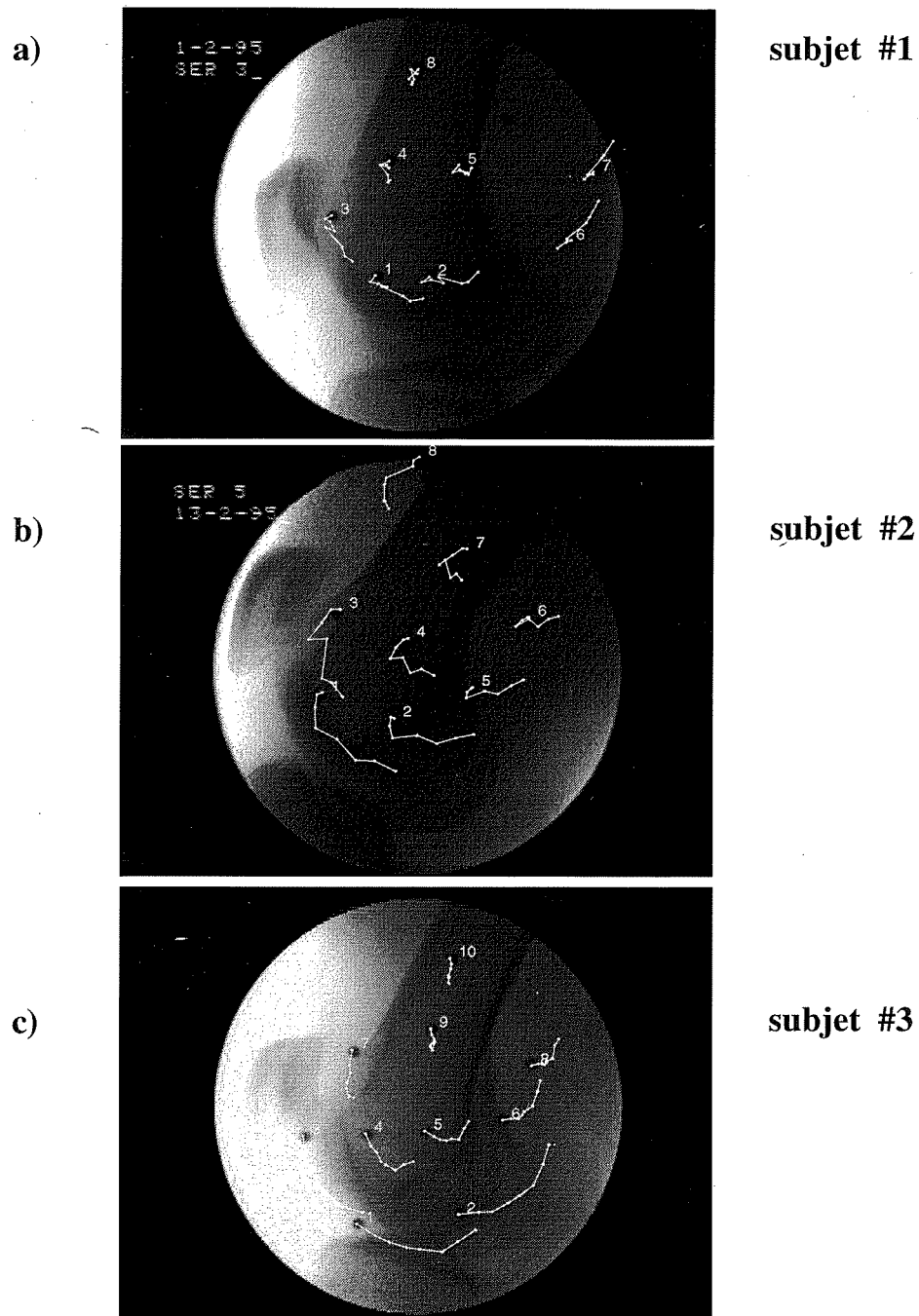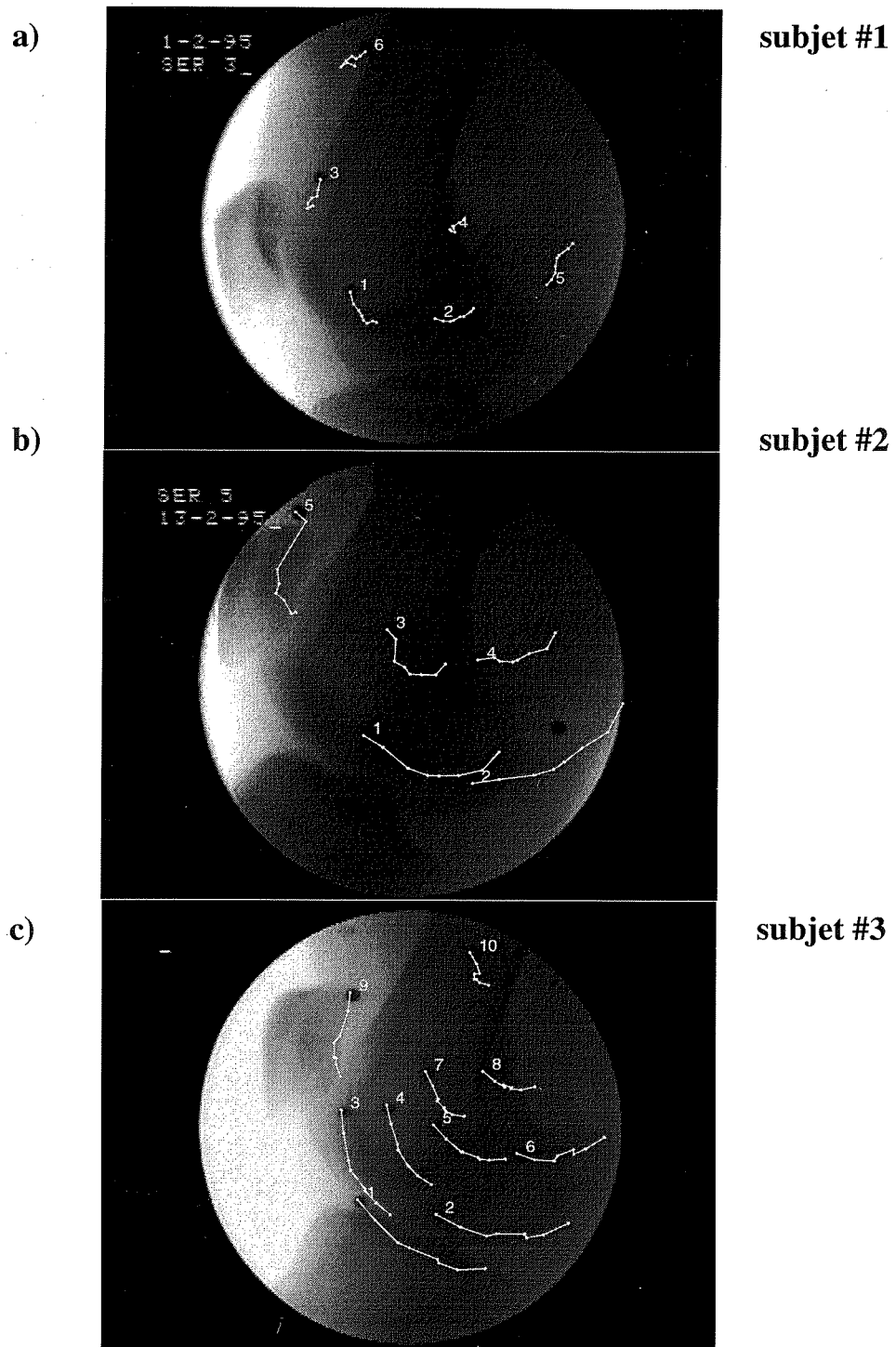c)   subjet #3

Figure 2–8 Movement of lateral skin–mounted markers with respect to the underlying bone during active knee flexion.

Figure 2–9 Movement of medial skin–mounted markers with respect to the underlying bone during active knee flexion.

Marker movement varied from 2.5 mm rms to 17 mm rms. The largest marker movements occurred when markers were placed on the joint line. These distally placed markers appeared to rotate in the sagittal plane about a point approximately 4 cm proximal to the joint line. The largest maximal range of lateral marker movement was for marker #1 on subject #3 with Dx= 42.5 mm and Dz= 20 mm (see Table 2-2). The order of magnitude of movement from subjects 2 and 3 was similar but larger than that of subject 1, despite the fact that the subjects' sizes did not vary greatly.

Table 2-2 RSMSd values of lateral marker movement on subjects

Marker #	1	2	3	4	5	6	7	8	9	10
Subject #1										
RMSd	8.90	9.13	8.02	3.47	2.93	8.72	6.57	2.58		
Dx	23.57	21.53	17.07	6.15	6.92	9.90	6.23	3.19		
Dz	3.19	12.92	12.92	7.80	4.45	23.31	15.09	6.31		
Subject #2										
RMSd	16.59	13.85	12.89	7.61	9.01	5.86	5.87	9.45		
Dx	41.6	31.22	22.34	18.21	16.44	12.31	10.63	6.89		
Dz	12.21	19.74	24.73	9.37	18.37	12.63	12.28	12.10		
Subject #3										
RMSd	16.77	15.40	12.57	7.78	6.51	7.18	6.03	4.96	2.47	2.86
Dx	42.51	21.33	33.19	21.37	13.79	8.02	8.24	6.13	4.15	3.67
Dz	20.60	33.27	14.35	6.13	11.20	19.08	14.93	13.20	6.19	7.73

For quantitative interpretation of the results, the reader is referred to Table 2-2, since data displayed on the bone is subject to variations in magnification and orientation depending on the positioning of the subject during the image acquisition.

Medial marker movement for all subjects varied from 2 to 17 mm rms. The largest movements were of the order of 15 to 17 mm rms for example marker #1 subject #3 (Dx= 44mm, Dz= 5mm) (see Table 2-3). Marker movement did, however, vary between subjects in both magnitude and direction. Subjects 2 and 3 had similarly large marker movements, as was the case on the lateral aspect, compared to subject #1 which had smaller movements. Marker movement of subject #3 tended to be much more posterior than the other two subjects.

Table 2-3 RMSd values of medial marker movement on subjects

Marker #	1	2	3	4	5	6	7	8	9	10
Subject #1										
RMSd	4.70	5.03	3.52	2.15	5.53	3.26				
Dx	12.20	11.78	2.33	3.72	4.01	6.26				
Dz	6.80	8.11	10.03	4.94	15.47	7.57				
Subject #2										
RMSd	14.95	17.12	7.80	8.41	10.83					
Dx	38.83	31.03	20.02	17.84	12.01					
Dz	16.41	39.21	7.34	16.99	24.34					
Subject #3										
RMSd	15.40	14.13	11.50	8.37	8.20	8.81	5.85	5.24	8.54	3.57
Dx	43.80	38.13	24.34	20.78	23.70	22.65	15.56	16.42	5.95	8.91
Dz	4.95	13.60	22.01	15.36	2.53	13.95	7.38	1.21	24.00	6.82

2.7 Discussion

2.7.1 Validation of the model

The cadaveric bone tests revealed an approximately linear (correlation > 0.98) and repeatable relationship between the model parameters **dx** and **dz** and rotations about the Z and X axes respectively. These results indicate that the **dx** and **dz** were reliable parameters to be used to track bone rotation in the model (see Figure 2-5).

By placing a marker in a fixed position with respect to the cadaveric bone, it was possible to evaluate the algorithm's accuracy in correcting data for both bone orientation and magnification. For typical movements and even for movements involving large rotations (10 to 15 degrees) about the X and Z axes, measurement error is smaller than 1mm rms Therefore the method accuracy is sufficient to accurately measure skin movement which is typically of the order of 5 to 15 mm rms. Furthermore, the validation study shows that, at the knee, the fluoroscopic technique is as accurate as intrusive techniques previously used to quantify skin movement at the knee (Lafortune, 1984;Cappozzo et al., in press).

By averaging data over several trials, rms error was reduced, indicating that there exists a component of random error in the method. The remaining error, inferior to 1mm rms, is a systematic error which was found through a sensitivity analysis to be mostly due to the difficulty in defining consistent reference axes on the bone.

2.7.2 Skin movement measurements

Small irregularities in the marker movement curves, even after averaging three digitizations, could be due to small systematic errors in the method. However, such

irregularities may in part arise from the diminished image contrast in live subjects since the irregularities were not as apparent during the cadaveric tests. This lower contrast could make identification of bone axes and condylar projections more difficult. It was also observed that for the slow movements studied, the subjects' muscles tended to "twitch" while controlling the movement. The small irregularities were less than one tenth the magnitude of marker movement, therefore they did not hinder interpretation of the data.

Skin movement varied significantly with marker position. Therefore, careful placement of surface markers can significantly reduce acquisition error of the underlying kinematics. By displacing the marker by about 2 cm in the condylar region, error due to marker movement can double. For example on the lateral side of subject #3, marker #5 moved by 7 mm rms whereas marker #1, placed approximately 2 cm distally, moved 15 mm rms (See Table 2-3). Such variance of marker movement with position was also true for markers placed on the medial side of the knee.

The direction of both medial and lateral skin movement can be explained in terms of the biomechanics of knee movement (see Figure 2-8, p. 52 and Figure 2-9, p. 52). The large movements of distally placed (on the joint line) markers can be explained by the posterior movement of the tibia with respect to the femur. The distal movement of anteriorly placed markers can be explained by the elongation of soft tissue (e.g. muscle) to enable the flexion of the tibia. The proximal movement of posteriorly placed markers can be explained by the contraction of soft tissue (e.g. of muscle) to enable tibial flexion. The posterior component of almost all markers in the condylar region indicates that the soft tissue is being stretched over the front of the knee and pulled towards the back of the knee during flexion. These observations shed light on the mechanisms by which marker movement is related to joint angle.

Even though general tendencies were found in the direction of marker movement, the magnitude of these movements varied significantly between subjects. The direction of the movement was also subject to variability, especially for markers on the medial aspect of the knee. Such findings do not encourage mathematical correction of marker position through modeling.

The importance of the correction method was seen by comparing marker movement with and without model corrections. For example, without corrections, the maximum range of skin movement of lateral markers 1 and 2 of subject #1 would have been underestimated by 10 mm.

The order of magnitude of skin movement in this study was similar to those found in the literature, however, comparison of the results is difficult because of the limited amount of subjects in all studies and the different ways in which skin movement was quantified. Previous studies have measured relative movement between surface markers (Macleod & Morris, 1987), used fluoroscopy without correction for three-dimensional bone orientation (Lafortune, 1984;Cappozzo et al., in press), and used invasive bone pins which reduced skin movement over the lateral condyle in some cases (Cappozzo et al., in press).

From the results of the present study, it can be seen to which point skin movement is often the largest source of error in movement analysis in the knee. It has been seen that skin can move D_x = 4 to 44 mm and D_z = 4 to 20 mm (or 2 to 17 mm RMSd) during active movements. Comparing this to the error in standard motion analysis systems, which is of the order of 1 mm rms, one can appreciate that skin movement error is by far the largest source of error in obtaining knee kinematics. Therefore, to improve the accuracy of acquisition methods, one should take steps towards reducing this large source of error. Furthermore, since skin movement is such a dominant error, motion analysis

equipment which is accurate to the order of millimeters is often overkill. Ironically, expensive motion analysis equipment is often purchased because of its accuracy which is often unnecessary since skin movement artifacts are such a dominant error.

Our method differs from those found in the literature. Previous attempts to evaluate skin movement via fluoroscopy were qualitative since rigorous definition of reference axes and correction for bone orientation and magnification were not elaborated (Cappozzo et al., 1993;Lafortune & Lake, 1991). Torzilli *et al.* (1981) used an X-ray method to measure AP laxity in the knee. They found a relationship between projected distances of bone landmarks and bone rotation which they used to correct X-ray measurements of A-P laxity in the knee. Their approach was to directly relate these parameters to the laxity values through a quadratic relationship which was obtained through statistical analysis of several human bone specimen. This differs from the present approach which explicitly calculates bone rotation of each individual knee to correct marker position for three-dimensional bone orientation.

2.7.3 Other applications of the method

Skin movement data found by the fluoroscopic method could help the choice of skin marker position for knee movement analysis. If skin movement error did not exist, placing a marker in proximity to the condyles would be best for measuring detailed condylar *displacements*. This is due to the fact that for a given error in marker (or sensor) position, error in the estimation of condylar position will increase the further this marker is placed from the region of interest. It has been seen, however, that skin movement increases as one approaches the condyles. Therefore, optimal marker placement is a compromise between distance from the region of interest and skin movement error as one approaches this region.

To avoid skin movement error which occurs near the condyles, one solution could be to place markers further from the joint line onto regions of the thigh. Spacing these markers can improve measurement accuracy of the orientation of the segment, however position accuracy is diminished due to the error amplification resulting from the distancing the markers from the region of interest. Such a solution could, however, be sufficient for certain gait analysis applications although Murphy (1990) and Cappozzo et al. (1995) have found that significant rotation error could still occur.

Markers placed on the medial side are hidden from conventional camera-based marker tracking equipment. It would however be possible to attach new motion tracking instrumentation not sensitive to this problem of "shadowing" onto such a medial attachment. Data must be obtained for other subjects before tendencies in skin movement can be generalized.

The non-intrusive nature of the method makes it conducive to further mathematical analysis of skin movement to reduce acquisition error. Having quantitative data on skin movement may make numerical correction of data obtained via surface markers possible. To accomplish this, skin movement for a large number of subjects must be obtained so that statistical correction factors can be derived for individuals of varying size and morphology. Although only three subjects were tested in this study, large variance in magnitude and direction of skin movement presents a challenge for mathematical marker position correction procedures. Modeling of marker movement requires marker positions which produce *consistent* movements between subjects. Therefore, marker placement should not only be chosen to reduce the relative skin-bone movement, but to remain relatively invariant for subjects of varying morphology (ex. fat vs. thin subjects). This implies that it may be advantageous to select marker positions where the movement is larger yet more constant between individuals.

Another way to reduce skin movement is to improve the physical attachment of markers non-invasively onto the underlying bone. The fluoroscopic method has been used to help place a recently developed mechanical device designed to physically reduce skin movement during data acquisition. The mechanical attachment device clamps non-invasively onto specific regions of the knee which have been observed to have both little soft tissue and little skin movement (Sati et al., 1993). Motion sensors are attached to the underlying bone by this attachment system to increase measurement accuracy. By placing radio-opaque markers in the attachment sites of this mechanical attachment device, it is possible to evaluate its movement with respect to the underlying bone in a similar fashion to the surface marker movement analyzed in this study. This method was employed to analyze several attachment designs to determine which best tracks the movement of the underlying bone.

Finally, the fluoroscopic method could be used to accurately measure three dimensional knee movement *in vivo*. The parameters **Rx** and **Rz** in the model indicate the knee's ab-adduction and femoral rotation respectively whereas knee flexion is the angle between the **Z** axis and the **Tib** axis. To report the relative rotations between femur and tibia would require physical attachment of reference markers onto the tibia. By attaching markers onto the bony anterior aspect of the tibia at its midshaft, little movement between these markers and the underlying bone occur (Sati et al., 1993). The method could be used to measure A-P as well as proximo-distal displacement between the femur and tibia, however, it would not permit measurement of medio-lateral displacement due to the fluoroscopic ML viewpoint. Such use of the fluoroscopic method would be interesting in an experimental environment to validate existing knee movement acquisition methods, yet it would not be practical as a clinical tool. Therefore, there remains an interest to use skin mounted marker movement data obtained in this study to improve present acquisition methods which are more practical for routine use.

2.8 Conclusions

Through the cadaveric study, the accuracy of the fluoroscopic method has been evaluated to be accurate below 1mm rms even for knee movements involving large rotations in all planes. This accuracy is slightly degraded when applied to live subjects since surrounding soft tissue reduces image contrast. Despite this reduced contrast and several assumptions of the model, the method is sufficiently accurate to report skin movement which has been found to vary from approximately 2 to 17 mm rms. A random error component in the method can be reduced by averaging data over several trials. The main source of the remaining systematic error component was found to be due to the difficulty in defining consistent reference axes on the bone images. The accuracy of the fluoroscopic method to evaluate skin movement at the knee is equivalent to that of previous intrusive techniques. Contrary to intrusive methods, the fluoroscopic method is more practical for extensive experimental analysis of marker movement at the knee.

Skin movement measured over several regions of both the medial and lateral sides of the knee were observed to vary from 2 to 17 mm rms (or $Dx = 4$ $Dz=4$ mm to $Dx = 44$ $Dz=20$ mm). Displacing the marker placement by 2 cm over the condylar region could double marker movement error.

This study illustrates to which point skin movement can be the largest source of error in knee movement analysis. Therefore, improving accuracy and acquisition methods of knee motion analysis requires an effort towards reducing this dominant error.

It is suggested that the data from this study be used to help improve acquisition methods. Skin movement data could be used to help mathematical correction procedures. Furthermore, data on both medial and lateral skin movement could help in the proper placement of knee ortheses or new mechanical sensor attachment devices which physically reduce movement between motion sensors and underlying bone. The fluoroscopic method is also being used to evaluate the accuracy with which these devices track bone movement to improve their design.

Finally, the accuracy of the method makes it possible to use as a research tool to measure detailed three dimensional knee kinematics without the need for tracking markers or other tracking instrumentation.

2.9 Acknowledgments

Annexes

2.9.1 Annex A: Explication of the nomenclature

Due to the multitude of measurement variables in this paper, variable names are comprised of three descriptive components. The first component indicates the type of variable, for example a distance or magnification. The second component indicates which view, AP or ML, the variable applies. The third component indicates what is measured, for example a marker position or a ruler magnification.

2.9.1.1 First component

Distance variables employ a capital first character, for example **Px**, to indicate that the value is measured in pixels. Once converted into real distance in mm, the variable name's first character is represented by a lowercase letter, for example **px**. Magnification variables start with the characters "mag".

2.9.1.2 Second Component

When distance is measured in the AP direction with respect to the AP reference position (the position of a ruler in the image), the letters "AP" follow the first character. Similarly for measurements in the ML directions, the characters "ML" follow the first character. If the characters AP or ML do not appear in a distance measurement, the measurement corresponds to one taken in the AP direction on an ML view. Distances measured along the axes defined on the bone, are indicated via that axes' name, for example "Y".

Magnification variables followed by the characters "AP" indicate that the magnification applies to an AP view. Similarly, the characters ML indicate that the magnification applies to an ML view.

2.9.1.3 Third Component

The characters in the third component are descriptive of the measured quantity. For example, for distances involving markers, the character "m" appears at the end of the variable name. Similarly "c" is used to indicate measurements of the condyles or "dc" for measurements involving the distal condyle, with optional subscripts "$_M$" or "$_L$" indicating medial or lateral condyles respectively. For example, the ML distance in mm between the reference ruler position and the medial condyle has the variable $\mathbf{dMLc_M}$. Similarly, the distance in pixels along the bone's Y axis to the i'th marker is termed $\mathbf{DYm(i)}$

The third component of magnification variables are subscripts describing to what object the magnification applies. For example the variable containing the magnification of the reference ruler in the ML view is $\mathbf{magML_{ruler}}$.

2.9.2 Annex B Geometric parameters of the model

Distance measured from the AP or ML rulers should be taken along a "horizontal line", which corresponds to the direction in which the magnification increases. To simplify matters, the $\mathbf{Z}$ axis should correspond approximately to the vertical directions in the ML view and AP view. In this way, one can approximate the "horizontal" direction to be perpendicular to the $\mathbf{Z}$ axis.

The ML view was used to measure the distance of markers and bone from the AP ruler position (Figure 2-2b):

DAPm(i) is the distance (or AP 'depth') in pixels perpendicular from the AP ruler to marker **i**

DAPc is the distance (or AP 'depth') in pixels perpendicular from the AP ruler to the average distal condyle. The average distal condyle is defined as the average position between the most distal point on the medial condyle and the most distal point on the lateral condyle.

The single AP view was used to measure parameters of bone geometry and marker position (Figure 2-2d):

DYm(i) is the distance in pixels along the 'Y'-axis, perpendicular from the Z axis to marker **i**.

DYc$_M$, DYc$_L$ are the distances in pixels, along the Y-axis perpendicular to the Z-axis, between the Z-axis and the most distal point of the medial and lateral condyles respectively.

The ML depth in pixels of the medial and lateral distal condyle from the ML ruler position was also digitized as **DMLc$_M$** and **DMLc$_L$** respectively, for magnification corrections.

2.9.3 Annex C: Magnification correction calculations

To find the true distance in mm between marker i and the Z-axis (Figure 2-2d), **dYm(i)**, the magnification in the plane of the marker must be known. From the ML reference image (Figure 2-2b), the distance of marker **i** from the AP ruler position is approximated as:

$$dAPm(i) = \frac{DAPm(i)}{magML_{ruler}}$$

$$(16)$$

In equation 16, one can use the magnification **magML_ruler** directly to calculate **dAPm** since the ML ruler is placed approximately in the same plane as the markers. Therefore, for marker movement on the medial side of the knee, the ML ruler is placed on the medial side. For measurement of marker movement on the lateral side, the ML ruler is placed on the lateral side of the knee. Generally, for measurements not physically near one of the reference rulers, one must first calculate the magnification in the plane of the measurement before calculating real distances.

Such a magnification calculation is required to estimate the distance **dYm**. Having calculated the depth **dAPm** of marker **i** from the AP ruler and knowing the slope of the magnification **slope_mag**, the AP magnification at the depth of marker **i**, termed **magAP_m(i)**, is calculated by:

$$magAP_m(i) = magAP_{ruler} + slope_{mag} \times dAPm(i)$$

$$(17)$$

Using this magnification, the real distance along the **Y** axis between marker **i** and the **Z** axis, **dYm(i)**, can be found:

$$dYm(i) = \frac{DYm(i)}{magAP_m(i)}$$

$$(18)$$

To find the true distance along the **Y** axis, between the distal condyles and the **Z** axis (Figure 2-2c, Figure 2-2 d), **dYc_M** and **dYc_L**, the magnification in the plane of the distal condyles must be found from the ML reference image (Figure 2-2a, Figure 2-2b). The real depth to the average distal condyle, is approximated as:

$$dAPc = \frac{DAPc}{magML_{ruler}}$$

$$(19)$$

In equation 19, to simplify the calculations, **magML$_{ruler}$** is used to approximate the magnification between the condyles. This approximation introduces a small error since the ML ruler is located near one of the condyles, not at the center of the condyles.

Knowing this distance and the slope of the magnification **slope$_{mag}$**, the AP magnification at the depth of the distal condyle, **magAP$_{dc}$**, is calculated to find the real distance **dYc$_M$** and **dYc$_L$** in mm:

$$magAP_{dc} = magAP_{ruler} + slope_{mag} \ x \ dAPc \qquad (20)$$

$$dYc_M = \frac{DYc_M}{magAP_{dc}} \qquad (21)$$

$$dYc_L = \frac{DYc_L}{magAP_{dc}} \qquad (22)$$

Once the static parameters have been calculated, values measured during active knee flexion (Figure 2-3) are corrected for image magnification for each image frame **f**. To correct measured distance between both the distal and posterior condylar projection, **Dz(f)** and **Dx(f)** respectively (Figure 2-3), the magnification of the "average condyle" **magML$_{avgc}$** is calculated. The "average condyle" magnification **magML$_{avgc}$** is defined as the average magnification between the medial and lateral condyles as seen in an ML view. From the depth of both medial and lateral condyles, **dMLc$_M$** and **dMLc$_L$**, and the slope of the magnification, the magnification at the average condyle **magML$_{avgc}$** is calculated:

$$dMLc_M = \frac{DMLc_M}{magAP_{DC}} \qquad (23)$$

$$dMLc_L = \frac{DMLc_L}{magAP_{DC}} \qquad (24)$$

$$magML_{avgc} = magML_{ruler} + slope_{mag} \ x \left(\frac{dMLc_M + dMLc_L}{2} \right) \qquad (25)$$

This magnification is used to correct the projected distance between the distal and posterior condyles $Dz(f)$ and $Dx(f)$ respectively for each image frame f:

$$dx(f) = \frac{Dx(f)}{magML_{avgc}}$$

(26)

$$dz(f) = \frac{Dz(f)}{magML_{avgc}}$$

(27)

where dx and dz are the projected distance between the distal and posterior condyles in mm.

The x and z components of marker position with respect to the bone axes, Pmx and Pmz, are corrected for magnification by:

$$pmx(f,i) = \frac{Pmx(f,i)}{magML_{ruler}}$$

(28)

$$pmz(f,i) = \frac{Pmz(f,i)}{magML_{ruler}}$$

(29)

where $magML_{ruler}$ is an accurate magnification since the ML ruler is placed in the same AP plane as the markers. Once corrected for magnification, the x and z components of marker position, pmx and pmz, are corrected for bone orientation.

CHAPTER III

3. ARTICLE #2: IMPROVING *IN VIVO* KNEE KINEMATIC MEASUREMENTS: APPLICATION TO PROSTHETIC LIGAMENT ANALYSIS

3.1 Situation of article in thesis

The first article, presented in Chapter 2, has highlighted the need to reduce skin movement errors to obtain accurate *in vivo* knee movement measurements. The quantitative data in this previous chapter provides basic skin movement data which is used in this article to develop an improved knee measurement method.

Possible complications associated with invasive methods has lead to the design of a device which reduces skin movement non-invasively. The fluoroscopic method presented in Chapter II is used in this chapter to evaluate the accuracy with which this new

mechanism tracks underlying bone movement. It is then evaluated whether it is feasible to predict prosthetic ligament deformations *in vivo* given this error. Feasibility of predicting prosthetic ligament deformations given this *in vivo* error is then evaluated.

IMPROVING *IN VIVO* KNEE KINEMATIC MEASUREMENTS: APPLICATION TO PROSTHETIC LIGAMENT ANALYSIS

Sati M.[0], de Guise J.A.[*], Larouche S.[0] and Drouin G.[0]

[0] Biomedical Engineering Department, École Polytechnique, Montréal, Canada; and
[*] Automated Production Department, École de Technologie Supérieure, Montréal, Canada.

Correspondence and Reprint Requests:

Marwan Sati, Biomedical Engineering Department, École Polytechnique, P.O. Box 6079 Station "Downtown", Montréal Québec, Canada H3C 3A7;

tel: (514) 340-4198 ; fax: (514) 340-4611; e-mail: sati@grbb.polymtl.ca

3.2 Abstract

The accuracy of three-dimensional (3D) *in vivo* knee measurement is presently limited by artifacts from movement of soft tissue surrounding the underlying bone. To improve 3D measurement, a mechanical fixation system is proposed which attaches sensors onto the underlying bone non-invasively. A 3D X-ray technique is used to show that the system can measure knee kinematics over 65 degrees flexion with an average accuracy of -0.4 degrees ab-adduction rotation, -2.3 degrees for axial rotation, 2.4 mm for antero-posterior translation and 1.1 mm for axial translation. To demonstrate a clinical application of the system, its use to predict prosthetic ligament bending and torsion deformations *in vivo* is reported.

3.3 Introduction

In vivo kinematic analysis of knee movement is difficult. Soft tissue structures surrounding the knee hinder the measurement of detailed knee kinematics. Traditional gait analysis equipment employs markers mounted on the surface of the skin overlying the knee to track the underlying bone movement. We have found that error arising from the movement between surface markers and the underlying bone during active flexion can be from 2 to 20 times that due to the equipment used to track the marker position (Sati et al., in press). This makes relative movement between skin and the underlying bone by far the largest obstacle to obtain accurate knee kinematics for precise biomechanical analysis. Furthermore, this movement artifact can significantly vary in both magnitude and direction between individuals.

The accuracy required to adequately describe the kinematics may, however, vary with the application. For instance, the accuracy required for the evaluation of below-knee prostheses has been met by gait lab apparatus which tracks markers mounted on the thigh and the prosthesis via optic tracking equipment. However, the accuracy required to evaluate the loading of a ligament prosthesis cannot be acheived with the above techniques (Gely et al., 1984).

3.3.1 Literature review

We can find in the literature three general methods which address the problem of relative skin movement: 1) elimination of skin movement error via transcutaneous attachments to the underlying bone (Cappozzo et al., in press;Levens et al., 1948;Holden et al.,

1994;Murphy, 1990;Karlsson & Lundberg, 1994), serial radiography (Frankel et al., 1971;Feudenstein & Woo, 1969;Hallen & Lindahl, 1966;Smidt, 1973) or roentgen stereophotogrammetry (Blankevoort et al., 1985;Huiskes et al., 1985;Kärrholm, 1989), 2) mathematical correction of the error by statistical analysis of the position of several markers mounted on the surface of the skin (Cappello et al., 1994;Wang et al., 1993;Veldpaus et al., 1988;Spoor & Veldpaus, 1980;Cheeze, 1993) or improved placement of markers (Söderkvist & Wedin, 1993;Crisco III et al., 1994) 3) physical reduction of this movement via marker "attachment systems"(Cappello et al., 1994;Ladin & Wu, 1991;Wu & Ladin Z., 1993;Mills & Hull, 1991;Quinn & Mote Jr., 1990).

The first and most accurate of these three approaches can involve implanting invasive bone pins or radio-opaque markers into the femur and tibia of the patient. Several studies report the use of fracture fixation devices (Cappozzo et al., in press), cortical pins (Levens et al., 1948;Lafortune, 1984;McClay et al., 1991;Murphy, 1990;Karlsson & Lundberg, 1994) and minimally invasive "halo ring" pin attachments (Holden et al., 1994) to obtain more accurate kinematics. Although very accurate, the potential complications and limited accessibility of invasive methods make them less practical in a clinical setting. Radiological methods or roentgen stereophotogrammetry are also not very practical for routine use.

Numerical methods to reduce skin movement error by using information from several markers have been attempted by several authors (Cappello et al., 1994;Wang et al., 1993;Veldpaus et al., 1988;Spoor & Veldpaus, 1980;Cheeze, 1993;van den Bogart et al., 1990). The basic principle behind most of these correction methods appeals to the theoretical rigid relative position of several markers mounted on the surface of the skin in three-dimensional (3D) space. If one of the surface markers moves with respect to the others, the rigid constraint attributes the relative movement to skin movement not bone movement. Some methods attempt to filter out skin movement noise. However, since

frequency components of skin movement are similar to those of the underlying bone (Cappozzo et al., in press), filtering has little effect.

Several authors have also proposed methods to mechanically restrain marker movement through an "attachment system". One example of a marker attachment system is to tightly wrap velcro straps around the segment in question. Position markers (or sensors), angular velocity meters and accelerometers can be mounted onto this tight wrap (Murphy, 1990;Wu & Ladin Z., 1993;Cappello et al., 1994). These methods tend to reduce movements of the skin during activities involving large accelerations. The tight wrap can also provide a solid basis for the mounting of both angular velocity and acceleration sensors (Wu & Ladin Z., 1993).

Other attachment systems have been conceived to attach goniometers onto the knee. Goniometers, which consist of robot-like linkages equipped with potentiometers to measure kinematics, have been attached to the knee via a combination of velcro straps and orthoplasts (Suntay et al., 1983;Marans et al., 1989;Isacson et al., 1986).

Two attachment systems, developped to measure knee laxity and kinematics in vitro (Quinn & Mote Jr., 1990) and knee laxity *in vivo* (Mills & Hull, 1991), combine two orthoplasts connected via a mechanical bridge to form a femoral clamp with velcro straps to hold this clamp in place. The medial and lateral attachment sites were placed on both the femoral medial and lateral epicondyles (femoral attachment sites of the lateral and medial collateral ligaments respectively). The mechanical bridge provides an inward clamping pressure between these sites while avoiding other soft tissue. The attachment sites of these systems could, however, be improved in light of recent findings that large amounts of skin-bone movement occur over the medial and lateral epicondyles (Sati et al., in press).

3.3.2 Objective of the present study

Our primary objective is to develop instrumentation of sufficient accuracy to study prosthetic ligament deformations *in vivo*. Our second objective is that this instrumentation be sufficiently practical to be used on a routine basis in a clinical setting.

The potential complications and impracticality of invasive methods for routine use has lead us to attempt a non-invasive approach to obtain accurate *in vivo* knee kinematics. The variance between individual anatomy and skin movement, the large magnitude of relative skin-bone movement and the similar frequency component with underlying bone movement makes elimination of error through mathematical correction difficult. Although possible in a gait lab, placement of several markers onto each limb for this type of analysis is not very practical on a routine basis in a clinical setting.

In this paper, a mechanical clamping system is proposed which attaches *non-invasively* onto specific areas of the knee to reduce movement between tracking sensors and the underlying bone. The system consists of an improvement over the most recent attachment systems by Quinn et al. (1990) and Mills and Hull (1991).

The accuracy with which the proposed system can track *in vivo* knee movement will be evaluated experimentally using a three-dimensional (3D) X-ray method. To demonstrate a clinical application, these accuracy values will then be input into a computer simulation to study the error in prosthetic ligament deformation calculations based on this experimental data.

3.4 Methodology

The design and placement of the attachment system was based in part on quantitative data of natural skin-bone movement obtained in a previous study in which small metallic beads were individually taped onto several regions of both the medial and lateral aspects of the skin overlying the femur[1]. The fluoroscopic (real-time X-ray) sagittal projection of both markers and underlying bone was recorded onto video tape at 30 frames per second during a subject's dynamic knee flexion. Both magnification and the three-dimensional (3D) orientation of the bone were taken into account in a mathematical model which calculated the movement of the markers with respect to the underlying bone. Figure 3-1 and Figure 3-2 illustrate the natural skin movement on the lateral and medial aspects of the knee with respect to the underlying bone during one active knee flexion for three subjects. The accuracy of the X-ray fluoroscopic method has been previously evaluated to track relative movements between marker and bone to below one millimeter. This method is also used in this study to evaluate the movement between the attachment system and the underlying bone.

3.4 Methodology

The design and placement of the attachment system was based in part on quantitative data of natural skin-bone movement obtained in a previous study in which small metallic beads were individually taped onto several regions of both the medial and lateral aspects of the skin overlying the femur[1]. The fluoroscopic (real-time X-ray) sagittal projection of both markers and underlying bone was recorded onto video tape at 30 frames per second during a subject's dynamic knee flexion. Both magnification and the three-dimensional (3D) orientation of the bone were taken into account in a mathematical model which calculated the movement of the markers with respect to the underlying bone. Figure 3-1 and Figure 3-2 illustrate the natural skin movement on the lateral and medial aspects of the knee with respect to the underlying bone during one active knee flexion for three subjects. The accuracy of the X-ray fluoroscopic method has been previously evaluated to track relative movements between marker and bone to below one millimeter. This method is also used in this study to evaluate the movement between the attachment system and the underlying bone.
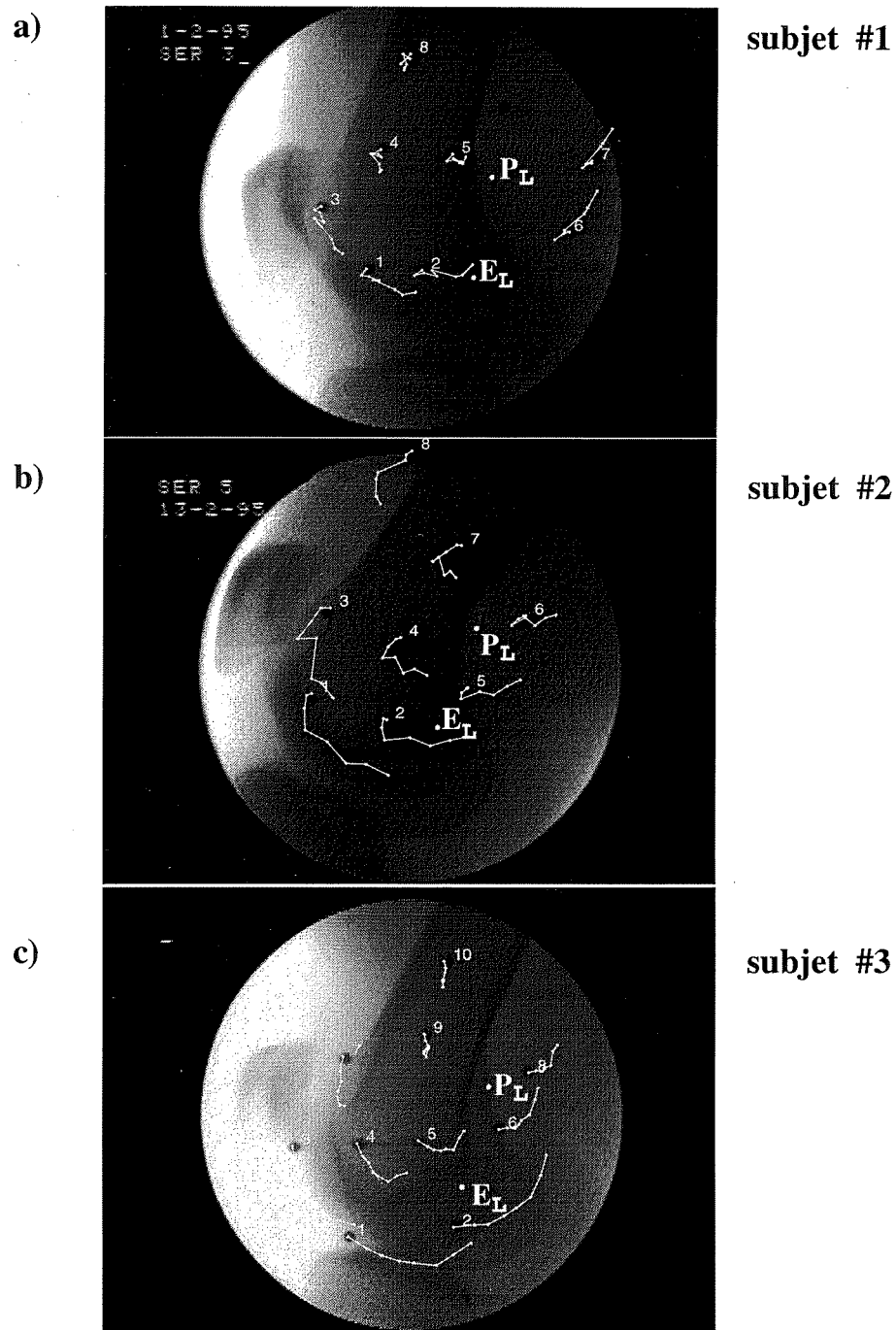
Figure 3–1 Movement of lateral skin–mounted markers with respect to the underlying bone during active knee flexion. Lateral epicondyle E_L and attachment point P_L.
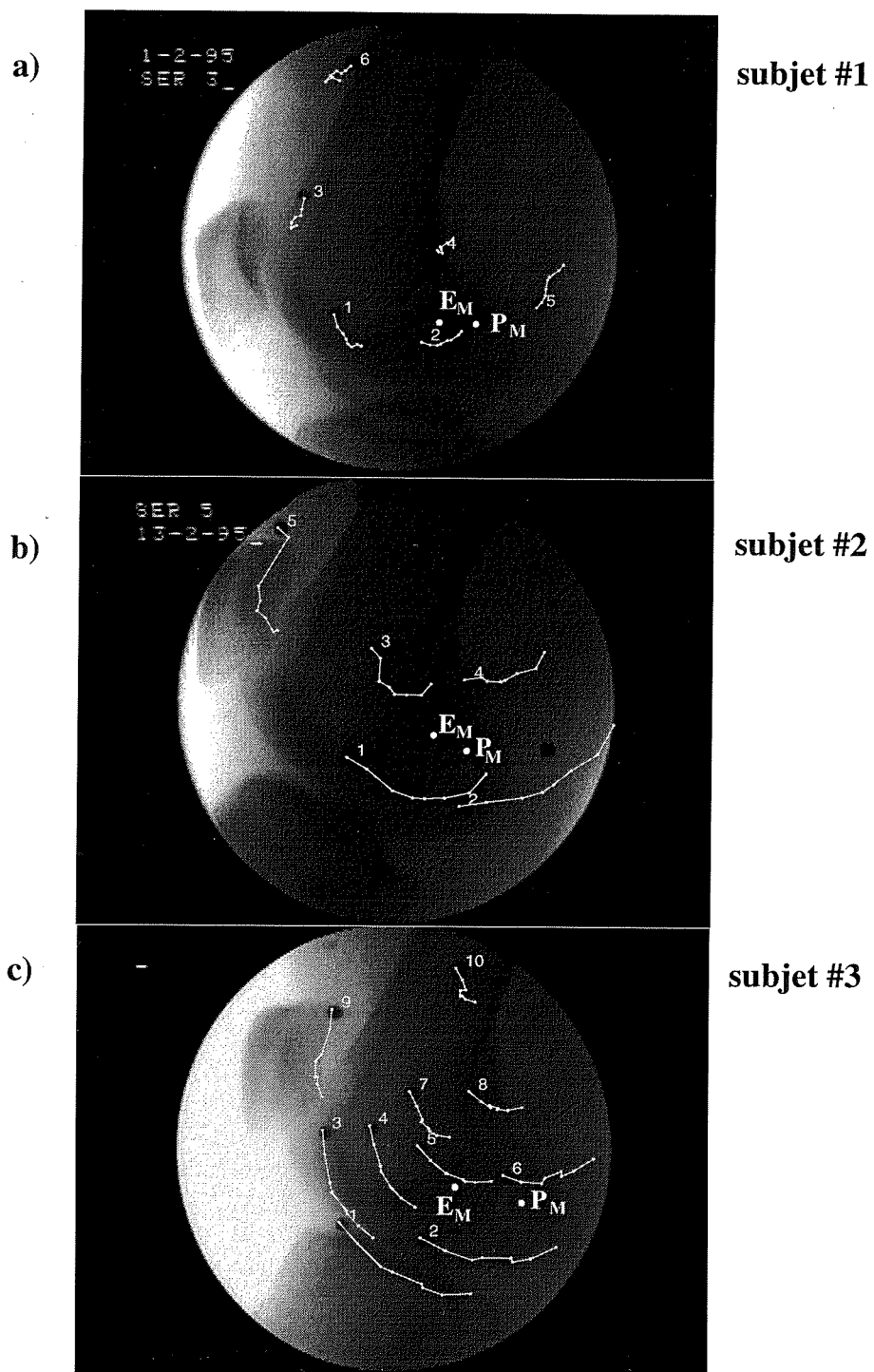
Figure 3–2 Movement of medial skin–mounted markers with respect to the underlying bone during active knee flexion. Medial epicondyle E_M and attachment point P_M.

Part of the attachment system is designed to remain stationary with respect to the underlying bone. Motion sensors placed on this part of the system can accurately track knee movement. The present system used magnetic sensors ("Flock of Birds", Ascension Technologies, Burlington Vermont) which give both position and orientation, thus requiring only one sensor per bone for 3D analysis. However, the use of other types of sensors is equally possible.

3.4.1 Design of the attachment system

Attaching sensors onto underlying bone is complicated by large amounts of surrounding soft tissue and anatomical structures which slide between the skin and the underlying bone. To avoid such parasitic movement, the underlying principle of the present design is to bridge over areas of thick soft tissue, attaching only onto selected areas of thin soft tissue that have little movement with respect to the underlying bone. Furthermore, to provide comfort and normal knee function, the system must have flexible components without compromising accurate measurement of the knee's three-dimensional movements, i.e. three rotations and three displacements.

3.4.1.1 Femoral attachment system design

Figure 3-3 shows several viewpoints of the attachment sites relative to a three-dimensional (3D) computer model of a selected knee anatomy. The choice of these attachment sites is explained by referring both to this figure of the anatomy and Figure 3-1 and Figure 3-2 of skin movement over the knee. Several of the previous attachement systems attached onto the lateral condyle (Mills & Hull, 1991;Quinn & Mote Jr., 1990;Isacson et al., 1986). Since the ilio-tibial band slips over the posterior half of the

lateral condyle during the first degrees of knee flexion, attachment is only possible on the anterior aspect of this condyle. However, it was observed that skin-bone movement over the anterior aspect of the lateral epicondyle is very large, of the order of 30 mm in the AP direction (Figure 3-1). Interestingly, skin-bone movement just above the lateral posterior condyle, termed P_L and seen in Figure 3-1, was smaller than on the epicondyle. Anatomically, as seen in Figure 3-3d, there exists a physical space between the ilio-tibial band (item#3) and the biceps femoris tendon (item#2), just above the posterior lateral condyle. Therefore, a 2 cm long, 0.5 cm wide orthoplast (item C) can be placed in this groove with its distal end formed to rest on the superior edge of the posterior condyle. This attachement is stabilized since it sits between the ilio-tibial band, the biceps femoris tendon and the top edge of the posterior condyle (see Figure 3-3c, Figure 3-3d). For reference landmark purposes, the lateral epicondyle (attachment of the lateral-collateral ligament) is denoted by E_L in both Figure 3-1and Figure 3-3

On the medial aspect of the knee, previous systems attached large circular pads or orthoplasts onto the femoral epicondyle E_M (site of the medial-collateral ligament femoral attachment) (Mills & Hull, 1991;Quinn & Mote Jr., 1990). However, skin moves significantly (up to 20 to 30mm) over both anterior and posterior aspects of the medial condyle (see Figure 3-2) The top of the posterior medial condyle offers a physical ridge, known as the adductor tubercle, onto which a contoured orthoplast can be placed (Figure 3-3 item#A). Placement onto this ridge reduces medio-lateral and proximo-distal displacements between the attachment system and the medial condyle, however it does not help reduce relative AP movements due to the naturally large skin movement in this area. To reduce relative clamp-bone AP movements, a region posterior to the medial adductor magnus tendon (item #1) and anterior to the sartorius tendon is selected (see Figure 3-3 item#B). Since the adductor tendon is attached onto the adductor tubercle on

a) Anterior view

b) Medial View

c) Posterior View

d) Lateral View
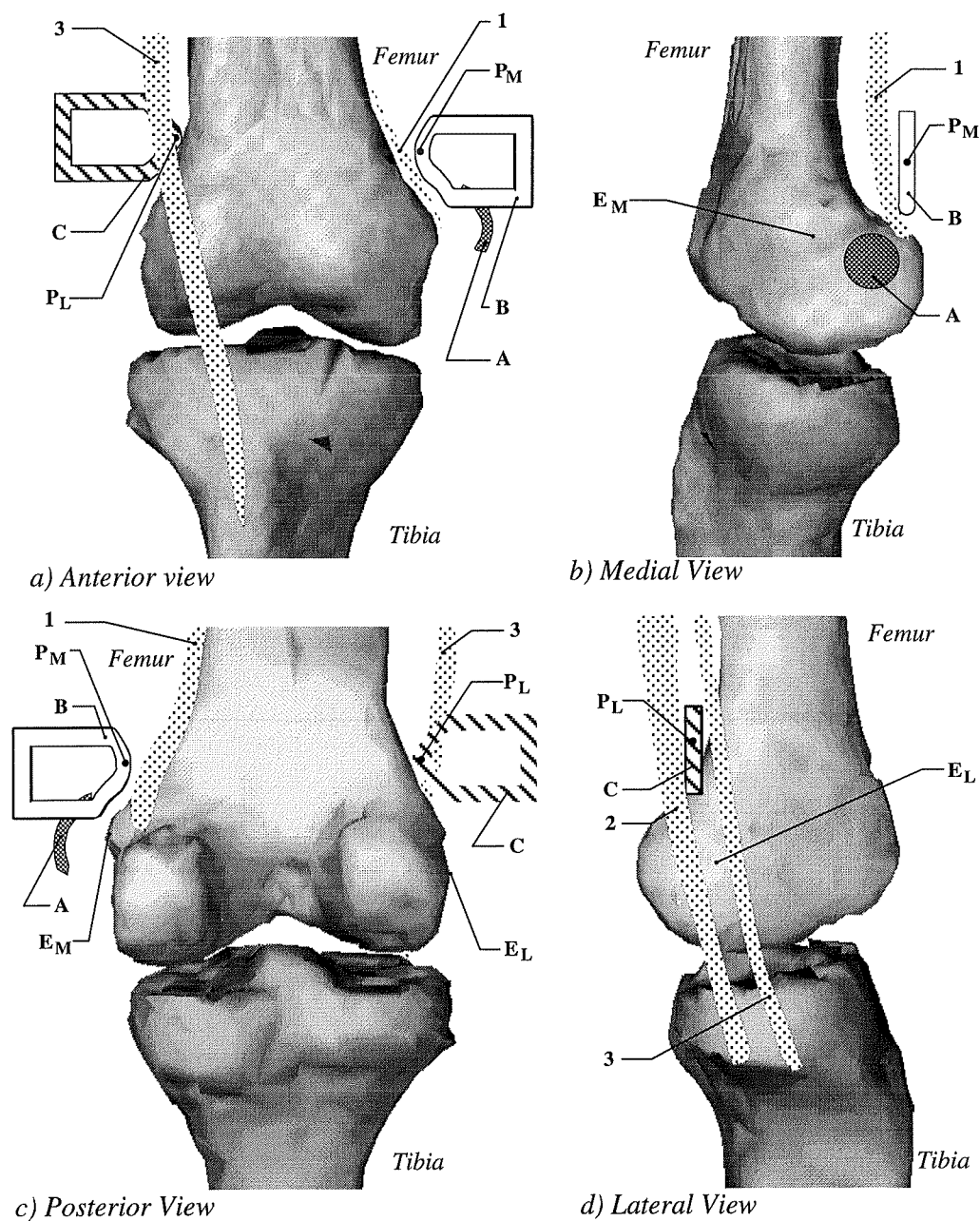
Legend: E_L, E_M : Lateral and medial epicondyles
  P_L , P_M : Lateral and medial attachment sites
  A: Medial orthoplast
  B: Medial Adductor orthoplast
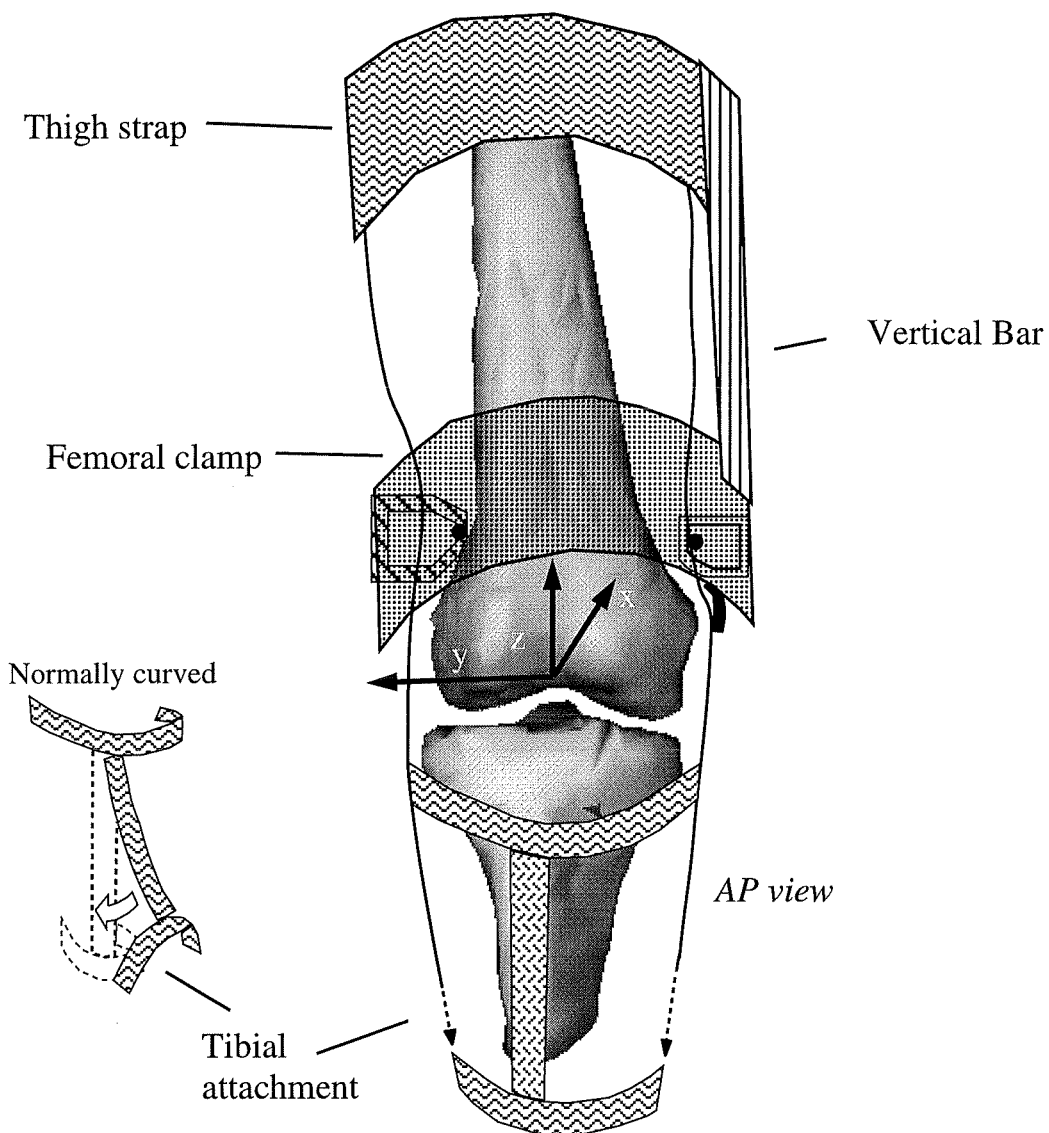 C: Lateral iliotibial–biceps long orthoplast

  1: Adductor Magnus t.
  2: Biceps Femoris t.
  3: Ilio–tibial band

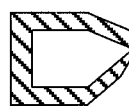**Figure 3–3 Views of attachment sites.**

which attachment "B" is placed, attachment "A" is slightly posterior and superior to attachment "B" (see Figure 3-3). Therefore, the superior aspect of the adductor tubercle and the posterior aspect of the adductor magnus tendon were the two *medial* attachment sites chosen for the new design.

Interconnections of the attachment sites can be seen in Figure 3-4. To further minimize the movement between the medial and lateral attachment sites and the underlying bone, an inward clamping pressure is applied via a mechanical "bridge" (Figure 3-4). For the system to accurately reflect the orientation of the femoral long axis, an attachment onto the proximal end of the thigh via a flexible velcro strap was employed (Figure 3-4). A second bridge, termed "vertical bar" attaches this femoral "clamp" to the proximal thigh (Figure 3-4).

Since it is impossible that each attachment site remain perfectly fixed with respect to the underlying bone, flexible material has been chosen for the design of some parts of the system to allow for subject comfort and freedom of movement without compromising precision. For example, the femoral "clamp" must be flexible enough to allow expansion of the arch during knee extension. This allows comfort for the subject since the biceps femoris tendon and iliotibial band approach one another during full extension and the attachment sits on the biceps femoris muscle (short head), which has the effect of pushing the lateral attachment away from the knee. Therefore, the motion sensor is (or sensors are) placed on the medial attachment site to track the real medio-lateral movement of the bone.

Thigh strap

Vertical Bar

Femoral clamp

Normally curved

AP view

Tibial attachment

Legend:

Medial orthoplast

Lateral iliotibial–biceps long orthoplast

Medial adductor magnus long orthoplast

Radio–opaque marker

Figure 3–4 The attachment system.

The thigh attachment is also given a certain flexibility. Radial and circumferential soft tissue movement on the thigh occurs during muscular contractions and femoral axial rotations. Furthermore, during knee flexion, the anterior soft tissue structures elongate while the posterior structures contract (Cappozzo et al., in press;Sati et al., in press) The elasticity in the thigh attachment allows dilation of the muscles while the friction of the elastic prevents proximo-distal displacement. This strap also has the effect of averaging the elongation and contraction movements of the anterior and posterior aspects of the thigh. To avoid parasitic circumferential rotation of the thigh's soft tissue about the femoral long axis, the vertical bar is allowed to pivot about its long axis at its attachment with the thigh. Therefore, the thigh attachment allows soft tissue dilation, rotation, elongation and contraction while maintaining the femoral clamp's orientation with respect to the femur's long axis.

The attachment system tends to produce a distal displacement due to its own weight which it must support. The large surface area of the thigh attachment offers frictional resistance against the weight of the attachment system. The upper ridge of the medial adductor tercule (see Figure 3-3b), and the superior ridge of the lateral posterior condyle (see Figure 3-3d), also provide a vertical force resisting the system's weight through the medial and lateral orthoplasts.

3.4.1.2 Tibial attachment system design

Qualitative fluoroscopic observations revealed that skin on the anterior aspect of the tibia was thin and underwent little movement with respect to the underlying bone making it a suitable tibial attachment area. The tibial attachment consists of a long bow-shaped plastic padded plate whose ends are strapped to the proximal and distal ends of the tibia to make

it conform with the relatively rectilinear anterior tibia (see Figure 3-4). Strapping onto the ends of the tibia avoids contact with large soft tissue of the calf. The tendancy of the bow to return to its normal shape exerts a posteriorly-directed pressure onto the anterior tibia which solidifies the attachment (see Figure 3-4 inset).

3.4.1.3 Femoral and tibial attachment system fabrication

The femoral clamp was heat-formed into an arch from a 6 mm thick, 5 cm wide and 35 cm long plexiglass sheet. The thigh strap was made from neoprene and linked to the femoral clamp via a 6 mm thick, 4 cm wide and 25 cm long plexiglass bar (referred to previously as "vertical bar"). The femoral attachment orthoplasts were machined from teflon and the tibial orthoplast was formed from 3mm thick, 27 mm long heat-deformable plastic which is held down at both the proximal and distal tibia of the subject via neoprene and velcro straps. The femoral attachment system is 15 cm wide and 30 cm long and weighs 200 g.

To accomodate individuals of different sizes and morphologies, the distance between the medial and lateral attachment sites and the length of the thigh strap are adjustable (Figure 3-4). Before the installation, care should be taken to identify the anatomical attachment regions which can be marked with an ink pen. The subjects should also be allowed a period of accomodation to the system before starting the tests.

3.4.2 Evaluation of the movement between the attachment system and underlying bone

To quantify the movement between the attachment system and the underlying bone, the aforementioned X-ray fluoroscopic method was applied to three subjects. Since the tibial attachment is inherently more solid than the femoral attachment, measurement accuracy analysis was concentrated on the femoral attachement. Three healthy adult subjects between the ages of 20-27, 1 female and 2 male, were made fully aware of the procedure and their consent was obtained before acquisition of the data.

For each subject, radioopaque markers were placed in both the medial and lateral orthoplasts near the underlying bone and a fluoroscope equipped with a super VHS videorecorder was used to register the data (Figure 3-5). The subjects were placed such that a lateral profile of both condyles and the superior aspect of the tibia were within the fluoroscopic window. Both an antero-posterior (A-P) and medio-lateral (M-L) fluoroscopic image were first taken to measure several geometric parameters used in later image correction calculations (Sati et al., in press). Once these images were obtained, active knee flexions in the sagittal plane were performed within the fluoroscopic window and data recorded in real time. Subjects were asked to raise their heel from the ground towards their buttock three times, keeping their knee joint within the fluoroscopic window during the X-ray recording. The attachment system was then removed, replaced and the procedure repeated.
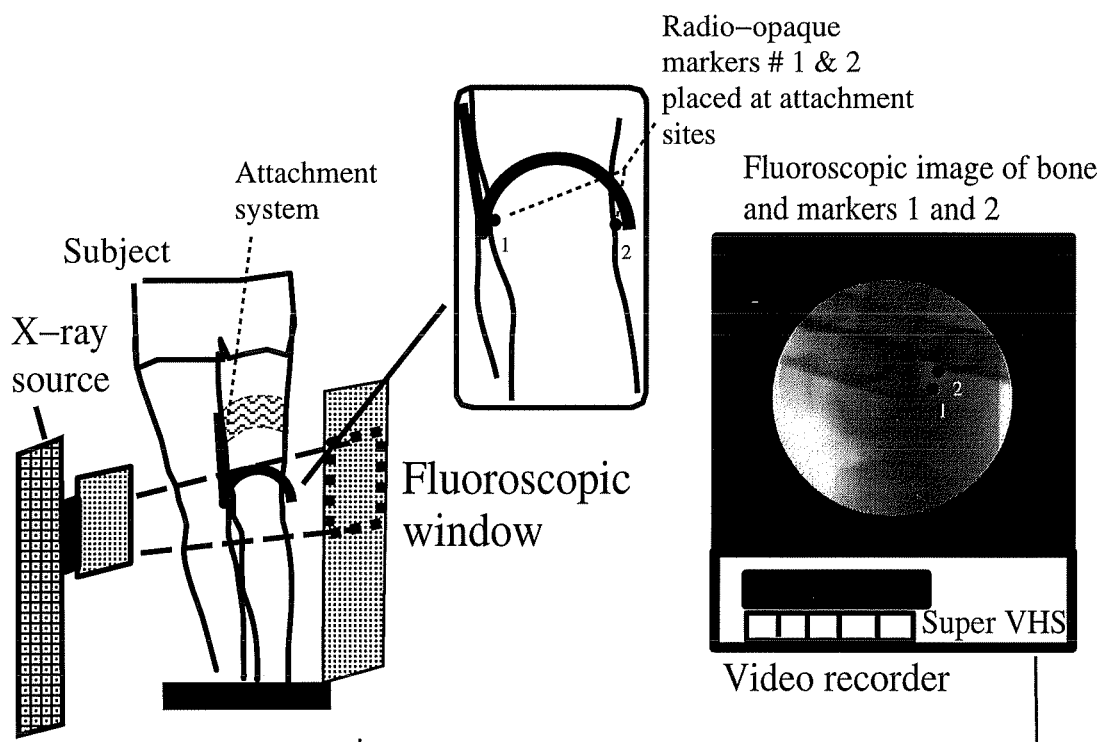
Figure 3–5 Fluoroscopic evaluation setup.

This study was limited to low acceleration movements since the primary application is to study the mechanical loading of prosthetic ligaments subject to low acceleration 3D knee kinematics. Fluoroscopic images were then digitized via a frame grabber on an IRIS Indigo Elan on which a MATLAB program was used to calculate the relative movements between marker and bone (Sati et al. in press).

Movement between markers and underlying bone was expressed in terms of a recently proposed standard error definition (Cappozzo et al., in press) which estimates error as the displacement of a marker with respect to its mean position. This error has been termed RMSd (or rmsd) and more recently "Position Artifact Standard Error" (PASE),

we will refer to this quantity by the former notation. Letting x_i and y_i be the components of marker position 'i', the RMSd error of this set of n marker positions is defined as:

$$RMSd = \frac{\left[\sum_{1}^{n}(x_i - \bar{x})^2 + (y_i - \bar{y})^2\right]^{1/2}}{(n-1)^{1/2}}$$

Eq. 3-1

where the measurement error is estimated as the difference between the position x_i where the mean position of x is obtained by:

$$\bar{x} = \frac{1}{n}\sum_{i=1}^{n}x_i$$

Eq. 3-2

The mean position of y is calculated in a similar fashion.

To characterize knee movement, joint kinematics (angles and displacements) must be calculated from the attachment system data. Figure 3-4 shows an axis system used to describe knee rotations and displacements. Displacements along the X, Y and Z-axes correspond respectively to anterior-posterior (A-P), medio-lateral (M-L) and axial translation of the tibia with respect to the femur. Rotations about these X, Y and Z axes correspond to ab-adduction, knee flexion and axial rotation respectively.

Movement between the attachment system and the underlying bone causes rotation and translation errors in the measured knee kinematics. Medial and lateral marker movements were used to explicitly determine these errors as a function of knee flexion. This was done by projecting the 3D vector which spans the medial and lateral markers (in the attachment sites) onto the X, Y and Z axes at approximately 10 degree intervals over 65

degrees knee flexion. From this data, both average and maximal rotation and displacement errors were investigated.

3.4.3 Predicting prosthetic ligament deformations *in vivo*

To demonstrate a clinical application of the system, its use to help analyze prosthetic ligament deformations *in vivo* is shown. The accuracy with which prosthetic ligament deformations can be predicted *in vivo* can be derived from the known accuracy of the attachment system to track knee movement. To evaluate the effect of experimental errors on prosthetic ligament deformations, a computer simulation was performed. A previously developed three dimensional computer program the "Prosthetic Ligament Information Generating System" (PROLIGS) (Sati et al., 1991) which can calculate prosthetic ligament deformations based on the "inverse deformation principle" was used. In this program, an individual's knee geometry is reconstructed in 3D from X-ray computed tomography (CT scan) (de Guise & Martel, 1988). Kinematics are then input from experimental measurements of the individual's knee movement via the sensor-equipped attachment. In the computer model, a prosthetic ligament can be simulated and its elongation, flexion and torsion calculated as a function of different ligament insertion orientations (see Figure 3-7).

The accuracy with which prosthetic ligament deformations could be predicted *in vivo* was determined through a perturbation analysis. Ligament deformations were first calculated from the *in vivo* kinematic data (see Figure 3-8 solid line). The knee movement measurement error was then simulated as a noise which perturbed the kinematics. Ligament deformation calculations were then performed on this perturbed movement data (see Figure 3-8 dashed line). The difference between the deformations calculated with and

without the perturbation is used to quantify the error in predicting *in vivo* ligament deformations (see Figure 3-8).

Errors in prosthetic ligament deformation calculations arise from errors in the measured knee kinematics and errors in the initial position estimate of the simulated ligament. The kinematic errors arise from the movement between the attachment system and the underlying bone as well as the inaccuracies of the tracking sensors used to record the knee movement. Since the focus of this paper is the evaluation of the attachment system, only ligament deformation difference arising from the system-bone movement error is considered.

Both average and maximal attachment system movements, found through the X-ray analysis described above, were input as perturbations to the experimental data. These perturbations were applied with respect to the femur's X, Y and Z axes, defined in Figure 3-4, at 10, 45 and 65 degrees knee flexion. Ligament deformations (torsion, bending and elongation) were then calculated according to Gely et al. (1984) with and without the perturbations for two typical prosthetic ligament insertion orientations **A** and **B** (see Figure 3-7). Ligament torsion is defined as the twisting of the functional part of the ligament about its long axis. Bending of the ligament is defined as the angle between the intra-articular part of the ligament and either the femoral insertion tunnel (femoral bending) or the tibial insertion tunnel (tibial bending) (see Figure 3-7).

The eventual goal of prosthetic ligament deformation analysis is to determine insertion orientation which will augment the fatigue life of prosthetic anterior cruciate ligaments (ACL) and posterior cruciate ligaments (PCL). The magnitude of ligament torsion and flexion deformations can be varied by changing the ligaments' insertion orientation (Gely et al., 1984). Hence the need to show that ligament torsion and flexion can be predicted from the attachment-generated data. Although it is not the focus of this study, ligament elongation calculation sensitivity to noise is also presented.

3.5 Results

3.5.1 Ergonomy of the attachment system

After the accustoming period alloted before the tests, all subjects felt comfortable and did not find the attachment system restricting for the movements they were asked to perform. The attachment felt solid for all the subjects during the prescribed movements.

3.5.2 Knee movement measurement error

The values of medial and lateral marker movement with respect to the underlying bone during 65 degrees knee flexion can be seen in Table 3-1 and Figure 3-6.

Table 3-1 Attachment System-Bone Movement on Subjects

Subject #	Side	RMSd (mm rms)	RMSd X (mm rms)	RMSd Z (mm rms)
1	Lateral	1.51	1.25	0.84
	Medial	2.49	2.29	0.98
2	Lateral	1.62	1.18	1.11
	Medial	2.67	2.19	1.54
3	Lateral	1.90	1.30	1.38
	Medial	3.55	3.42	0.92
Avg.	Lateral	1.68	1.24	1.11
	Medial	2.90	2.63	1.15

The three-dimensional standard error RMSd, the RMSd in the X direction and the RMSd in the Z direction are all reported for both medial and lateral marker movements. Table 3-2 summarizes average rotation and displacement errors in knee kinematics calculated from these movement artifacts.

Average ab-adduction rotation error was -0.4 degrees and average axial rotation -2.3 degrees over 65 degrees knee flexion. Average translation error was 2.4 mm rms AP and 1.1 mm rms axially. Maximal errors over 65 degrees knee flexion, reported in Table 3-2b, averaged 1.8 degrees (ranging from 1.2 to 2.1 deg.) for ab-adduction rotation, 5 degrees (ranging from 2.2 to 7.6 deg.) for axial rotation, 5.3 mm (ranging from 5.1 to 6.1 mm) for A-P translation and 2.5 mm (ranging from 2.0 to 3.2 mm) for axial translation. Although displacement error along the Y-axis and rotation about the Y-axis were not reported with

the X-ray method, quantitative fluoroscopy revealed these errors to be small compared to the other values reported.

Table 3-2 Kinematic Artifacts

a) Typical Kinematic Artifacts

Subject #	Axial Rotation (deg.)	Ab-adduction (deg.)	A-P translation (mm rms)	Axial translation (mm rms)
1	0.74	-0.90	2.20	0.63
2	-3.12	0.31	2.52	1.76
3	-4.44	-0.50	2.50	0.92
Average	-2.27	-0.37	2.41	1.10

b) Maximal Kinematic Artifacts

Subject #	Axial Rotation (deg.)	Ab-adduction (deg.)	A-P translation (mm rms)	Axial translation (mm rms)
1	|2.22|	|-2.13|	|5.05|	|1.98|
2	|-5.23|	|1.22|	|4.77|	|3.23|
3	|-7.59|	|-1.99|	|6.14|	|2.28|
Average (of absolute values)	5.01	1.78	5.32	2.50
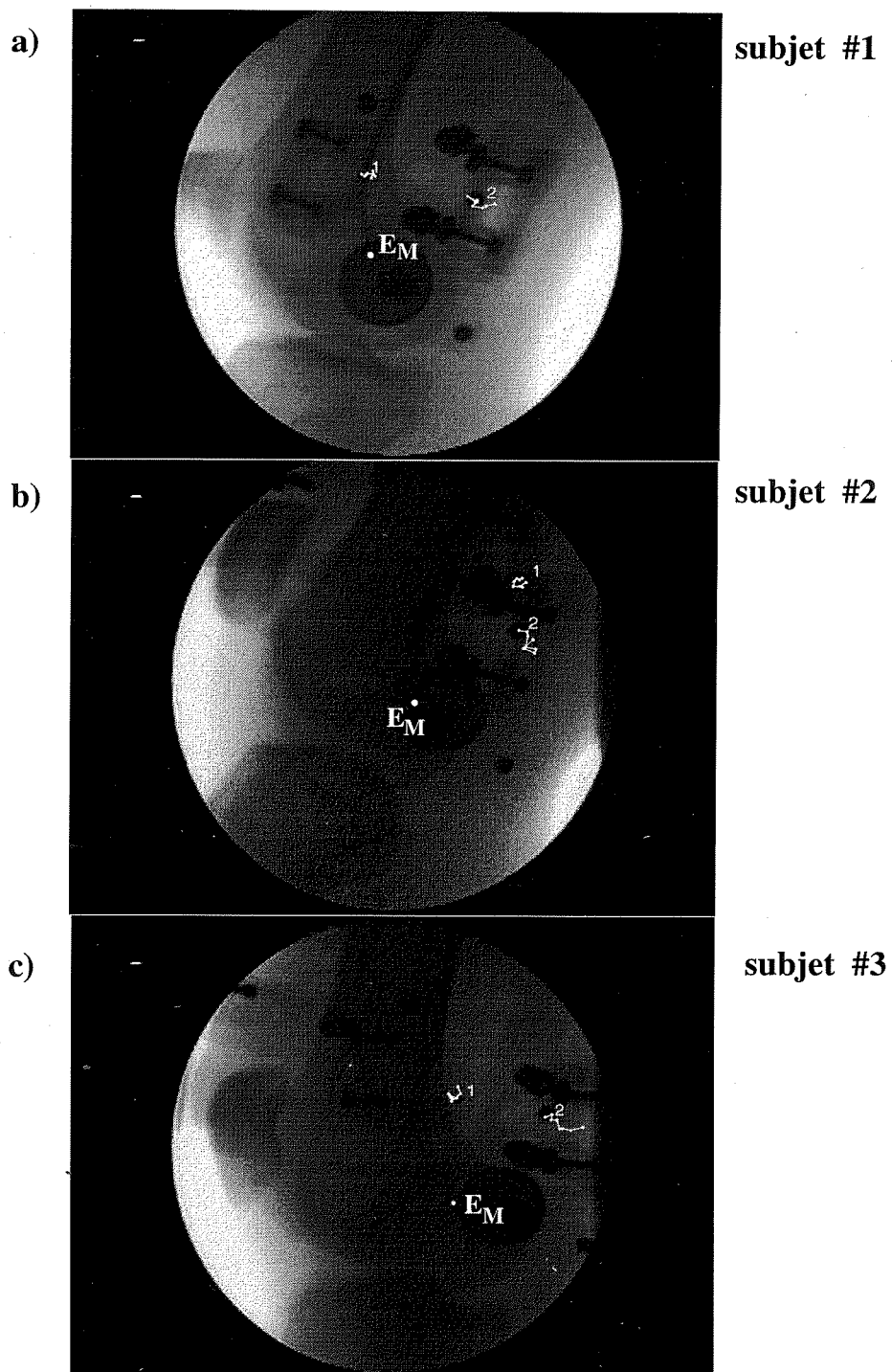
Figure 3–6 Fluoroscopic tracking of attachment system movement over 65 deg. knee flexion.
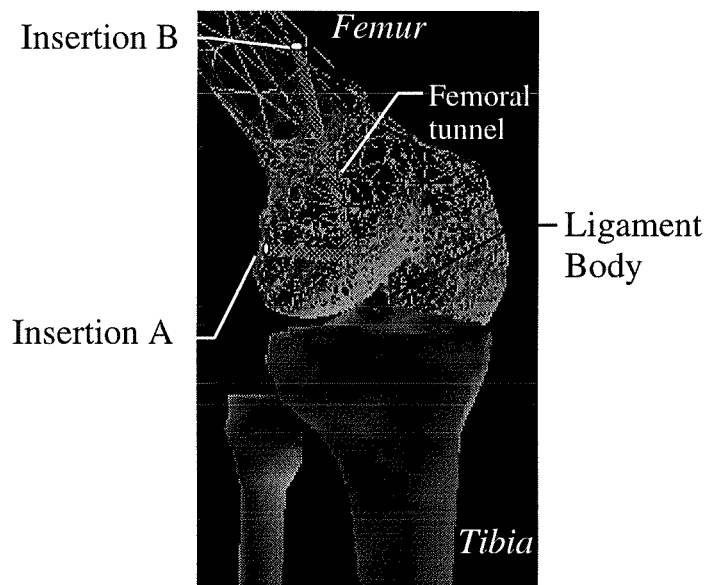
a) Ligament positions in bone model
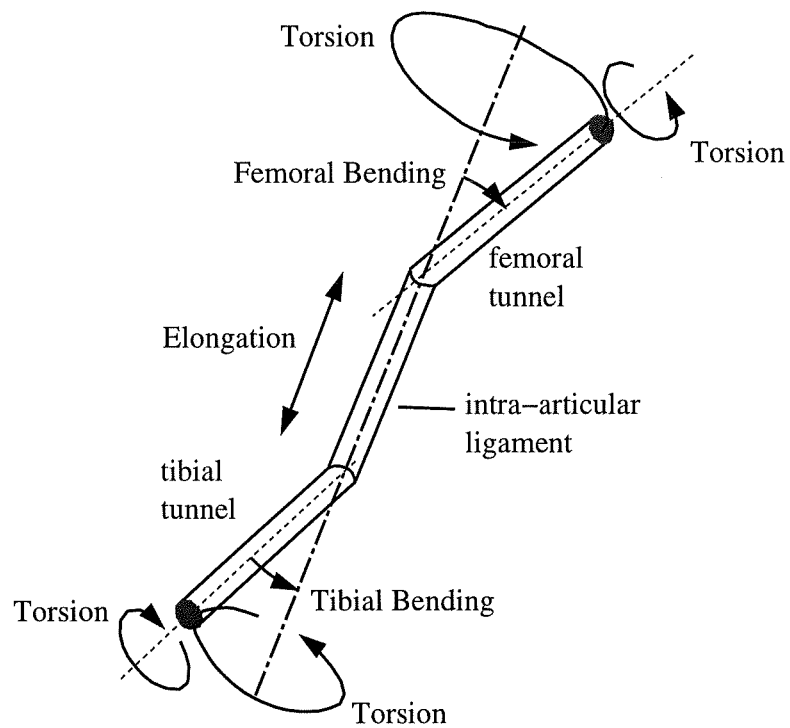
b) Ligament torsion, bending and elongation

Figure 3–7 Computer model of prosthetic ligament deformations.
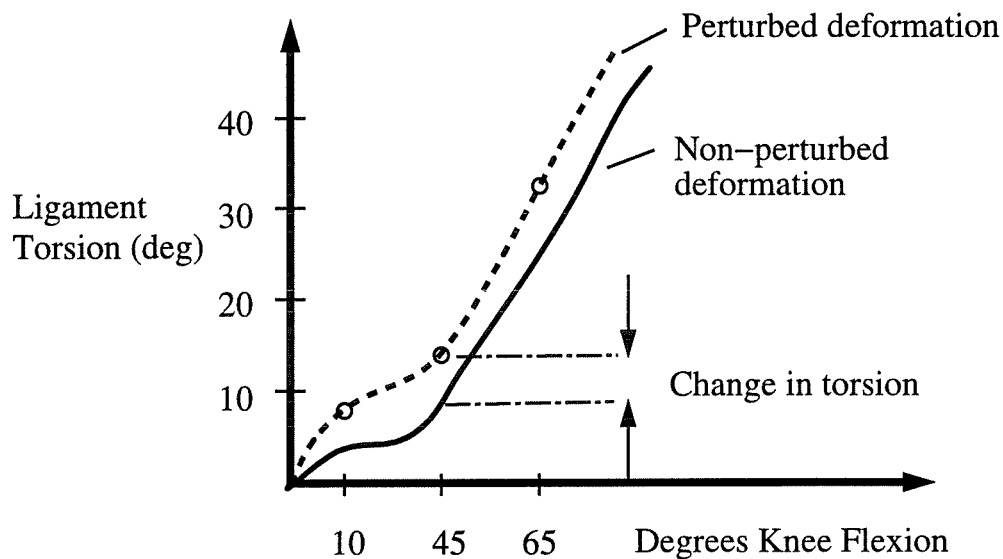
Figure 3-8 Sensitivity analysis. Simulation of error in kinematics at 10,45 and 65 degrees knee flexion.

3.5.3 Ligament deformation sensitivity analysis

Since sensitivity values of the calculations did not vary greatly with knee flexion angle, results at 45 degrees knee flexion for two very different ligament insertion orientations **A** and **B** (seen in Figure 3-7) are reported in Table 3-3. Sensitivity of calculations due to translation along and about the Y-axis were not reported since these errors were found to be relatively small as mentioned above. However, the calculations were found to be not particularily sensitive to these perturbations.

Table 3-3 Sensitivity of calculations at 45 deg. knee flexion for two ligament insertions A and B

a) Sensitivity to average errors

Applied perturbation	Magni-tude	Femoral Bending (deg.)		Tibial Bending (deg.)		Ligament Torsion (deg.)		Ligament Elongation (mm)	
		A	B	A	B	A	B	A	B
A-P displace. (Tx)	2.41 mm	-1.35	5.53	4.42	4.42	-4.34	0.32	-0.52	-0.52
Axial displace. (Tz)	1.10 mm	-0.15	-0.37	-0.49	-0.49	0.38	0.05	-1.08	-1.08
Ab-ad. rotation (Rx)	-0.37 deg.	-1.20	-0.30	-1.26	-1.26	0.87	-0.02	-0.10	-0.10
Axial rotation (Rz)	-2.27 deg.	-3.35	0.36	-1.70	-1.70	3.06	1.92	-0.58	-0.58

a) Sensitivity to maximal errors

Applied perturbation	Magni-tude	Femoral Bending (deg.)		Tibial Bending (deg.)		Ligament Torsion (deg.)		Ligament Elongation (mm)	
		A	B	A	B	A	B	A	B
A-P displace. (Tx)	5.32 mm	-3.01	10.6	2.63	2.63	-9.39	0.69	-1.44	-1.44
Axial displace. (Tz)	2.50 mm	-0.33	-0.81	-1.06	-1.06	0.83	-0.11	-2.46	-2.46
Ab-ad. rotation (Rx)	1.78 deg.	-2.28	1.03	0.48	0.48	-0.46	-0.47	0.40	0.40
Axial rotation (Rz)	5.01 deg.	4.31	0.12	3.14	3.15	-7.18	-4.23	-0.05	-0.05

Average attachment system movement, applied as a perturbation at 45 degrees knee flexion, resulted in changes of torsion and bending deformations less than 5 degrees for both ligament insertions **A** and **B**. Maximal attachment system movement resulted in less than 10 degree changes in torsion and bending calculations for both ligament insertions. Relative sensitivities of bending and torsion varied with the type of ligament insertion orientation. Elongation calculations changed by less than 1 mm from average attachment system movement and less than 2.5 mm from maximal movement. Ligament elongation measurements were most sensitive to translational movements between the attachment system and underlying bone.

3.6 Discussion

3.6.1 Attachment system

Non-invasive mechanical reduction of sensor-bone movement is a desireable option for routine use over invasive techniques which place pins through the skin into underlying bone or radiological-based techniques. However, it is important that the subject feel comfortable for both humanitarian and practical reasons. Pain or a restrictive feeling results in an unpleasant experience for the subject (and eventually the patient) and can restrict normal movements.

Flexibility of the system's parts allows natural soft tissue movements to provide comfort while one part of the system precisely tracks the underlying bone movement. The concept of a flexible yet precise system is a general concept which can be applied to other human-

machine interfaces. Furthermore, the surface area of the attachement sites had to be sufficiently large and properly placed to reduce local contact pressure and avoid sensitive innervated regions which cause pain.

From the fluoroscopic analysis, it was shown that medial attachment A-P movement was greater than lateral attachment movement. This implies that future improvement of the medial attachment could increase the accuracy of measurements. It also implies that for unique measurement of A-P and axial displacements (i.e. sagittal plane movements), one should place the sensor on the lateral attachment. However, M-L displacement is smaller on the medial attachment since the lateral attachment is pushed away from the knee by underlying soft tissue movement during knee flexion.

Skin movement artifacts were significantly reduced by the use of the attachment system. Surface mounted markers traditionally placed on the lateral epicondlye E_L (Figure 1), were found to move from 9 to 14 mm rmsd compared to the new attachment system's lateral attachment site (P_L) movement of 1.5 to 1.9 mm rmsd. Skin movement over the medial epicondyle E_M (Figure 2) moved 5 to 12 mm rmsd compared to the attachment system medial attachment site (P_M) movement of 2.2 to 3.6 mm rmsd.

This reduction in sensor-bone movement allowed average knee movement measurement accuracy to under 2.5 degrees in rotation and 2.5 mm in translation. It must be noted that the attachment-bone movements are reported over 65 degrees knee flexion. Analyses involving relative movements less than 65 degrees would have less error and vice versa. Furthermore, it is stressed that these values apply to the movements studied, namely active knee flexion. The use of the system to measure other movements or knee laxity will be analyzed in later publications.

Axial rotation error was almost twice the ab-adduction error. Similarily, antero-posterior displacement error was also almost twice that of proximal-distal error. Values varied slightly between individuals, yet it was observed in the fluoroscopic data on all three subjects that the lateral attachment sites presented less relative movement with respect to the underlying bone than the medial attachment. Axial rotation error was larger than ab-adduction error mostly due to the medial A-P movement of the attachement system. The fact that the attachment system movements varied in both magnitude and direction between individuals implies that the variance between individuals must be better understood before further noise-reduction via mathematical modelling can be performed.

This level of accuracy of the attachment-generated data opens the door to some previously impossible biomechanic and orthopedic applications. Examples of such applications could include detection of rotational instabilities, optimal placement of knee orthotics, *in vivo* analysis of knee prostheses, the effect of foot orthotics on knee kinematics and the planning of surgical correction procedures.

3.6.2 Ligament sensitivity values

On a practical basis, it is surgically difficult to place a prosthetic ligament with a ligament tunnel flexion or tunnel orientation accuracy greater than 5 to 10 degrees in the knee. Since average and maximal errors from attachment system movement result respectively in less than 5 and 10 degree changes in bending and torsion deformations, movement data from the attachment system can be used to provide clinically significant prosthetic ligament deformation values.

3.7 Conclusions

The semi-flexible design of the attachment system allows subject comfort while providing precise *in vivo* measurements.

The attachment system significantly reduced skin movement artifacts over the lateral condyle from 11mm rms to 1.7 mm rms and over the medial condyle from 8.5mm rms to 2.9 mm rms. The reduction of skin movement artifacts provides *in vivo* measurement of joint kinematics over 65 degrees knee flexion to an average -0.4 deg for ab-adduction rotation, -2.3 deg for axial rotation, 2.4 mm for A-P translation and 1.1 mm for axial translation. The medial attachment generally moved more than the lateral attachment. The variance of attachment system movement between individuals must be better understood before further noise reduction through mathematical modelling can be performed.

The clinical application to *in vivo* prosthetic ligament deformation calculation was shown through a sensitivity analysis. The system-bone attachment is sufficiently accurate to provide *in vivo* clinically relevant prosthetic ligament deformation values to help improve surgical placement. This system will be used to determine surgical placement of prosthetic ligaments which reduce cylic torsion and bending deformations in the hope of augmenting their fatigue life.

This paper has shown that the attachment system accuracy is more than sufficient to predict ligament torsion and bending *in vivo*. However, the attachment system is to be used in combination with other components to measure and visualize knee movement. A future study will analyze the effect of combined error of all the components on ligament deformation calculations.

3.8 Acknowledgments

CHAPTER IV

4. COMPUTER-ASSISTED KNEE SURGERY: DIAGNOSTIC AND PLANNING OF PROSTHETIC LIGAMENT INSERTION

4.1 Situation in thesis

In the previous chapter an article was presented proposing a mechanical fixation device to improve knee movement measurements. The discrepancy between the accuracy of movement measurement sensors and the accuracy with which they are fixed with respect to the bone has often been overlooked in the literature. In light of the large magnitude of marker-bone displacement error, navigation sensor accuracy requirements can be less demanding than previously thought. For this study, the magnetic system was chosen because of its relatively good accuracy, simple computer interface, compact nature, portability, relatively low cost and its capacity to be used to perform real-time analyses.

The mechanical attachment system is integrated into the three dimensional knee analyzer, presented in the present article, for analysis of prosthetic ligament deformations. This computer-assisted knee analyzer system can be considered to be a virtual interface since it allows user interaction with subject bone geometry and movement for analysis and planning of ligament surgery.

Serial photography followed by cine film were major breakthroughs to help past biomechanists elucidate and communicate human movement by capturing it on static film. Virtual interfaces may be the modern parallel to these previous technologies, allowing analysis to go one step further by allowing 3D interaction with subject-generated movement data. A virtual environment can be defined as having both sensorial input and output through which the user can interact. An interesting aspect of a virtual environment is that reality can be represented in any number of ways such that learning or analysis through interaction is most efficient.

To assist analysis and surgical planning in the knee, computer animation of the underlying bone geometry is incorporated into the proposed system. Movement data is fed into the computer bone model in which the examiner can interactively simulate some surgical procedure and receive feedback from the computer's analysis of the intervention. The computer interface intends to improve both data comprehension and communication from the knee analysis system.

The system's sensitivity in calculating ligament deformations is determined in this article through mathematical simulation of component error. Accuracy of deformation calculation is also evaluated through comparison of ligament elongation values with those from the literature. This validation is to support the future use of the system for prosthetic ligament analysis introduced at the end of this chapter and elaborated in the following chapter.

COMPUTER-ASSISTED KNEE SURGERY:
DIAGNOSTICS AND PLANNING OF PROSTHETIC LIGAMENT INSERTION

Sati M.°, de Guise J.A.*and Drouin G.°

° Biomedical Engineering Department, École Polytechnique, Montréal, Canada; and
* Automated Production Department, École de Technologie Supérieure, Montréal, Canada.

Correspondence and Reprint Requests:

Marwan Sati, Biomedical Engineering Department, École Polytechnique, P.O. Box 6079 Station "Downtown", Montréal Québec, Canada H3C 3A7;
tel: (514) 340-4198 ; fax: (514) 340-4611; e-mail: sati@grbb.polymtl.ca

4.2 Abstract

Cruciate ligament rupture, a common injury among young active adults, disrupts the knee's complex movement and often leads to premature degenerative arthritis of the joint. Prosthetic cruciate ligaments can be used for replacement but often fail due to incorrect surgical placement. To aid in the planning of cruciate prosthetic substitution, a computerized system has been developed to provide the surgeon with a virtual interface allowing him to accurately visualize three dimensional (3D) bone structure and movement normally hidden beneath layers of soft tissue.

Pre-operatively, precise *in vivo* kinematics are quantified, with the help of 3D medical images. 3D imagery techniques based on computed tomography (CT) have been developed to obtain accurate 3D reconstruction of knee geometry pre-operatively. The system allows the surgeon to know the real-time spatial position of the patient via magnetic position and orientation sensors attached non-invasively onto the femur and tibia via a portable system. An interactive computer program has been developed to allow the user to simulate different prosthetic ligament insertions and compute elongation, bending and torsion values which will be imposed on the prosthesis. Through comparison with cadaveric studies and a perturbation analysis, the system is shown to be sufficiently accurate to predict *in vivo* ligament deformations.

4.3 Introduction

The large amount of soft tissue surrounding the knee makes diagnosis of pathologies and surgical planning difficult. Rupture of the cruciate ligaments of the knee is an injury which can destabilize complex interactions between ligament stiffness and muscle action which characterize this sensitive mechanism. Surgical replacement of a ruptured anterior cruciate ligament (ACL) or posterior cruciate ligament (PCL) via a prosthesis, autograft or allograft is difficult because of surrounding soft tissue and the anatomical location of these ligaments between the femoral condyles.

ACL and PCL prostheses have not gained widespread acceptance largely because they have been known to fail prematurely *in vivo*. It has been long suspected that this premature failure is in part due to non-optimal insertion orientation of the prosthesis resulting in combined elongation, flexion and torsion deformations in the ligament (Gely et al., 1984). This hypothesis has been more recently supported by mechanical testing (Drouin et al., 1991).

To aid in the diagnosis and correction of knee pathologies, such as an ACL or PCL rupture, we have developed a computer-assisted virtual interface with the knee. The proposed system consists of instrumentation to measure and visualize underlying bone movement and an interactive computer program to help plan and implement corrective measures.

The objective of this paper is to present this new instrumentation, the evaluation of its accuracy in measuring knee movement and, more specifically, its capacity to simulate prosthetic ligament deformations *in vivo* for surgical planning purposes.

A brief review of the literature will be followed by a description of the system's components. The evaluation of the system's accuracy in measuring knee movement and in predicting prosthetic ligament deformation *in vivo* is then described.

4.4 Literature Review

Soft tissue surrounding the knee hinders both the measurement and viewing of underlying bone movement making detailed analysis difficult.The accuracy of three-dimensional (3D) *in vivo* knee measurement is presently limited by artifacts from movement of soft tissue surrounding the underlying bone (Cappozzo et al., in press;Sati et al., in press). We can find three general methods in the literature that address the problem of relative skin-bone movement: 1) elimination of skin movement error via transcutaneous attachments to the underlying bone (Cappozzo et al., in press;Levens et al., 1948;Holden et al., 1994;Murphy, 1990;Karlsson & Lundberg, 1994), serial radiography (Frankel et al., 1971;Feudenstein & Woo, 1969;Hallen & Lindahl, 1966;Smidt, 1973) or roentgen stereophotogrammetry (Blankevoort et al., 1985;Huiskes et al., 1985;Kärrholm, 1989), 2) mathematical correction of the error by statistical analysis of the position of several markers mounted on the surface of the skin (Cappello et al., 1994;Wang et al., 1993;Veldpaus et al., 1988;Spoor & Veldpaus, 1980;Cheeze, 1993) or improved placement of markers (Söderkvist & Wedin, 1993;Crisco III et al., 1994) 3) physical reduction of this movement via marker "attachment systems" (Cappello et al., 1994;Ladin & Wu, 1991;Wu & Ladin Z., 1993;Mills & Hull, 1991;Quinn & Mote Jr., 1990). A mechanical fixation system which attaches sensors onto the underlying bone non-invasively has been developed to improve 3D measurement (Sati et al., submitted). This mechanical system is employed in the present study to help reduce skin movement artifacts.

Although work has been done to improve knee movement measurement, analysis is still difficult since the spatial position of the articular geometry is unknown. Detailed 3D articular geometry is presently incorporated into some kinematic measurements (Couteau et al., 1994;Ronsky et al., 1995), some mathematical knee models (Blankevoort & Huiskes, 1991;Essinger et al., 1989;Wismans et al., 1980;Bendjaballah et al., 1995;Lin et al., 1995) and some commercial packages (SIMM, MusculoGraphics Inc., Evanston IL; ADAMS, Mechanical Dynamics Inc., Ann Arbor, MI). Aside from cadaveric measurements (Lin et al., 1995) or animation purposes, a system providing real-time detailed 3D articular geometry and movement does not presently exist.

There is no comprehensive experimental data available in the literature measuring the combined prosthetic ligament elongation, bending and torsion deformation. However there has been some work on the analysis of ligament elongation as a function of surgical insertion. Grood and Hefzy used an instrumented space linkage (ISL) to measure cadaveric knee movement with submillimeter accuracy. Relative displacement between femur and tibia (elongation) during knee flexion was described for several interior insertion points into the femur. This analysis was performed to help determine which ligament placements result in minimal elongation changes during knee flexion; this is also referred to as "isometric" placement (Flemming et al., 1992). In this study, we use these elongation patterns to evaluate the accuracy of the new knee analysis system.

4.5 Virtual interface description

The system integrates several technologies which are combined together and can be seen in Figure 4-1. Instrumentation captures the subject's personalized bone movement (Figure

4-1a) while the personalized geometry of the subject, obtained via medical imagery, is represented in the computer (Figure 4-1b). The movement data is fed into the computer and mathematically calibrated with the knee geometry such that when the subject's knee moves, the virtual knee moves accordingly.

This system provides a virtual interface with the knee since both the geometry and movement of the real knee are reproduced by the virtual knee. The virtual environment augments reality by providing a detailed medical image of the patient's knee which allows the user to effectively "see through" the skin. The virtual interface provides an interactive environment in which measurements and simulations can be performed to diagnose pathologies, plan and implement corrective measures.

4.5.1 Data acquisition of personalized geometry

Bone geometry is obtained via X-ray computer aided tomography (CAT) scan. Along with the articular geometry, the tomographic images of the patient's knee reveal the coordinates of calibration objects placed within the scanned region (see Figure 4-2). Calibration objects are placed on the knee such that slices used to reconstruct knee geometry also serve to locate the calibration points. One-millimeter thick tomographic slices are used to obtain the maximal resolution of the anatomical structure. The slice acquisition protocol was developed to fulfill two objectives: 1) minimize the radiation dosage and 2) to ensure maximal detail of the articular surface.
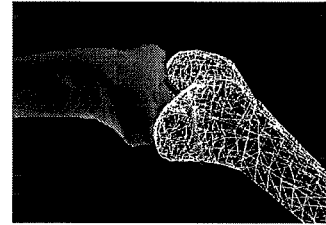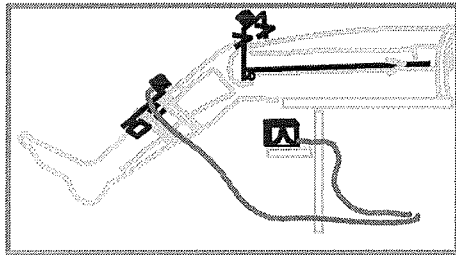
Figure 4–1 Components of 3D knee analysis system.

a)

b)

Figure 4-2 Medical imagery protocol for 3D reconstruction of personalized geometry.

Normally, to reconstruct only the articular surfaces and a small portion of the bone axes, a CAT scan of a patient's knee with slices spaced at 2 mm intervals would require approximately 60 tomo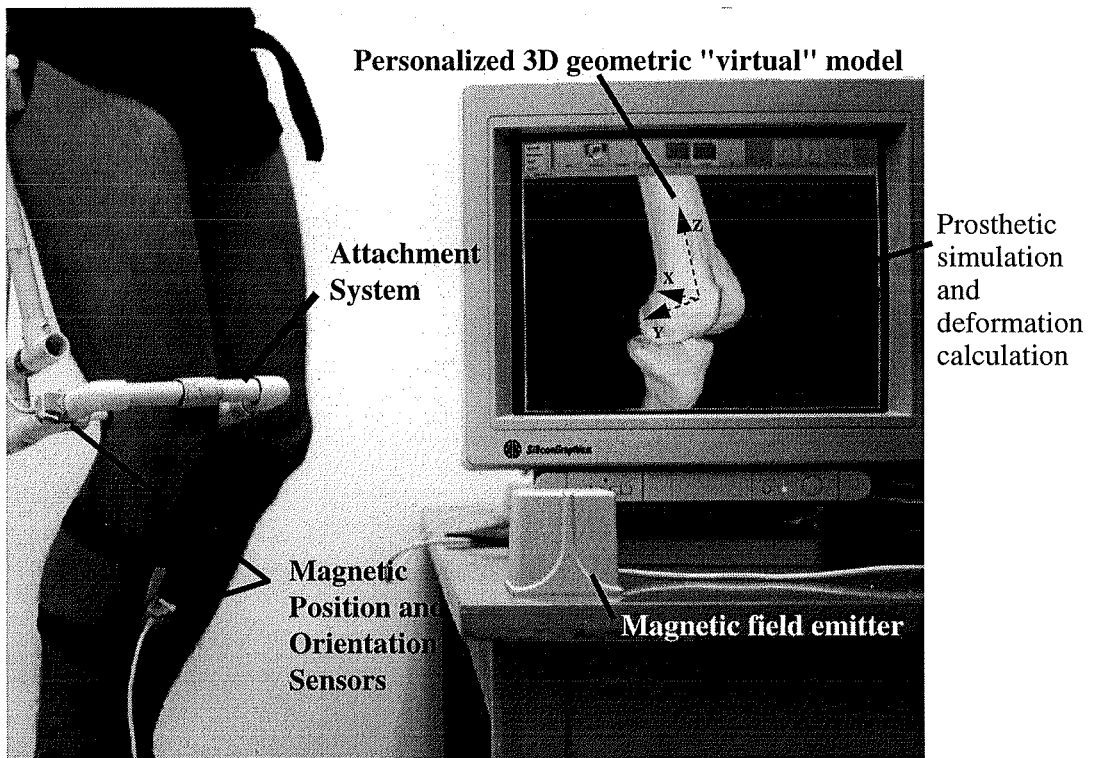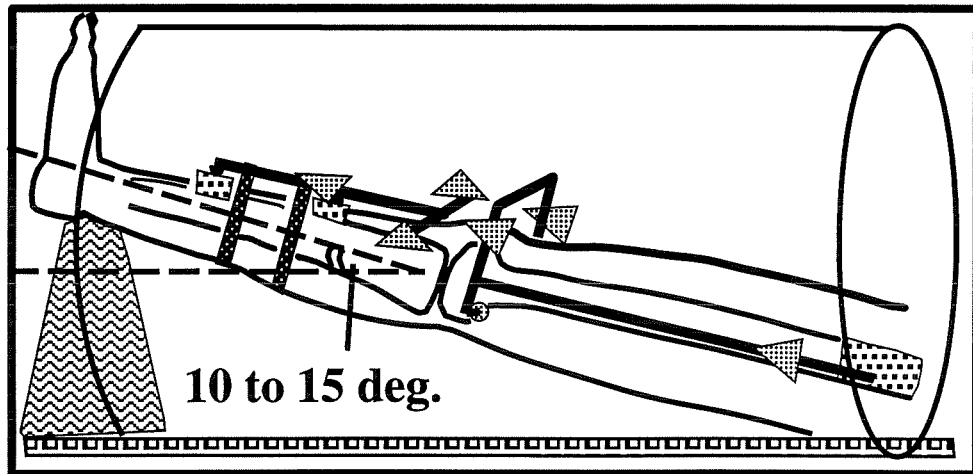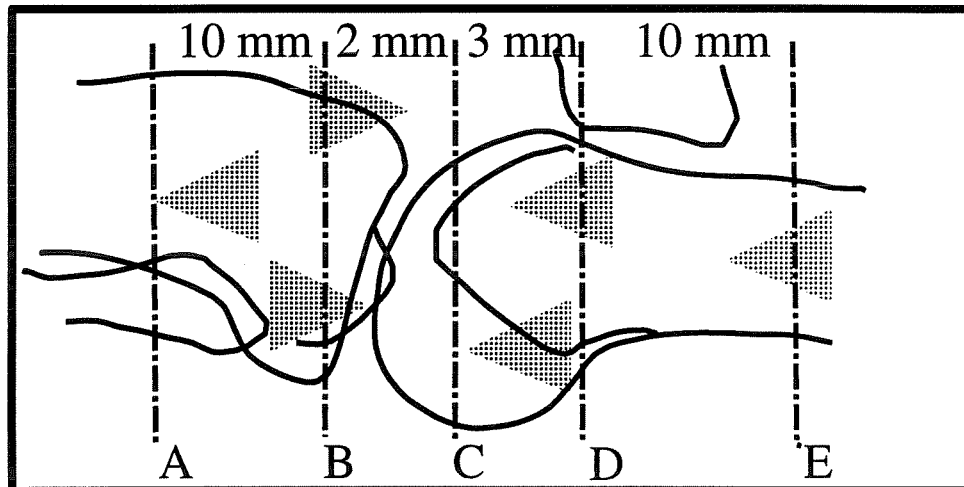graphic slices. To minimize both the radiation to the patient and the time taken in the scanner, we developed an image acquisition protocol requiring under 30 image slices to reconstruct both the femur and tibia. To ensure maximal detail of the articular surface, the images are taken with the patient's heel raised on a cushion in full extension so that the femoral axis forms a 10 to 15 degree angle with respect to the horizontal, as seen in a Figure 4-2. This angle ensures that several slices cross the tibial plateau to improve reconstruction accuracy of its geometry. Furthermore, these slices intersect both the plateau and the distal condyles reducing the number of slices to required to reconstruct the articulating portion of the joint.

To further increase the slice number to accuracy ratio, the three-dimensional (3D) curvature of the bone is inspected to define four regions (see Figure 4-2). Slices are spaced more closely in regions of large curvature and vice versa. An interpolation algorithm is then used in regions of large slice spacing to fill in the gaps (Pouliot et al., 1989).The regions are defined using a lateral pilot scan (Figure 4-2) by anatomical reference points A to E:

A- on the tibia, 30 to 40 mm distal from the tibial plateau

B- the most posterior point on the tibial plateau

C- the most posterior point on the femoral condyles

D- the inflection point between the femoral condyle and the femoral shaft

E- 30 to 40 mm proximal to point D.

It should be noted that landmark C is the posterior point with respect to the femur which is slanted at 10 to 15 degrees. Slice spacing between landmarks is 10 mm from A to B, 2 mm from B to C, 3 mm from C to D and 10 mm from D to E. With 1 mm slice spacing, the 3D reconstruction method has been previously evaluated to generate geometric

models accurate to 1 mm rms (de Guise & Martel, 1988;Aubin et al., submitted), which would be the case for region between landmark B and C which is most critical. Accuracy is lower as slice spacing is increased. However, it will be seen that this error is relatively small and therefore not a determining factor in overall system accuracy.

4.5.2 Data acquisition of personalized kinematics

Femoral and tibial kinematic data is measured via a magnetic field "navigation system" (Ascension Technology "Flock of Birds", Burlington Vermont) which consists of a base DC magnetic field emitter and small "position & orientation" sensors or "tracking receivers" (seen in Figure 4-1). The magnetic field position sensor can be thought of as a three-dimensional computer mouse which returns both position and orientation data. We have evaluated the magnetic tracking system's accuracy in our experimental environment to be 2 mm RMS in displacement and 0.7 deg. RMS in rotation over a 1 meter radius from the emitter (Sati & Vaillancourt, 1992). To maintain this level of accuracy, care must be taken with the use of magnetic tracking devices to control interference from the environment. Metals interfering with a magnetic field, such a most ferro-magnetic metals, must be avoided as well as electrical instrumentation which generates a magnetic field. Stainless steel series 300 and good quality aluminum are examples of metals which do not perturb magnetic devices.

The magnetic sensors are solidly attached onto the underlying bone via a mechanical attachment system (see Figure 4-1). Without this attachment, position artifacts from skin-bone movement can be 10 to 20 times higher than that from conventional motion sensors (Sati et al., in press). The mechanical system attaches non-invasively onto regions of soft tissue which are thin and have little natural movement with respect to the underlying bone

(Sati et al., submitted). This system reduces sensor-bone movement which can be as high as 17 mm root mean square (rms) to 2 or 3 mm rms.

4.5.3 Calibration

The basic principle for calibration is to identify the coordinates of three points in both the geometrical model and the navigation reference systems.

Figure 4-3 represents the two reference systems: the scanner (image or geometric model frame) and the magnetic motion tracker (or kinematic measurement frame). Knowing the coordinates of three points in both the image reference frame and the navigation reference frame for each limb segment allows the calculation of the homogeneous coordinate transformation between these two frames for the femoral segment ($M_{ScanNavF}$) and the tibial segment ($M_{ScanNavT}$). Homogeneous transformation matrices, also referred to as position and orientation matrices are used to describe all three dimensional transformations and are of the form:

$$\begin{bmatrix} r_{11} & r_{12} & r_{13} & 0 \\ r_{21} & r_{22} & r_{23} & 0 \\ r_{31} & r_{32} & r_{33} & 0 \\ tx & ty & tz & 1 \end{bmatrix}$$

Eq. 4-1

Where r_{ii} are the components of a 3x3 rotation submatrix and tx, ty, tz the components of the translation.

Calibration objects having the triangular form seen in Figure 4-3 allow the identification of the reference points in both the geometric model and navigation reference frames. The

apex of each triangle defines a calibration point. In the scanner, direct imaging of this apex is difficult since the slice position can only be controlled to ± 1 mm. Therefore, during the scan of the subject's knee, several CT slices are obtained on each of the three calibration objects and these images are used to calculate the apex via the intersection of the triangles' longest sides.
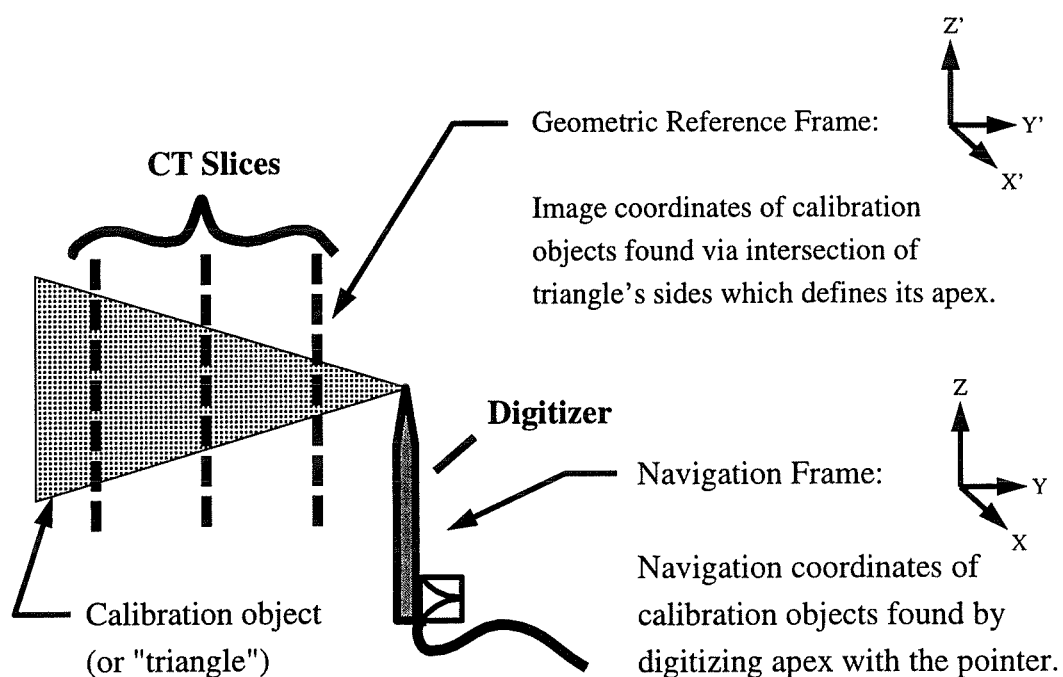
Figure 4-3 Calibration between image and navigation system reference frames.

After the image acquisition, the patient is exited from the scanner, and the magnetic position sensors used as a 3D pointing device to directly digitize the apexes of each calibration triangle. Use of the magnetic sensor as a pointer is made possible through an

additional transformation between the sensor and the tip of the pointer described in the system's device manual. The geometric model and navigation system coordinates of the three calibration objects permitted the calculation of the necessary transformation between the navigation frame and the geometric model frame. The system also registers the magnetic sensor's position and orientation in space during the digitizing for both the femur ($M_{InitPosF}$) and tibia ($M_{InitPosT}$) which is stored in a calibration file along with the coordinates of the calibration objects.

To generate an animation, the femoral and tibial position sensors are assumed to behave as rigid bodies with the femoral and tibial geometric models respectively. The inverse of the initial position and orientation matrix is multiplied by the calibration matrix to give the matrix Mcal for the femur ($_F$) and tibia ($_T$).

$$M_{CalF} = M_{InitPosF} \times M_{ScanNavF}$$
$$M_{CalT} = M_{InitPosT} \times M_{ScanNavT}$$

Eq. 4-2

This calibration matrix is multiplied by the recorded kinematics matrices for the femur M_{KinF} and the tibia M_{KinT} and the matrix describing points on the geometric model M_{GeoF} and M_{GeoT} to give the total animation matrix M_{TotF} and M_{TotT} :

$$M_{TotF} = M_{CalF} \times M_{KinF} \times M_{GeoF}$$
$$M_{TotT} = M_{CalT} \times M_{KinT} \times M_{GeoT}$$

Eq. 4-3

The resulting computer animations of 3D knee movement are performed on an IRIS Indigo Elan (Silicon Graphics) using an interactive program developed in our laboratory.

4.6 Methodology

4.6.1 System accuracy evaluation

Errors in prosthetic ligament deformation calculations arise from errors in the measured knee kinematics and errors in the initial position estimate of the simulated ligament. The kinematic errors arise from the movement between the attachment system and the underlying bone as well as the inaccuracies of the tracking sensors used to record the knee movement. Error in the initial position of the prosthetic ligament arises from error in the geometric model and the calibration procedure which mathematically matches the kinematics to the geometry.

The largest source of kinematic error arises from the movement between the attachment system and the underlying bone; a quantity which has been previously evaluated (Sati et al., in press) to be on average below 2.5 degrees in axial and ab-adduction rotation and below 2.5 mm in AP and axial displacement. Maximal errors from the attachment system were found to be below 5 mm in displacement and 5 degrees in rotation. Kinematic error arising from the magnetic sensor was obtained through another previous study to be on average 1 mm in displacement and 0.35 degrees in rotation and maximally 2 mm in displacement and 0.7 degrees in rotation (Sati & Vaillancourt, 1992).

Calibration error was defined as the residual between the calibration point coordinates in the navigation system frame and the image coordinates which were transformed into the navigation system frame during the calibration. Geometric error was obtained from previous papers describing the reconstruction method (de Guise & Martel, 1988;Aubin et al., submitted).

To estimate total system error, both average and maximal component errors were expressed with respect to the X, Y and Z axes defined in Figure 4-1. The root of the sum of the squares of the X, Y and Z component errors were calculated to determine total system X, Y and Z errors.

4.6.2 Prosthetic ligament placement

The interaction between active structures (muscles) and passive structures (connective tissue) determines the kinematics of *in vivo* knee movement. For example, forces generated by the associated muscle define tendon loading. Ligaments, unlike tendons, are loaded by bone movement since their function is to maintain the knee within a safe "envelope" of movement unless a large load exceeds their mechanical strength. Therefore, we can fully describe the displacements and rotations of the ends of the ligament by accurately tracking the kinematics of the femur and tibia during dynamic movements. Therefore, to help predict prosthetic ligament deformations, kinematics generated from the precisely attached magnetic sensors are to be employed.

The function of the prosthetic ligament replacement is to restore normal knee movement. It is therefore assumed that normal knee kinematics can be used to predict prosthetic ligament deformations.

Unlike the natural anterior cruciate ligament (ACL) and posterior cruciate ligament (PCL), prosthetic ACL's and PCL's are anchored via tunnels in the femur and tibia (see Figure 4-4). The angle formed between the tunnels and the ligament body create combined elongation, flexion and torsion deformations in the ligament as the knee is flexed. Elongation of the ligament is defined by the relative displacement of the femoral and tibial intra-articular attachment points. Keeping these entry sites constant, it is possible to change flexion and torsion in the ligament by varying the angle between the

tunnel and ligament body. Ligament torsion is defined as the twisting of the intra–articular part of the ligament about its long axis. Bending of the ligament is defined as the angle between the ligament functional body with respect to either the femoral insertion tunnel (femoral bending) or the tibial insertion tunnel (tibial bending) (see Figure 4–4). Therfore the term deformation in this paper refers to the relative elongation, bending and twisting of the insertion tunnels with respect to the ligament body.

a)   b)
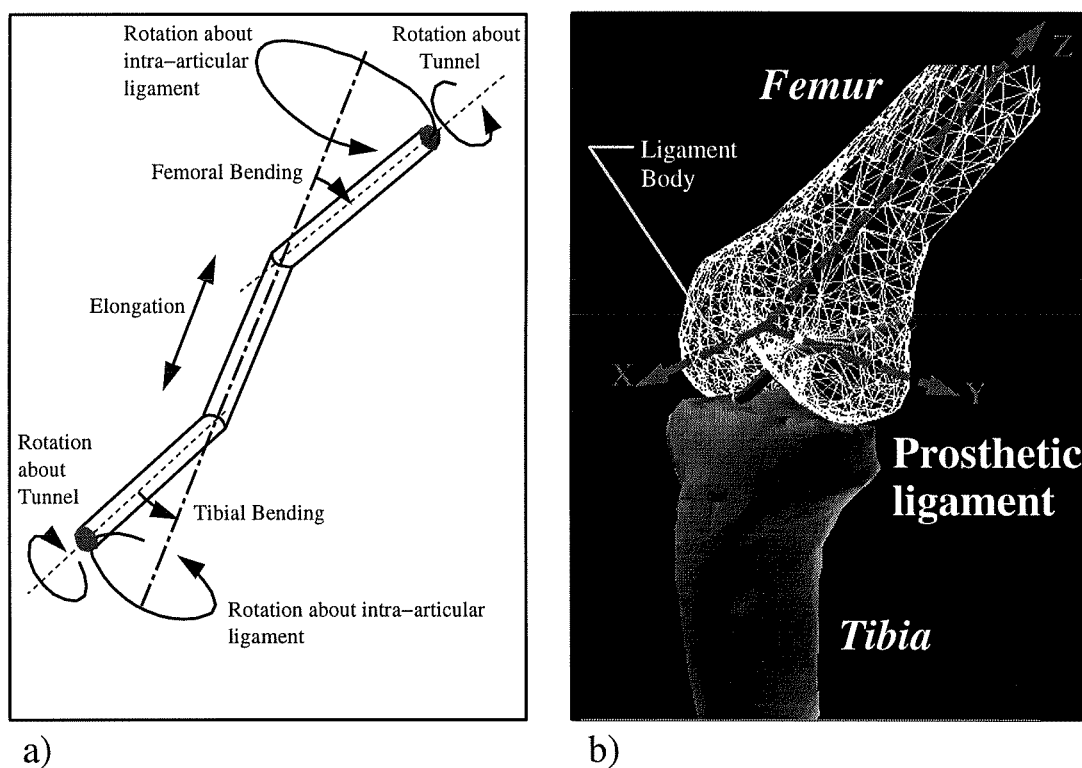
Figure 4–4 PROsthetic Ligament Information Generating System (PROLIGS).

A previously developed interactive computer program, the "Prosthetic Ligament Information Generating System" (PROLIGS) (Sati et al., 1991), was used to calculate

prosthetic ligament deformations based on the "inverse deformation principle" (Gely et al., 1984). To calculate prosthetic deformations, the ligament is first simulated within the 3D kinematic model of the knee. The ligament insertion tunnels are simulated via cylindrical objects, one in the femur and one in the tibia, through which a simulated artificial ligament is passed (see Figure 4-4). The intra-articular attachment points of both femoral and tibial tunnels often correspond to the attachment sites of the natural ligament. In this study, these intra-articular points were chosen according to a suggested placement in the literature (Cazenave & Laboureau, 1990). The exterior entry point of both the femoral and tibial tunnel therefore determine the orientation of the ligament's femoral and tibial insertion respectively. Once the ligament was placed, the customized kinematics were applied to the bone-ligament geometry and deformations on the ligament calculated. *In vivo* data analysis was performed on three subjects to demonstrate the feasibility of the approach. The subjects were asked to perform knee squats and a heel raise off the ground towards the buttock, over approximately 0 to 80 degrees knee flexion. The results for one of the subjects is reported in detail.

To ensure that ligament deformation calculations were correct, known deformations were generated by a simulator written in MATLAB™ and applied directly to a simulated prosthetic ligament (see Figure 4-4a). PROLIGS was then used to decompose the torsion, bending and elongation deformations resulting from the simulated movements. Comparing the simulated and calculated deformations for many 3D rotation combinations ensured the proper function of the algorithm.

In the previous section, the average and maximal system error in generating 3D knee geometry movement was determined. The accuracy of prosthetic ligament deformations calculated from this data must be evaluated to prove that the results are clinically significant. To evaluate errors in prosthetic ligament deformations, the total system error was considered to be a noise which perturbed the 3D geometry's movement

instantaneously when the knee reached 45 degrees flexion. The deformations of a prosthetic ligament, inserted in a typical surgical orientation, were then calculated from these kinematics. The difference between ligament deformations calculated with and without this perturbation was used to quantify the error in predicting ligament deformations *in vivo*.

This methodology is described in great detail in a previous paper (Sati et al., submitted), where the perturbation analysis was used to evaluate the error in prosthetic ligament deformation calculations arising only from the attachment system component of knee analyzer system. The movement with respect to underlying bone of the attachment system represents the largest source of error in the knee analyzer, even though it reduces sensor-bone movement significantly over traditional attachment methods (Sati et al., submitted).

Once the accuracy of the system was explored via the perturbation analysis, the manufacturer suggested insertion of a commercially available ACL and PCL ligament prosthesis was simulated and deformations calculated. The surgeon selects the desired entry and exit points to interactively simulate the prosthesis's placement in the 3D geometric model of the knee. This procedure involves manipulating the 3D model in the computer interface and hitting enter on the keyboard when the cursor overlies the desired position for each point. A point is placed on the intra-articular surface of both the femur and tibia to specify the position of the intra-articular portion of the ligament. These intra-articular points were chosen in this study according to a suggested placement in the literature (Cazenave & Laboureau, 1990). An external entry point on the tibia determines that of the tibial tunnel and an external entry point on the femur determines the orientation of the femoral tunnel. Both femoral and tibial ligament insertion tunnels are graphically simulated via cylindrical objects, through which a simulated artificial ligament is passed in the computer interface. After placement of the ligament, the customized kinematics are applied to the bone-ligament geometry and deformations on the ligament calculated. To

demonstrate the feasibility of the approach, data analyses were performed on three subjects. Kinematic data were obtained from active knee squats and heel raises off the ground towards the buttock, over approximately 0 to 90 degrees knee flexion.

To further validate the accuracy of the knee analyzer, ligament elongation data is compared with that found in the literature. Femoral insertion as described by Hefzy et al.(1989) and Grood et al. (1989) were reproduced in this study on the 3D personalized geometry and elongation calculations performed to compare the present non-invasive *in vivo* results with those obtained by the invasive cadaveric studies.

4.7 Results

4.7.1 System accuracy evaluation

Geometric model error has been previously evaluated to be a maximum of 1 mm rms (de Guise & Martel, 1988;Aubin et al., submitted). Kinematic error arising from relative movement between the attachment system and the underlying bone have been previously evaluated (Sati et al., submitted) and are summarized in Table 4-1b. The maximal kinematic error from the tracking sensor is 2 mm rms and 0.7 degrees over the 1 meter radius in which the tests were performed (Sati & Vaillancourt, 1992). Maximal calibration error was evaluated to be 2 mm in displacement and 1.5 deg in rotation (see Table 4-1b). The root mean square total errors along the X, Y and Z axes can be seen at the bottom of the table. Average component errors and their root mean square totals are presented in Table 4-1a.

Table 4-1 Component errors of system

a) Average System Errors

Component	X		Y		Z	
	Pos. (mm)	Orient. (deg)	Pos. (mm)	Orient. (deg)	Pos. (mm)	Orient. (deg)
Geometry	0.5	0	0.5	0	0.5	0
Kinematics Attach. Sys.	2.41	-0.37	0	0	1.1	-2.27
Nav. Sys.	1	0.35	1	.35	1	0.35
Calibration	1	0.75	1	0.75	1	0.75
Total	2.84	0.91	1.50	0.83	1.86	2.42

b) Maximal System Errors

Component	X		Y		Z	
	Pos. (mm)	Orient. (deg)	Pos. (mm)	Orient. (deg)	Pos. (mm)	Orient. (deg)
Geometry	1	0	1	0	1	0
Kinematics Attach. Sys.	5.32	1.78	0	0	2.50	5.01
Nav. Sys.	2	0.7	2	0.7	2	0.7
Calibration	2	1.5	2	1.5	2	1.5
Total	6.11	2.43	3.00	1.66	3.91	5.28

4.7.2 Prosthetic ligament placement

Known simultaneous bending, torsion and elongation values generated by the MATLAB simulator, were reproduced exactly by PROLIGS (see Table 4-2). This held true even for torsion and bending values greater than 90 degrees.

Table 4-2 Verification of program function through simulation

a) Stimulated deformations

frame #	Femoral Bending (deg)	Tibial Bending (deg)	Torsion (deg)	Elongation (mm)
0	20	20	0	0
1	30	30	-20	0
2	40	40	-60	0
3	50	50	-100	0
4	60	60	-140	0
5	70	70	-180	0
6	80	80	-220	0

b) Calculated deformations

frame #	Femoral Bending (deg)	Tibial Bending (deg)	Torsion (deg)	Elongation (deg)
0	20.0013	20.0013	0	-0.0000
1	29.9613	29.9613	-20.0166	-0.0100
2	39.9905	39.9905	-60.1078	-0.0120
3	49.9860	49.9860	-100.0373	-0.0040
4	59.9681	59.9681	-140.0656	-0.0100
5	69.9785	69.9785	-180.0877	-0.0100
6	80.0173	80.0173	-220.0354	-0.0000

The perturbation analysis revealed that both average ligament bending and torsion deformation errors were below 5 degrees (see Table 4-3a). Maximal bending error was 6.5 degrees (femoral bending) and maximal torsion error was 5 degrees (see Table 4-3b). Average elongation errors were below 1.8 mm and maximal elongation errors were below 3.8 mm.

Table 4-3 Sensitivity of calculations at 45 deg. knee flexion for a typical ligament insertion

a) Sensitivity to average errors

Applied perturbation	Magni-tude	Femoral Bending (deg.)	Tibial Bending (deg.)	Ligament Torsion (deg.)	Ligament Elongation (mm)
A-P displace. (Tx)	2.84 mm	-1.65	4.84	5.30	-0.66
M-L displace (Ty)	1.50 mm	-3.53	-1.89	0.82	0.28
Axial displace. (Tz)	-1.86 mm	-0.25	-0.80	0.63	-1.83
Ab-ad. rotation (Rx)	0.91 deg.	-1.91	-0.54	0.35	0.44
Flexion rotation (Ry)	0.83	0.27	0.09	0.74	-0.27
Axial rotation (Rz)	2.42 deg.	0.93	1.19	-3.19	0.03

b) Sensitivity to maximal errors

Applied perturbation	Magni-tude	Femoral Bending (deg.)	Tibial Bending (deg.)	Ligament Torsion (deg.)	Ligament Elongation (mm)
A-P displace. (Tx)	6.11 mm	4.55	1.23	-3.80	-1.74
M-L displace (Ty)	3.00 mm	-6.41	-4.59	-0.82	0.46
Axial displace. (Tz)	-3.91 mm	-1.37	-1.57	0.30	-3.84
Ab-ad. rotation (Rx)	2.43 deg.	-1.21	2.08	-1.52	-0.53
Flexion rotation (Ry)	1.66 deg.	1.05	2.54	0.30	-0.67
Axial rotation (Rz)	5.28 deg.	2.70	1.66	-4.91	0.03

Ligament elongation, bending and torsion calculated by the system can be seen in Figure 4-5 and Figure 4-6 for the placement of a commercial ACL prosthesis and a commercial two-band PCL prosthesis (Laboureau & Bercovy, 1993). Both medial and anterior viewpoints of the simulated ligament in the knee can be seen at the top of each figure. Values of ligament bending at the femur, bending at the tibia, torsion in the ligament and

elongation of the ligament are seen plotted at the bottom of each figure. The position of the ACL ligament was accurately reproduced by two surgeons. Placement of the two–band PCL ligament proved to be difficult to reproduce between the surgeons.

For the comparison of deformation data with that in the literature, Figure 4–7c shows ligament elongations generated from experimental data in this study corresponding to

cACL #1

a) Medial view

b) Anterior view

FE

c)
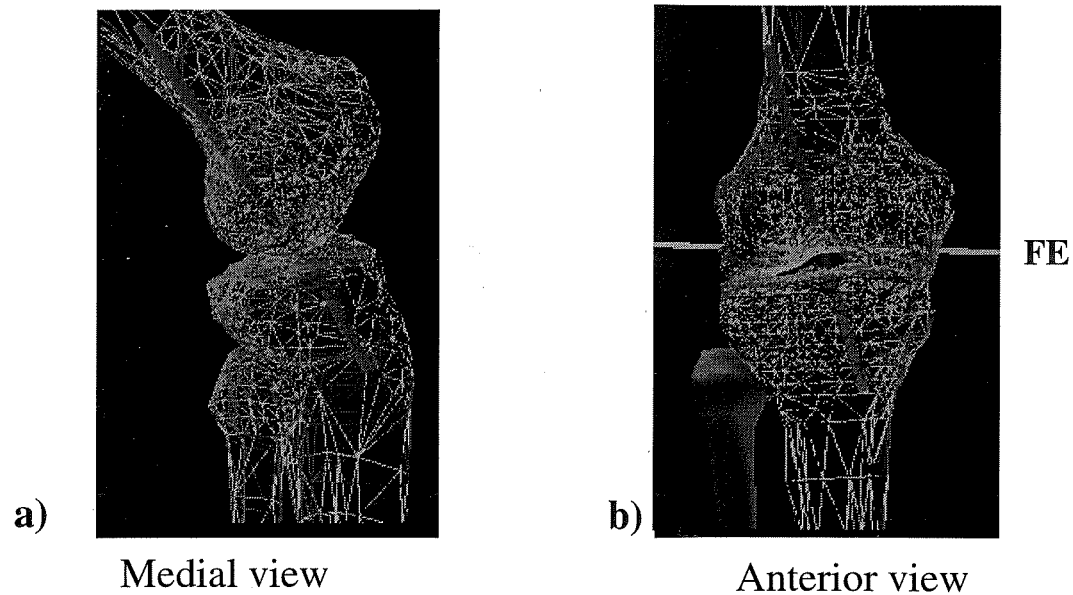
Figure 4–5 Deformation resulting from a placement suggested for commercial ACL prosthesis #1.

cPCL #1
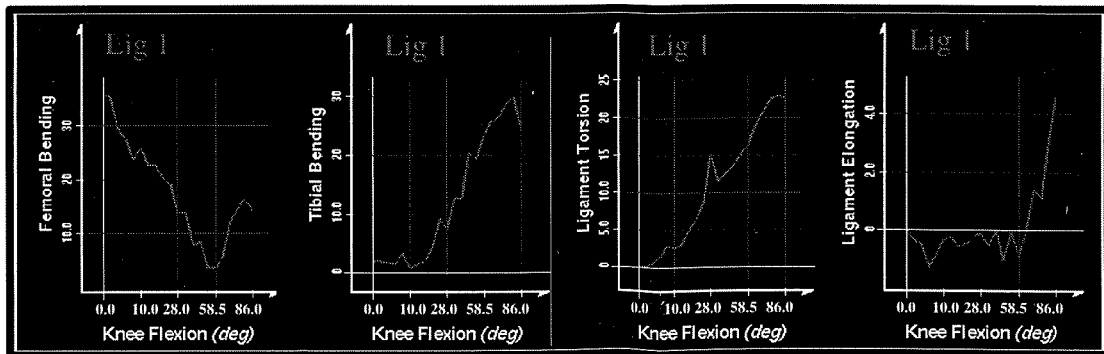

a) Medial view   b) Anterior view

c)
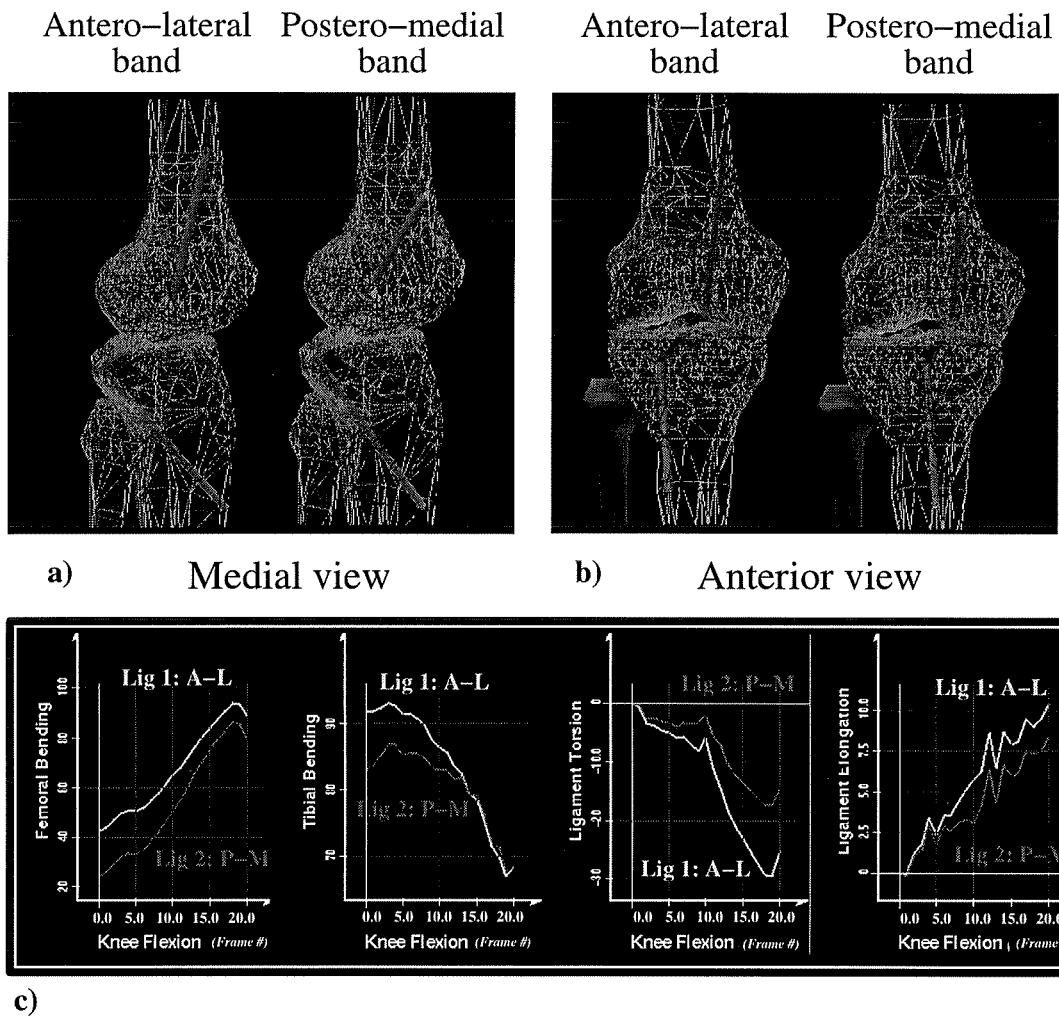
Figure 4–6 Deformation resulting from a placement suggested for commercial PCL prosthesis #1.

femoral insertions a to f in Figure 4–7a. Data for PCL deformations can be seen in Figure 4–8c corresponding to several femoral insertion locations Figure 4–8a.
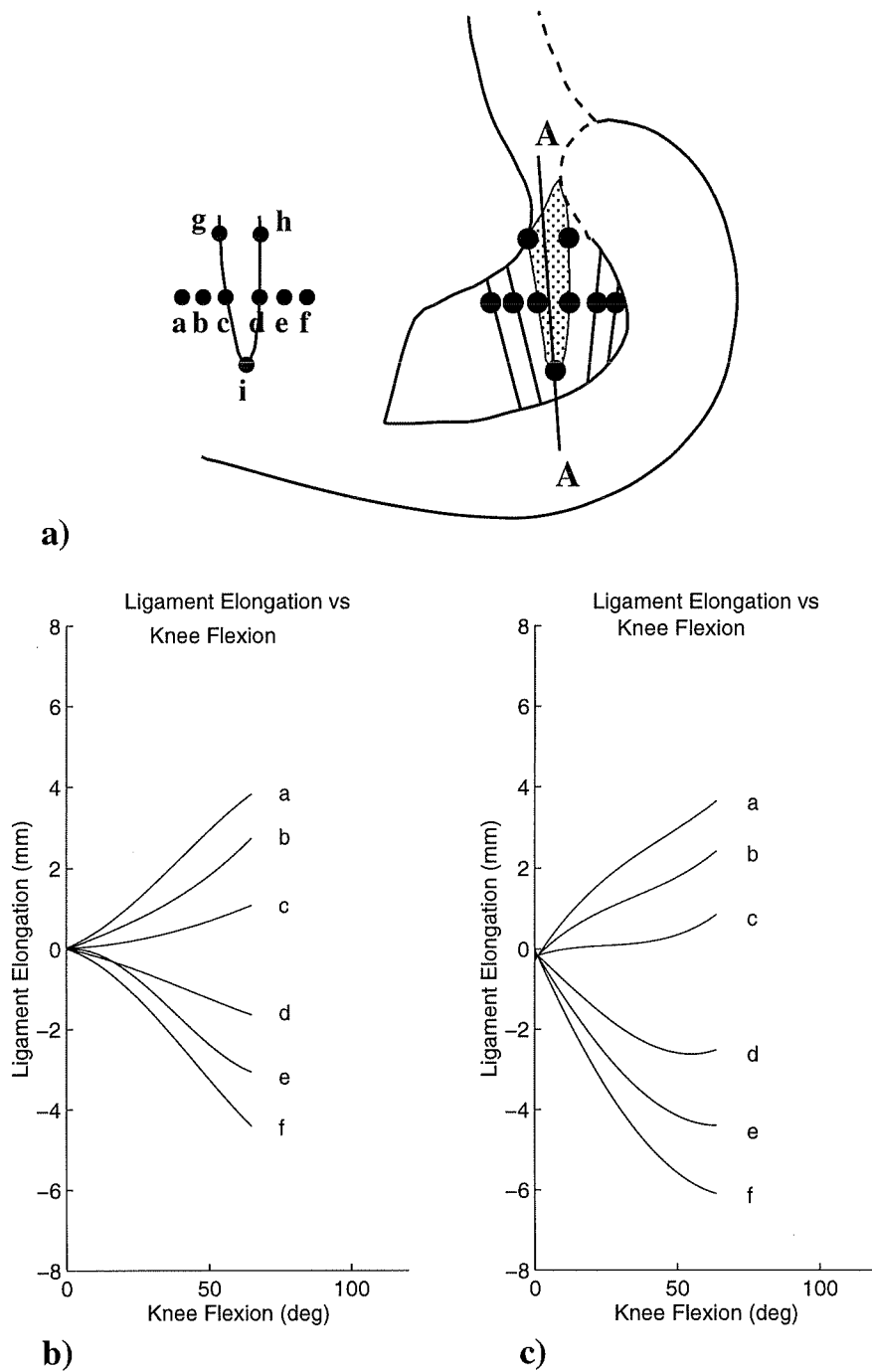
Figure 4–7 ACL elongation a) femoral insertion points investigated by Hefzy et al. (1989) b) elongation values found by Hefzy et al. c) elongation values calculated in the present study.
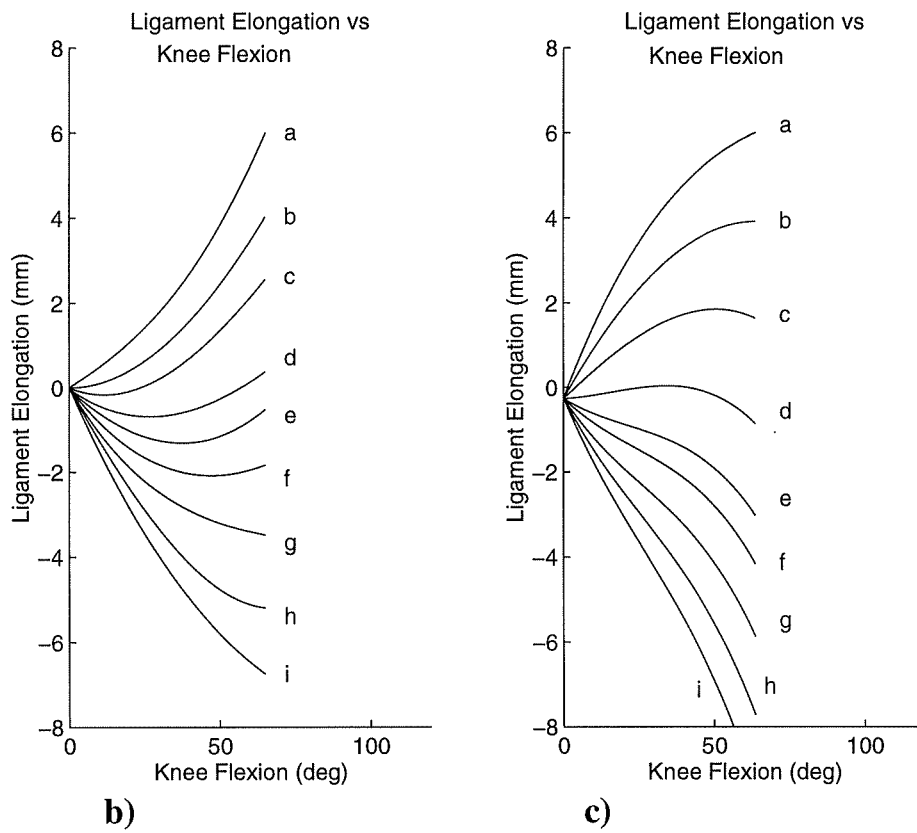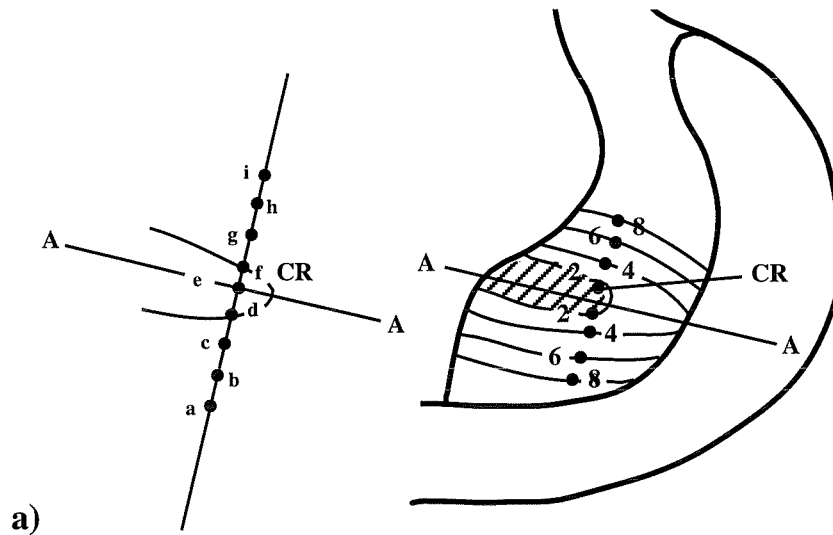
Figure 4–8 PCL elongation a) femoral insertion points investigated by Grood et al. (1989) b) elongation values found by Grood et al. c) elongation values calculated in the present study.

4.8 Discussion

To our knowledge, the knee analyzer represents the first virtual interface with the knee of its kind allowing 3D knee movement analysis for surgical planning. The system provides direct representation of *in vivo* bone movement and geometry with which the user can interact. Since the "virtual knee" reproduces 3D movement and geometry of the real knee, *in vivo* deformations in the real knee can be predicted through simulations in the virtual knee. Before the present work, 3D *in vivo* bone movement had never been seen.

4.8.1 System accuracy evaluation

It was found, by combining component errors, that the system average error in measuring knee kinematics, was 2.8 mm in displacement and 2.4 degrees in rotation and the maximal error was 6.1 mm in displacement and 5.3 degrees in rotation. These error values are not much higher than those previously calculated for the attachment system movement with respect to the underlying bone (Sati et al., submitted). This level of accuracy represents a significant improvement over data obtained using skin mounted markers (Sati et al., in press). The compact nature of the technology encourages its transformation into a clinical tool which could help both in the diagnosis of previously hard to detect pathologies and the surgical planning of corrective measures.

4.8.2 Prosthetic ligament placement

The precise calculation of prosthetic ligament deformations imposed on the ligament by the simulator showed the software gave accurate results provided that the input

kinematics were correct. The perturbation analysis helped quantify the error in *in vivo* prosthetic ligament deformations arising from the total error of the system. Since it is difficult to surgically place prosthetic ligaments with accuracy greater than 5 degrees, we believe that the system error is sufficiently low to provide clinically significant deformation values. Elongation deformation was not the primary objective of the study, however average error below 1.8 mm and maximal error below 3.8 mm could be useful for certain clinical studies.

Simulation and calculation of the manufacturer-suggested ACL placement demonstrated the feasibility of such analysis. Work needs to be done to improve the reproducibility of PCL insertion before analysis of this two-band prosthesis can be performed. To improve repeatability of placement a more rigid protocol must be developed and the computer interface slightly modified to provide surgeons with viewpoints of the knee that they are more accustomed to. The surgeons also require simultaneous representation of both bands of the PCL prosthesis in the computer model, since they rely on their relative position for proper placement.

Non invasive estimation of ligament elongation is difficult since it is very sensitive to noisy movement data. The present system was not designed to measure ligament elongation or study the question of isometry, however the similarity of elongation data with invasive studies by Grood and Hefzy helps validate its accuracy. It can be seen that over 65 degrees knee flexion, ACL elongation calculated from the non invasive *in vivo* data closely resemble those of Hefzy et al. (Figure 4-7b and c). PCL deformations from non invasive *in vivo* data (Figure 4-8c) also closely resemble those reported by Grood et al. through 0 to 65 degrees knee flexion.

Differences in ligament elongation for high flexion values can be expected since it is known that the attachment system has a small displacement with respect to the underlying

bone which increases with knee flexion, especially during high degrees of knee flexion (Sati et al., submitted). Other discrepancy is that cadaveric tests involved knee flexion with 100N loads, whereas *in vivo* tests involved raising the heel off the floor towards the buttock. Further study must be performed, however, before data from the present system is to be used to find the so-called "isometric point" of ligament insertion.

4.9 Conclusions

This paper has presented a unique virtual interface and its use for the calculation of prosthetic ligament deformations. The system provides knee movement kinematics with maximal errors of 6.1 mm in position and 5.3 degrees in orientation.

Through the perturbation analysis, prosthetic deformations calculated from *in vivo* data were shown to be accurate to below 6.5 degrees for bending and 5 degrees for torsion. We believe this accuracy is sufficient to give meaningful data for planning surgical placement. Similarity observed between elongation data calculated with the system and that in the literature further demonstrates the accuracy of the system. The system is ready to be used for analysis of prosthetic ACL ligament deformations to help improve the surgical placement of these devices. Consistency of surgical placement needs still to be obtained before PCL ligaments can be properly placed.

4.10 Future Work

The use of prosthetic ligaments is presently limited due to past failures. We believe that this is largely due to a lack of understanding of both the biological and physical conditions that the ligament experiences *in vivo*. This system will be used in future studies

to help explain the relationship between surgical insertion and *in vivo* deformation conditions. Improved surgical placement based on quantitative data will hopefully augment the long term survival of these prostheses and help in the design of future prostheses. We also hope that the least-squares flexion-extension axis will serve as a functional reference to help in the surgical insertion of these implants.

The instrumentation and software developed for planning of prosthetic ligament placement could form a basis for other computer-aided knee surgery applications. Correction of a knee pathology requires accurate diagnostics, surgical planning and surgical implementation of the appropriate procedure. A computer-assisted clinical system could help improve consistency in this process. The knee analyzer would first be used to help evaluate the patient's knee pathology. The computer environment could then be used to help plan an "optimal" surgical procedure. Finally computer-assisted guidance of surgical tools could ensure proper implementation of the optimally planned procedure. Computer-assisted diagnosis, planning and image-guided intervention may help to improve efficiency, precision and reduce trauma by avoiding open surgery. Computer-assisted surgery applications based on this technology could include: ligament allograft/autograft replacements, total knee replacements, selection and placement of knee orthoses and planning of correctional osteotomies. The use of the knee analyzer to help diagnose ligament insufficiencies is presently under study.

4.11 Acknowledgments

CHAPTER V

5. APPLICATION OF THE SYSTEM TO ANALYSIS OF PROSTHETIC ACL AND PCL DEFORMATIONS

5.1 Introduction

In the previous chapter, the 3D knee analyzer has been described in detail as well as its accuracy to measure knee movement and predict prosthetic ligament deformations. The present chapter describes the analysis of prosthetic ligament deformations using the 3D analyzer.

Ligament deformation is first investigated as a function of different simulated surgical placements. With this analysis, a relationship between surgical insertion orientation and deformation is established.

It is difficult to interpret and communicate three-dimensional ligament deformations to ligament orientation in space. Finite helical axes (Veldpaus et al., 1988) and gyroscopic

angles (Grood & Suntay, 1984) can be used to help in the interpretation and communication of kinematic data. Helical axes describe knee movement by finite rotation axes which move in space during knee flexion. Euler-based systems like that of Grood and Suntay (1984) describe knee movement as a sequence of rotations about orthogonal axes. Interpretation of ligament deformations with respect to such moving or multi-parameter descriptions is complex. The relative merits of Euler-based and Helical-based methods have been actively debated over the past decade within the biomechanical community, especially through discussions over the internet (Biomch-L, 1991;Biomch-L, 1992). Both helical and Euler-based methods have their relative advantages and disadvantages, however neither is perfect for all applications.

Therefore, a simpler parameter, the flexion-extension (FE) axis of the knee was calculated in this thesis to serve as a three-dimensional reference direction to help interpret the relationship between ligament insertion orientation and deformation.

As a concrete example of the usefulness of the knee analyzer and the flexion-extension reference parameter for surgical planning, the placement of a commercially available prosthesis is analyzed.

5.1.1 Methodology

Kinematic data from three subjects was analyzed for this study according to the protocol described in the previous chapter. The subjects were asked to perform knee squats and raise their heel off the ground towards their buttock, over approximately 0 to 90 degrees knee flexion. Since data from all subjects showed the same tendencies, data for only one of the subjects studied is presented in detail.

The purpose of prosthetic ligament deformation calculations is to determine insertion orientations which will augment the fatigue life of prosthetic ACL's or PCL's. Therefore, several insertion orientations were investigated in the interactive computer graphics environment to determine relationships between ligament tunnel orientation and ligament deformations.

5.1.2 Flexion-extension (FE) axis

The "average" flexion-extension (FE) axis of the knee is calculated as a 3D functional reference landmark. A least-squares algorithm is employed to find the axis which "best fits" the knee's rotation. To calculate this axis, the coordinates of a point on the FE axis is described in the femoral reference frame by $[a]_F$ and the tibial reference frame by $[b]_T$. For this situation, the co-ordinates of $[a]_F$ and $[b]_T$ remain constant with respect to the femoral and tibial reference frames respectively for all knee positions "i" and are related by:

$$[a]_F = R_i \, \mathrm{x} \, [b]_T \, \mathrm{x} \, [t_i]$$

Eq. 5-4

where R_i and $[t_i]$ are respectively a 3x3 rotation matrix and a translation vector relating the two reference frames at some kinematic knee position "i". We cannot hope to attain exact equality in an experimental situation but a good solution of $[a]_F$ (or$[b]_T$) can be obtained using a least-squares optimisation on the data (Genoud, 1994;Richard, 1995).

To study the range of possible deformations, prosthetic ligament tunnels were oriented either parallel or perpendicular to the knee's FE axis. It will become clear below that the use of the FE axis as a reference orientation helps to interpret the results (see Figure 5-1).
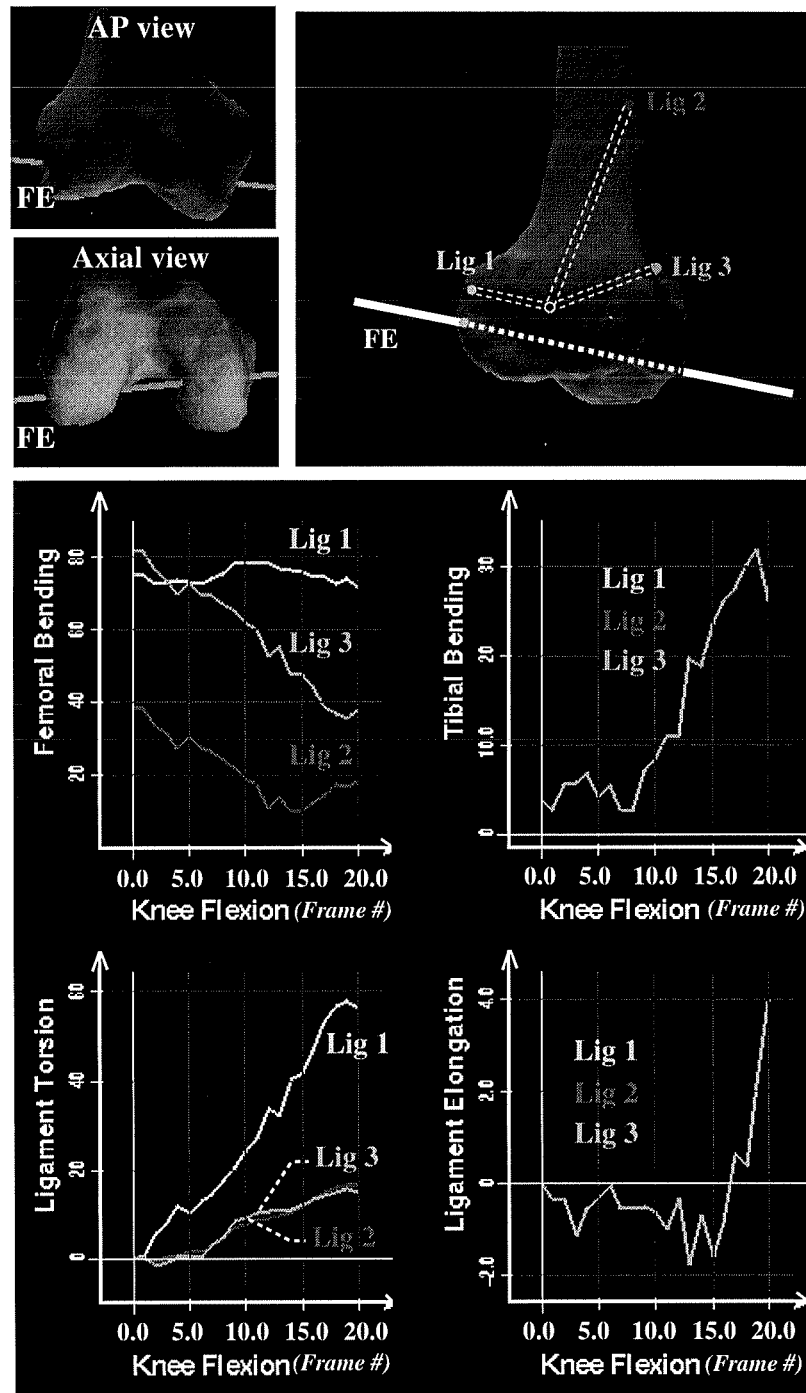
Figure 5–1 Deformations of ligaments placed in extreme orientations with respect to the flexion–extension (FE) axis. Ligaments placed parallel (Lig 1), perpendicular and proximal (Lig 2), perpendicular and anterior (Lig 3).

In this study, the intra-articular entry points of the ligament into the femur and tibia were held constant so that only the effect of orientation on bending and torsion could be studied. The intra-articular points were chosen according to a suggested placement in the literature (Cazenave & Laboureau, 1990) for all the analyses. Since the elongation of the ligament depends only on its intra-articular entry points, ligament elongation remains constant for all orientations investigated.

A suggested orientation for a commercially available ACL and PCL (Laboureau & Bercovy, 1993) (LARS, France, company manual), referred to as cACL#1 and cPCL#1, was also investigated as a practical example of how ligament deformations can be explained and analyzed to help improve their insertion (see Figure 5-1). The surgical orientation of these ligaments with respect to the FE axis was used to help describe the deformations they are subjected to.

It must be noted that placement of the ACL was more precise than that of the PCL for the above-suggested placements. Several surgeons were able to accurately reproduce similar ACL insertions whereas two-band PCL tunnels varied significantly.

5.2 Results

For the real knee movement data, prosthetic ligament deformation values varied more with changes in femoral tunnel orientation than tibial tunnel orientation. Therefore, the effect of changes in femoral tunnel orientation were studied in detail. In Figure 5-1a, tunnel 'lig1' is oriented parallel to the FE axis, tunnel 'lig2' is oriented perpendicular to the FE axis and oriented proximally and tunnel 'lig3' is also oriented perpendicular to the FE axis but oriented anteriorly. Deformations of 'lig1', 'lig2' and 'lig3' can be seen at the

bottom of the figure as a function of frame number in the animation. The movement recored for this study involved a knee flexion from 0 to 85 degrees which is represented by frames 0 to 20 in the graphs.

cACL #1

a) **Medial view**

b) **Anterior view**

FE

c)
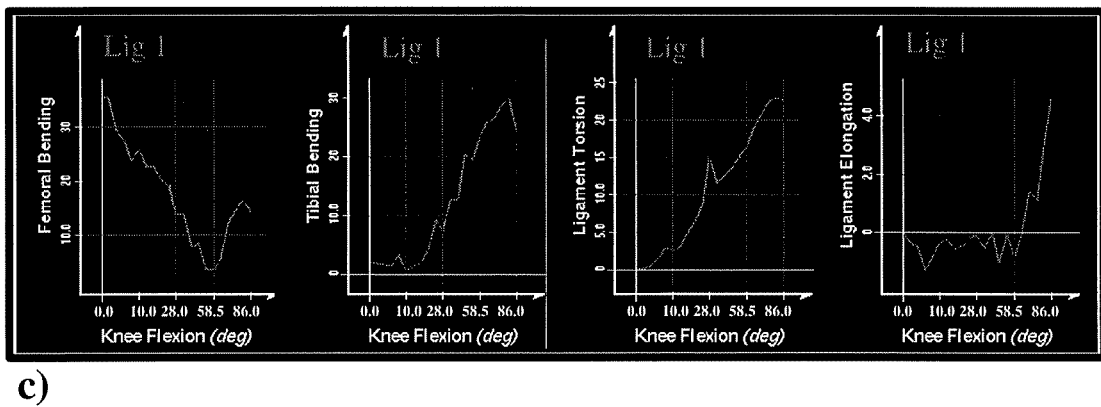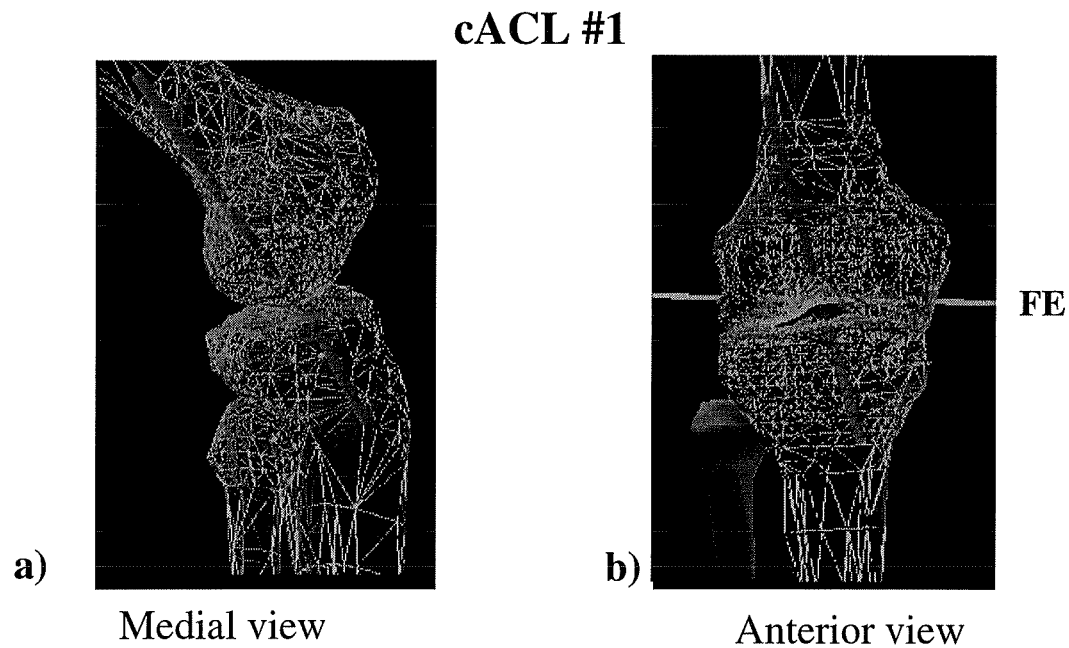
Figure 5–2 Deformations resulting from a placement suggested for commercial ACL prosthesis #1.

It was found that the orientation of ligament #1 resulted in maximal ligament torsion values and minimal changes in bending values. Orientations of ligaments #2 and #3

had very low torsion values, but both had large changes in bending values which were of similar magnitude. However ligament #3 had a much higher initial bending value than liagment #2. Therefore, bending and torsion deformations on ligament #2 and #3 had similar changes in torsion and flexion yet different initial bending values.
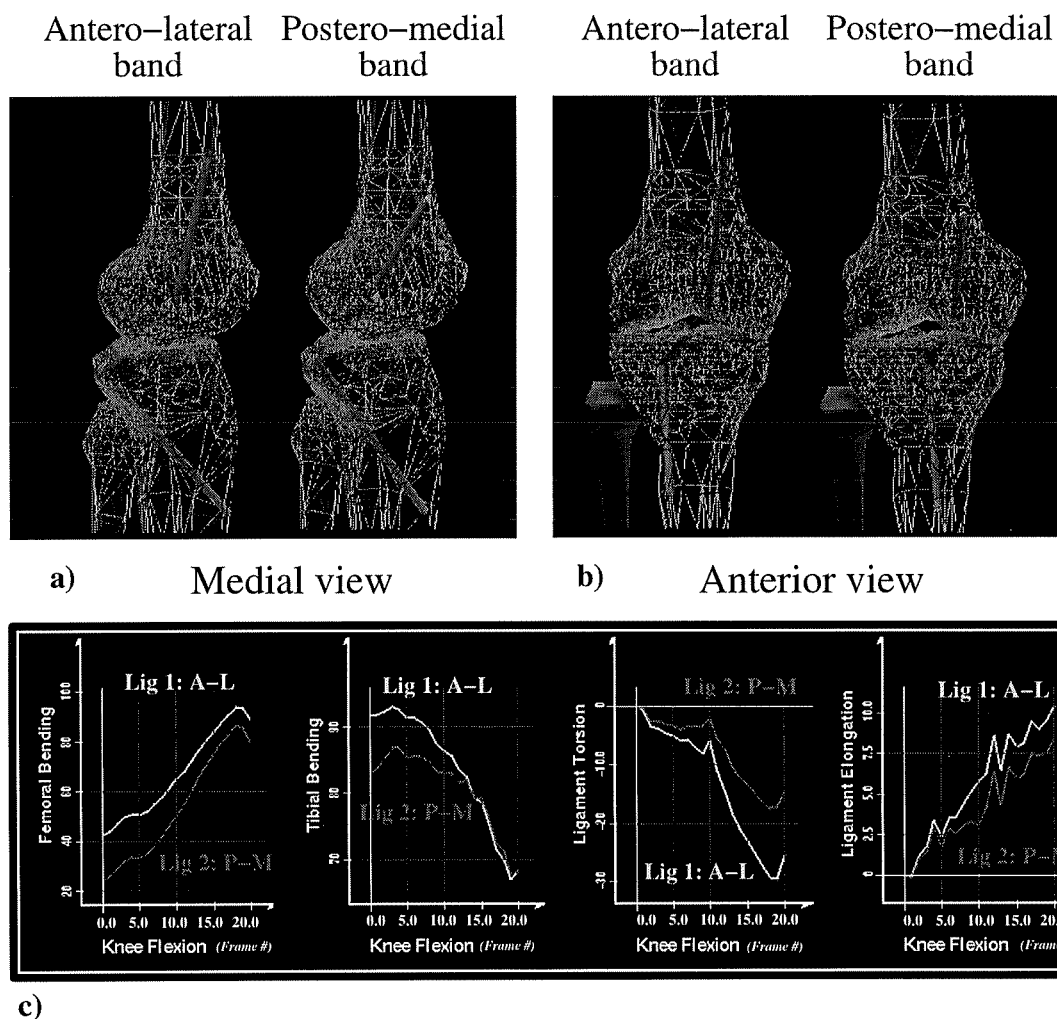
cPCL #1

a) **Medial view** b) **Anterior view**

c)

Figure 5–3 Deformations resulting from a placement suggested for commercial PCL prosthesis #1.

Deformations on the commercially-available ligament cACL#1 and cPCL#1 can be seen in Figure 5-2 and Figure 5-3 respectively. It was noted that the orientation of cACL#1 was close to that of 'lig2' which is perpendicular to the FE axis. Change in torsion was therefore small and change in femoral bending high. Femoral bending reached a minimum near mid-flexion of the knee.

5.3 Discussion

Interpretation of the results may be simplified by relating the ligament tunnel orientation to the average flexion-extension axis "FE" of the knee (Figure 5-1). For ligament **lig1**, the femoral tunnel is approximately parallel to the average flexion axis of the knee. Therefore flexion of the knee rotates the femoral tunnel about its axis, creating torsion in the ligament. Since the intra-articular portion of the ligament is approximately perpendicular to the **FE** axis, the bending angle between the femoral tunnel and the ligament is high yet approximately constant throughout the flexion. For ligament 2, the femoral tunnel is approximately perpendicular to the average flexion axis. Therefore, flexion of the knee will rotate the femoral tunnel about an axis perpendicular to its long axis, causing much change in bending yet little torsion in the ligament. Ligament 3 is also perpendicular to the **FE** axis but is oriented differently than ligament 2, therefore it has the same change in torsion and bending as ligament 2, but starts out with a higher initial flexion angle, which explains the offset in the bending calculations.

It can be appreciated from these tunnel placements resulting in maximal deformations that the ligament insertion tunnel orientations can be varied to provide a broad range of possible ligament deformations. Studying these extreme placements helps our

understanding of the relationship between tunnel orientation and ligament deformation and allows us to situate presently proposed ligament placements with regard to possible deformations.

The ACL #1 prosthesis showed relatively little change in torsion deformation and a large change in bending deformation. This ligament is designed to have pre-twisted fibers in the intra-articular portion of the knee which un-twist during knee extension. This pre-twist is set at 90 degrees clockwise or counterclockwise depending if it is to be used for a left or right knee. However, it was observed from the calculations that ligament torsion remained below 25 degrees over 90 degrees knee flexion. Therefore, the present twist in the ligament is much higher than required an may even be detrimental to the ligament in the long run due to excessive rubbing between inter-twisted fibers.

The design of the twist is based on the observed rotation of the natural ligament's attachment site. Since the natural ligament is attached on the medial aspect of the lateral condyle, its femoral attachment rotates in the sagittal plane. This is true for the natural ligament since its "attachment orientation" is perpendicular to the articular surface where it enters the femur. This is similar to having a prosthetic ligament tunnel oriented medio-laterally (or parallel to the FE axis) which would also result in a large change in torsion. The much lower torsion value for ACL #1 is due to the fact that the suggested femoral tunnel insertion is *perpendicular* to the FE axis.

The large change in femoral bending is not good for the fatigue life of the ligament. However, the minimum near 0 degrees in femoral bending at mid-flexion of the knee reduces the effect of this large change. Fatigue is therefore lessened because the ligament is relatively straight at a frequent knee flexion angle.

Detailed description of the PCL deformation is not described here since the variance between placement by several surgeons was too large. For future analysis, more work has to be performed to help consistently define two-band PCL insertions.

5.4 Conclusions

It was suggested that prosthetic ligament deformations could be explained in reference to their orientation with respect to the FE axis of the knee. Insertion of the tunnel parallel to the FE axis maximized torsion while minimizing bending and vice versa for tunnels placed perpendicular to this axis. This indicated and explained a tradeoff which exists when choosing a prosthetic ligament insertion orientation.

The analysis in this chapter showed that the pre-torsion designed into the cACL#1 prosthesis was too high and should be reduced to fine-tune its desired function. It was also shown that the ligament was placed in a region where femoral bending deformation is very high and torsion very low, since the femoral tunnel is oriented perpendicularly to the FE axis. The relative straight position of the ligament at a common knee flexion angle however reduces the fatiguing effect of the large change in bending. This and other such information from the knee analyzer system should help the understanding of prosthetic ligament fatigue *in vivo* to help augment their long-term survival and their future designs

CHAPTER VI

6. GENERAL DISCUSSION

Instrumentation and software has been developed and validated to help determine the relationship between prosthetic ligament insertion and deformation. The fluoroscopic method has accurately quantified relative skin-bone movement and provided the basis for the development and analysis of a new mechanical device for improving knee movement measurement accuracy. This device was equipped with movement sensors and integrated into a novel 3D virtual knee analyzer interface. Additionally, software has been developed in this environment has allowed calculation of prosthetic ligament deformation corresponding to personalized geometry and *in vivo* knee kinematics.

Results from the fluoroscopic skin movement study and the performance of the knee analyzer are compared with information in the literature in the section 6.1. Analysis of prosthetic ligament deformations are then discussed in section 6.2. The performance of the entire virtual interface is discussed with respect to the literature in section 6.3. Future improvement and suggested developments are presented in the respective sections.

6.1 Movement data acquisition

The fluoroscopic study identified skin-bone movement to be by far the largest source of error in knee movement analysis. It also provided detailed quantitative information on the magnitude and direction of this error over the entire medial and lateral aspects of the knee.

The order of magnitude of skin movement, reported to range from 4 to 44 mm (or 2 to 17 mm rms), was similar yet more detailed than that found in the literature. Macleod and Morris (1987) found relative movements between knee and ankle markers to vary by 15 mm. Lafortune et al. (1991), using raw fluoroscopic sagittal projections of subjects performing squats, found skin movement over the lateral epicondyle of approximately 20 mm AP and 18 mm axially which compared to the 22 mm and 15 mm displacements respectively found in the present study. Using a similar protocol to Lafortune et al., Cappozzo et al. (in press) reported AP displacements of 20 mm and axial displacements of 9 mm over the lateral condyle. Cappozzo et al. went on to use internal fixators to obtain more quantitative data over the lateral condyle during cycling movements. They reported 4.7 mm rms AP displacement and 2.5 mm rms axial displacement. In contrast, the present study found movement over the lateral condyle of 8 mm rms AP and 4 mm rms axially.

The fluoroscopic study in the present work was quantitative since corrections for magnifications and bone orientation were taken into account, whereas those by Lafortune et al. and Cappozzo et al. were intended to be qualitative. One drawback of the fluoroscopic approach is that only sagittal plane movement is reported. It is, however, possible to observe fluoroscopic AP projection of markers during knee flexion to gather qualitative data on this movement. The quantitative medical imagery approach is advantageous over intrusive measures since it does not cause complications or reduce

natural knee or skin movements. The fixators used in the study by Cappozzo et al. (1995) were often attached onto underlying bone near the lateral condyle. Skin movement over the lateral condyle was therefore difficult to obtain. This provides an example of how a measurement method can interfere with the desired quantity to be measured.

The information on skin movement obtained in this study, along with a study of the knee anatomy, was the basis for the design of the proposed attachment system. The attachment system reduced skin movement, which can range from 2 to 17 mm rms, to 1.5 to 3.6 mm rms. With this reduction of the artifact, knee movement measurement error was below 2.5 degrees for both ab-adduction and axial rotation and below 2.5 mm rms for both AP and axial translation over 65 degrees knee flexion.

These results compare favorably with the few methods presented in the literature which have attempted to reduce skin movement error. Murphy (1990) has compared data from invasively pinned sensors to that acquired with arrays strapped carefully onto bony prominences. He found that skin movement artifacts attenuated rotation angles by fifty percent and made smooth movement look noisy, complex and unrepeatable. Murphy concluded that a better attachment method was required to obtain sufficient accuracy to fully characterize knee kinematics. Hart et al. (1991) evaluated the accuracy of one of the ancestors of the present attachment system on cadaveric specimen. They found a total difference of 4.9 degrees in orientation and 3.6 mm rms in position between the attachment system and bone over 20 to 80 degrees knee flexion. More recently, Cappozzo et al. (1993) have reported some preliminary studies on the accuracy of plates mounted with straps onto the proximal or distal thigh during cycling. They found that plate marker movement (of the order of 3 to 4 mm rms) was less than skin marker movement (of the order of 3 to 8 mm rms over different regions of the thigh). However, it was noted that the relatively large distance between the plate markers and the articulation would affect bone axis definition. At the time of their study, it was suggested that improved design of

coupling between bone and plate would make the use of plates preferable, although this suggested approach seems to have been abandoned for mathematical correction procedures of skin movement (Cappozzo et al., in press).

Observations by Cappozzo et al. (1993) of the error in bone axis definition due to the distance between markers and the joint center of mechanical axes raise an interesting discussion. Skin mounted markers have been traditionally placed directly onto anatomical structures which define the joint's mechanical axes for biomechanical analysis. These marker placements do not, however, minimize skin movement artifacts. This dilemma has resulted in the recent distinction between marker placement and bone axis definition (Cappozzo et al., 1993) termed the "Calibrated anatomical system technique" (CAST). This technique allows the placement of markers in regions with less skin-bone movement away from the joint center. However, errors in marker position far from the joint causes errors in mechanical axis definition according to the CAST technique. Presently, research is being conducted to mathematically correct skin movement error, however the variance in subject size, morphology and skin movement (Sati et al., in press), represents a significant challenge to this approach.

The proposed mechanical sensor-bone system has the advantage of being directly attached to the knee joint near its mechanical rotation axes (Pennock & Clarck, 1990). In this way, skin movement is reduced and the problem of the distance between markers and joint mechanical axes is eliminated. Although not a substantial problem in the present study, the mechanical system can be more cumbersome than skin mounted markers for use in movement analyses such as walking. Reduction of the system's weight and the size of its interconnections should be the subject of future work to make its use practical for such situations. The effect of the system on "natural" movements such as walking should also be evaluated for these applications.

Information on the phenomenon of skin-bone movement could be used for future studies and applications. For example, this quantitative data is already being used as a basis for a new mathematical method to help reduce errors induced by skin movement. Skin movement information could also help in other applications such as the placement of orthotic devices on the knee or to assist understanding of the physiology of soft tissue movement about the knee.

6.2 Prosthetic ligament deformations

The perturbation analysis in Chapter 4 demonstrated how prosthetic ligament deformations could be simulated *in vivo* using the proposed instrumentation. Comparison of elongation results with those in the literature improved confidence in the system's accuracy. Elongation values matched best with those in the literature when knee flexion did not exceed 65 degrees. Above 65 degrees, there was a divergence from the ACL elongation results found by Hefzy et al. (1989). The PCL deformations closely resembled those found by Grood et al. (1989). The discrepancies between the results for flexion angles greater than 65 degrees can be explained by the attachment system's known tendency to move with respect to bone increasingly with knee flexion (Sati et al., submitted). Other differences could be in part due to the fact that the studies by Grood et al. and Hefzy et al. were performed on cadaveric specimen with different loading compared to the *in vivo* loading in the present study. The current study presents the first bending and torsion calculations from *in vivo* knee movement.

These results encourage the use of the knee analysis system to help understand the mechanisms of prosthetic ligament failure. The understanding of prosthetic ligament failure has been difficult, especially with respect to explaining why prosthetic devices fail differently than their natural counterparts, namely through permanent elongation, fatigue

wear and immune response. The study of ligament fatigue itself has evolved from cyclic tension to combined elongation, bending and rotation analysis.

From the ligament deformation analysis, we see that prosthetic ligaments can be subjected to large bending and torsion deformations *in vivo* if improperly placed. Unlike the natural ligament, the prosthesis does not possess the capacity to regenerate its material over time. Furthermore, also unlike the natural ligament, the prosthesis is usually anchored via a bone tunnel, whose movement with respect to the ligament is responsible for changes in bending and torsion. It is these *changes* in bending and torsion, coupled with tension and fraying (from rubbing against bone) that may cause premature failure (Gely et al., 1984;Drouin et al., 1991;Claes et al., 1995). These results indicate that prosthetic ligaments fail due to fatigue failure, whereas natural ligaments fail due to sudden impacts. This is the reason that the minimization of bending and torsion deformations is such an important consideration for ligament prostheses.

The results of ligament deformations presented in chapter V indicate a tradeoff between minimizing flexion and torsion in the ligament. That is, an insertion orientation which decreases torsion will augment bending in the ligament.

Deformation data generated from this study can help to determine optimal placement of prosthetic ligaments. Fatigue properties of a prosthesis are a function of its material and its design. Data on the relative displacements of tunnel insertion for some surgical insertion could be reproduced by an *in vitro* "Tension Torsion Flexion" (TTF) fatigue testing machine previously developed (Drouin et al., 1991) to closely simulate *in vivo* conditions. Information on the number of cyclic loads to rupture could help understand the mechanisms of particle wear and ligament failure to better predict the *in vivo* survivorship. Since it has been observed that changing ligament insertion orientation can result in a wide range of deformation values, ligament placement can be customized as a

function of the specific ligament's fatigue properties. For example, a prosthetic ligament whose fatigue life is low when subjected to bending deformations should be placed such that bending is minimized. A choice between bending and torsion deformations must be made since it has been found, and explained through the relative orientation of the ligament tunnel and the FE axis, that insertions which reduce torsion increase bending and vice versa.

It should be eventually possible to design prosthetic ligaments so that their design is a function of the deformations they will be subjected to *in vivo*. For example, a ligament could be designed to have little sensitivity to torsion deformations and be inserted in a region of high torsion and constant bending. As we saw in the previous chapter, one specific ligament was given a pre-twist of 90 degrees whereas the calculations indicated that it should be of the order of 10 to 25 degrees. *In vivo* data from the present study therefore suggests a change in this ligament design is required. So it is now possible with this new technology to match design criteria, for example the twist of the ligament, with the twist the ligament will undergo *in vivo*.

Further work on the consistent placement of two-band PCL prostheses must be performed before analyses can be performed. On a practical level, the surgeon must see both bands simultaneously and in standard views since their placement is relatively complex. Much work needs to be done to help describe PCL deformations since relatively little work has been done in this field.

Of course the choice of optimal insertion will be a function of many factors. The placement must 1) be surgically accessible 2) not disturb or interfere with anatomical structures involved in the knee's function 3) have sufficient amounts of cortical bone to allow proper fixation 4) not alter the joint's normal kinematics.

A similar analysis of insertion versus deformation may be useful for non-prosthetic ligament replacement. Presently, replacement of a ligament by an autograft or allograft is quite popular. The future surely holds in store the development of "bioprostheses" (DesRosiers et al., in press) which consist of biodegradable scaffolds which promote natural tissue regeneration of the ligament. Living tissue ligament replacements are generally inserted into the knee via insertion tunnels in a similar fashion to a prosthesis. They will therefore undergo similar deformations as an artificial prosthesis before they "heal" in the knee. It has been observed that cells which produce the natural ligament matrix do so as a function of mechanical strain or stress (DesRosiers et al., in press; Yen et al., 1990). Therefore, it could be eventually possible to insert the prosthetic ligament such that strains or stresses are "optimal" to favour matrix production.

6.3 Virtual interface

A great divide presently exists between equipment available in human movement laboratories and that available directly to the clinician. Gait labs are equipped with expensive equipment, a spacious walkway and specialized staff to analyze complex human movements. In contrast, the clinician often will quantify a pathology by visual observation and may have access to certain instruments to measure one-dimensional (1D) knee laxity for example (KT1000™, KT2000™ Medmetric, San Diego, CA; Telos™, Germany) or complex and cumbersome instrumentation to measure 3D kinematics (Genucom, Faro Medical Technologies Inc., FL, U.S.A.). The present work shows how slight modification of gait lab technology can bring quantitative 3D data to a more compact clinical form. However, since the clinician does not typically have a technical background, the challenge lies in the simplification of both technological components and interpretation of the data.

In this thesis, we have presented a three-dimensional computer interface with representation of both the subject's knee geometry and movement. The virtual interface provides a direct 3D image representation in space and time of the real knee. Therefore, interaction for surgical planning is more realistic and intuitive than previous systems which generated only numerical output of knee movement data. Unlike previous one-dimensional devices (KT 1000, Telos) and three-dimensional (Genucom) systems the present system is portable and can therefore potentially measure a variety of active knee movements performed by the subject. The compact nature of the computer and attachment system makes it more convenient in a spatially restricted clinical environment and for shared use between clinicians than the existing 3D system.

If a picture is worth a thousand words, a virtual 3D environment could be an interactive book of information. The proposed knee analyzer represents a "virtual knee" environment with which the user can interact and learn. The capacity to visualize underlying bone movement can be seen as giving the user "see through vision" to underlying articular interaction. The numerical feedback on kinematic data and simulated prosthetic ligament insertions makes it a powerful analysis tool. The virtual environment is interactive and allows knee movement to be observed from any point in 3D space. For example, by setting the user's viewpoint of the virtual knee animation from below the floor looking up as the subject walks by, abnormal tibial rotation could be easier to detect than from a lateral or frontal view. The capacity to record and replay movements in slow motion could also be a beneficial feature to detect subtle movements.

With slight modifications, the virtual knee presented in this work could become an educational tool to teach medical students the proper placement of prosthetic ligaments and health science students the kinematics of the knee. Another such application is in rehabilitation where patients often quit due to the monotony of prescribed exercises.

Visual feedback routed through a game-like environment could make rehabilitation exercises mentally challenging and physically beneficial. Here we see that communication of clinical data is not only important for the examiner but also for the examinee. It is becoming increasing important to communicate clinical data to well informed patients and the interface should eventually cater to both.

The graphical interface must convey clinically significant data. While the 3D knee analyzer generates accurate *in vivo* kinematics in several formats, there remains work to be done in the interpretation of these kinematics for the system to be used for other applications. A least-squares method has been used in this study to determine the average flexion-extension (FE) axis in the knee. The FE axis may serve as a useful tool to help explain ligament deformations. There has been some recent research in the literature indicating that the flexion-extension axis of the knee is constant during knee flexion (Hollister et al., 1986), which challenges the traditional view of the knee as an articulation possessing a moving flexion axis or helical axis. The improved accuracy of the current instrumentation and the FE axis calculation could permit *in vivo* confirmation of this hypothesis. Study of both the FE axis and the helical axes of the knee generated by the system could help to understand the relationship between these two forms of movement description which appear to give controversial results. The location of this axis with respect to knee anatomy and the variability of this location could give insight into the knee's function and support its use clinically.

The FE axis is a parameter which could help to better define the knee mechanism. For example, the fundamental problem with Eulerian-type kinematic descriptors is that they require accurate bone axis definition. The FE axis could be used to help define these axes more consistently since it is a function of the knee's characteristic movement. This would not be true for pathological cases, where the contralateral knee would be the only

reference of normality. However, in the case of a pathology, the FE axis itself could be used to help evaluate knee movement pathologies. There has been some recent evidence that the knee's flexion axis is changed following ligament rupture. Re-establishment of the FE axis could therefore eventually be the objective for corrective measures. The relationship between corrective measures and their influence on the FE axis must first be established for this to be possible.

Data generated from the 3D knee analyzer could be useful for several applications where accurate knee kinematics could help in the diagnosis of pathologies and planning of correctional procedures. Knee kinematics and laxity are the basis for detection of ligamentous instability in the knee. To date, detection of pathologies is performed principally through one-dimensional analyses such as the AP drawer or Lachman test. A common and increasingly popular 3D laxity test is the pivot shift for which is presently difficult to quantify numerically.

Correction of ligament instability can be provided by an orthotic brace. For the correction to be effective, the right orthosis must be chosen and properly placed. Evaluation of the kinematics with the system could help in choosing the right orthosis. The calculation of the average flexion-extension (FE) axis of the knee is being presently used to try to help properly place the orthosis. After placement of the orthosis, evaluation of the brace's efficacy could be performed through analysis of the corrected kinematics.

Ortheses placed in the soles of shoes are suspected to alter knee kinematics (BIOP, Joliette, Canada). Knee kinematics with and without foot ortheses are being presently studied using the instrumentation developed in this work to determine their effect on knee movement.

Knee kinematics can also be used for the evaluation of successful total knee replacement. Pre-surgically, quantification of knee kinematics could help plan prosthetic placement and the associated osteotomy. Post-surgically, verification of the correction could be performed. This and other post-intervention analyses could provide feedback to the surgeon or orthesist on the quality of the correction.

In this thesis, we have presented a 3D computer-assisted knee analyzer with potential for diagnostics and planning purposes. Interpretation of knee movement data helps in the diagnostics of pathologies and planning of the corresponding corrective measures. There must, however, be continuity between diagnostics, planning and intervention for the system to be efficient. For example planning of the perfect procedure could lead to catastrophic results if it is not properly implemented. Continuity between these elements ensures quality and efficiency.

The technology used by this system can be directly applied to surgical intervention by placing a motion sensor on a surgical pointer or tool and performing the same mathematical correlation between the image and navigation system reference frames. This allows the system to track surgical tool position during an intervention. The surgeon that is controlling the surgical instrument is therefore provided with visual feedback of his instruments and patient bone position throughout the procedure. Similarly to the knee movement analysis application, sensors can be directly placed on the bones of the subject allowing the surgeon to perform complex manipulations, typical of orthopedics, without losing valuable image-generated data.

The future scenario to resolve a ligamentous instability in the knee could involve diagnosis of the pathology through kinematic analysis, pre-operative planning of "optimal" surgical placement and per-operative guidance towards the predetermined trajectory. Per-operative guidance by the virtual interface could be fulfilled via visual,

auditory or tactile cues to improve accuracy of the intervention. Visual control of surgical tool movement, even when working on structures normally hidden from view, gives image-guided orthopedic surgery the potential to diminish trauma by avoiding open surgery.

A working surgical assistance prototype, based on some concepts presented in this work, has been developed and applied for the placement of pedicle screws in the spine (Amiot et al., submitted). This approach is however not specific to any one type of surgery and can therefore find other applications. Some examples of surgical applications include: 1) hip 2) knee 3) maxio-facial 4) ankle. However, development of a practical minimally invasive registration technique remains to be developed to permit correspondence between the patient and the image-generated data (Amiot et al., 1995).

CHAPTER VII

7. CONCLUSIONS

This thesis has fulfilled its desired objectives. The relationship between prosthetic ligament insertion and deformation has been established through the development of new instrumentation and analysis software. The main artifact from traditional methods has been understood and quantified. Based on this information, a method to reduce this error has been developed to improve movement measurement by an order of magnitude. Software has been developed to simulate prosthetic ligaments and calculate their deformations. This combination of the analysis software and hardware forms a 3D knee analyzer capable of predicting *in vivo* ligament deformations. Using this technology, ligament deformations were explained in reference to their surgical placement relative with a new knee parameter, the FE axis of the knee.

The fluoroscopic method, presented in the second chapter and developed to quantify relative sensor-bone movement, was shown to be accurate to below 1 mm rms through cadaveric studies, with accuracy on live subjects predicted to be slightly less due to decreased image contrast from surrounding tissue. Small fluctuations in sensor position

data arose mainly from the difficulty in defining consistent reference axes on the bone images but were not significant. This method was sufficiently accurate to evaluate the movement of skin relative to bone during knee flexion without and with the mechanical system attached. The fluoroscopic method has similar accuracy to intrusive methods but is more practical for extensive analysis of marker movement of the knee.

Skin movement measured over several regions of both the medial and lateral sides of the knee were observed to vary from 2 to 17 mm rms and varied significantly with marker placement. The information obtained through this study is the most detailed to date. This data identified skin movement as the largest source of error in knee movement analysis and stressed the necessity for improved methods.

The third chapter responded to this need by the design of a non-invasive clamping system whose accuracy was evaluated using the same fluoroscopic method. Knee anatomy and fluoroscopic data formed the basic knowledge required to design the mechanical system.

The semi-flexible design of this system provides subject comfort without compromising precision. Skin movement over the medial condyle was reduced from 11 to 1.7 mm rms and over the lateral condyle from 8.5 to 2.9 mm rms. This allowed measurement of joint kinematics over 65 degrees knee flexion to -0.4 degrees for ab-adduction rotation, -2.3 degrees for axial rotation, 2.4 mm for AP translation and 1.1 mm for axial translation. Medial attachment was mostly responsible for these small errors.

This attachment system was one of several components which form the 3D knee analyzer. This analyzer represents a virtual interface which was used in this work to analyze prosthetic ligament deformations based on *in vivo* kinematic data. The interactive interface and the prosthetic ligament deformation calculation software makes analysis and

surgical planning possible. The FE axis was shown to be a promising parameter to help explain ligament deformations as a function of their insertion orientation.

The system provides *in vivo* knee movement of the 3D bone geometry with accuracy under 6.1 mm in position and 5.3 degrees in orientation. The perturbation analysis showed that the average errors in prosthetic ligament deformations was below 6.5 degrees for bending and 5 degrees for torsion and 3.8 mm for elongation. These values for elongation were similar to those in the literature.

It was shown that prosthetic ligament deformations could be explained in reference to their orientation with respect to the FE axis of the knee. This helped explain the deformations of commercially available prostheses. This information should help the understanding of prosthetic ligament fatigue *in vivo* to help augment their long-term survival and their future designs. Through this analysis, a design flaw was found in the ACL#1 prosthesis. Pre-torsion designed in the ligament was far too high and should be reduced in the future. More work has to be done on consistently defining two-band PCL placement before further analysis can be performed.

This work has resulted in the realization of unique instrumentation and software for 3D knee analysis. To our knowledge, the system is the first to have succeeded in the challenging problem of predicting ligament deformation *in vivo*. With this level of precision and its compact nature, this system may form the basis for a clinical system to help improve the quality of diagnostics, surgical planning and post-operative evaluation for the knee.

8. References

AMIOT, L. P., LABELLE, H., DE GUISE, J. A., SATI, M., BRODEUR, P., & RIVARD, C. H. (submitted) Computer Assisted Pedicular Screw Fixation:1sr three cases. *SPINE.*

AMIOT, L. P., LABELLE, H., DE GUISE, J. A., SATI, M., BRODEUR, P., & RIVARD, C. H. (1995) Computer Assisted Pedicular Screw Fixation: a feasability study. *SPINE, 20*, 1208-1212.

ANDREWS, J. G., & YOUM, Y. (1979) A Biomechanical Investigation of Wrist Kinematics. *Journal of Biomechanics, 12*, 83-89.

AUBIN, C. E., DANSEREAU, J., PARENT, F., LABELLE, H., & DE GUISE, J. A. (submitted) Morphometric validation of personalized 3-D reconstruction fo the Human spine. *M.B.E.C..*

BENDJABALLAH, M. Z., SHIRAZI-ADL, A., & ZUKOR, D. J. (1995) Biomechanics of the human knee joint in compression: reconstruction, mesh generation and finite element method analysis. *The Knee, 2*, 69-79.

BIOMCH-L. (1992) *ANGLES3D Topic* Internet: LISTSERV@HEARN.nic.SURFnet.nl.

BIOMCH-L (1991) *ICR Topic*, Internet: LISTSERV@HEARN.nic.SURFnet.nl.

BLANKEVOORT, L., & HUISKES, R. (1991) ACL Isometric is not the criterion for ACL reconstruction. In *37th Annual Meeting, Orthopaedic Research Society.*

BLANKEVOORT, L., HUISKES, R., & DE LANGE, A. (1990) Helical Axes of Passive Knee Joint Motions. *Journal of Biomechanics, 23*, 1219-1229.

BLANKEVOORT, L., HUISKES, R., & DE LANGE, A. (1985)The reproducibility of passive human knee joint motion characteristics In *Biomechanics: Currrent Interdisciplinary Research* (PERREN, S. M., & SCHNEIDER, E., editors) pp. 309-314, Martinus Nijhoff Publishers, Dordrecht, The Netherlands.

CAPPELLO, A., LEARDINI A., CATANI, F., & PALOMBARA, P. F. (1994) Selection and validation of skin array technical references based on optimal rigid model estimation. In *International conference on 3-D analysis of human movement,* pp. 15-18.

CAPPOZZO, A., CATANI, F., DELLA CROCE, U., & LEARDINI A. (1993) Calibrated Anatomical Systems Technique in 3-D Motion Analysis-Assessment of Artefacts. In *Proceedings of the International Symposium on 3-D Analysis of Human Movement*, pp. 45-52.

CAPPOZZO, A., CATANI, F., LEARDINI A., BENEDETTI, M. G., & DELLA CROCE, U. (in press) Position and orientation in space of bones during movement: experimental artifacts. *Clinical Biomechanics*.

CAZENAVE, A., & LABOUREAU, J. P. (1990) Reconstruction isométrique du ligament croisé antérieur. Détermination pré et post-opératoire du point fémoral. *Rev. Chir. Orhtop. 76*, 288-292.

CCP (1986) *Classification canadienne de procédures de diagnostique, thérapeutique et chirurgicales*, Statistics Canada.

CHAO, E. Y. S. (1980) Justification of Triaxial Goniometer for Measurement of joint Rotation. *Journal of Biomechanics, 13*, 989-1006.

CHEEZE, L. (1993) *Contribution à l'étude cinématique et dynamique in vivo de structures osseuses humaines par l'exploitation des données internes.* Thèse, Université C. Bernard.

CLAES, L. E., LUDWIG, J., MARGEVICIUS, K. J., & DÜRSELEN, L. (1995) Biological Response to Ligament Wear Particles. *Journal of Applied Biomaterials, 6*, 35-41.

COUTEAU, B., HOBATHO, M. C., BAUNIN, C., DARMANA, R., & CAHUZAC, J. P. (1994) In Vivo Description of the Flexion Movement of the Human Tibia Relative to the Femur. In *Second World Congress of Biomechanics*, p. 147.

COVEY, D. C., SAPEGA, A. A., SHERMAN, G. M., & TORG J.S. (1992) Festing for isometry during PCL reconstruction. In *38th Annual Meeting of the O.R.S.*.

CRISCO III, J. J., CHEN, X., PANJABI, M. M., & WOLFE, S. W. (1994) Optimal marker placement for calculating the instantaneous center of rotation. *Journal of Biomechanics, 27*, 1183-1187.

CROWNINSHIELD, R., POPE, M. H., & JOHNSON, R. J. (1976) An analytical model of the knee. *Journal of Biomechanics, 9*, 397-405.

DE GUISE, J. A., ALLARD, B., SATI, M., & FALLAHA, M. (1993) Evaluation d'une méthode radiologique pour la mesure de la taille d l'échancrure intercondylienne du genou

à l'aide de la tomographie axiale et de l'infographie tri-dimensionelle. In *Proceedings of the Canadian Orthopaedic Research Socienty (CORS)*, p. Abstract 60.

DE GUISE, J. A., & MARTEL, Y. (1988) 3D-biomedical modelling: merging image processing and computer-aided design. In *Proceedings of the IEEE EMBS 10th Int. Conf.*, pp. 426-427.

DESROSIERS, E. A., MÉTHOT, S., YAHIA, L. H., & RIVARD, C.-H. (in press) Réponse des fibroblastes ligamentaires à la stimulation mécanique. *Annales De Chirurgie*.

DORLOT, J. M., AIT BA SIDI, M., TREMBLAY, G. R., & DROUIN, G. (1980) Load Elongation Behavior of the Canine Anterior Cruciate Ligament. *Journal of Biomechanical Engineering, 102*, 190-193.

DROUIN, G. (1986) The Prosthetic Replacement of the Cruciate Ligament. *Clinical Orthopaedics and Related Research, 208*, 59-60.

DROUIN, G., MASSON, M., & L'HOCINE YAHIA (1991) In Vitro Fatigue Testing of Prosthetic Ligaments: A New Concept. *Bio-Medical Materials and Engineering, 1*, 159-165.

DROUIN, G., MASSON, M., & YAHIA, L. (1991) In Vitro Fatigue Testing of Prosthetic Ligaments: A New Concept. *Bio-Medical Materials and Engineering, 1*, 159-165.

ENGIN, A. E., & CHEN, S. M. (1988) On The Biomechanics of the Human Hip Complex In Vivo-I. Kinematic for Determination of the Maximal Voluntary Hip Complexes Sinus. *Journal of Biomechanics, 21*, 785-795.

ENGIN, A. E., & PEINDL, R. D. (1987) On the Biomechanics of Human Shoulder Complex-I. Kinematic for Determination of Shoulder Complex Sinus. *Journal of Biomechanics, 20*, 103-117.

ENGIN, A. E., PEINDL, R. D., BERME, N., & KALEPS, I. (1984) Kinematic and Force Data Collection in Biomechanics by Means of Sonic Emitters-I:Kinematics Data Collection Methodology. *Journal of Biomechanical Engineering, 106*, 204-211.

ESSINGER, J. R., LEYVRAZ, P. F., HEEGARD, J. H., & ROBERTSON, D. D. (1989) A mathematical model for the evaluation of the behaviour during flexion of condylar-type knee prostheses. *Journal of Biomechanics, 22*, 1229-1241.

FEUDENSTEIN, F., & WOO, L. S. (1969) Kinematics of the human knee joint. *Bulletin of Mathematical Biophysics, 31*, 215-232.

FLEMMING, B. C., BEYNNON, B. D., NICHOLS, C. E., & RENSTROM, P. (1992) In vitro comparison between predictive isometry measurement and elongation in the reconstruction of ACL. In *38th Annual Meeting of O.R.S.*.

FRANKEL, V. H., BURSTEIN, A. H., & BROOKS, D. B. (1971) Biomechanics of internal derangement of the Knee. *Journal of Bone and Joint Surgery., 53A*, 945.

GELY, P., DROUIN, G., THIRY, P. S., & TREMBLAY, G. R. (1984) Torsion and Bending Imposed on a New Anterior Cruciate Ligament Prosthesis During Knee Flexion: An Evaluation Method. *Journal of Biomechanical Engineering, 106*, 285-294.

GENOUD, P. *Personal Communication* (1994) .

GILLQUIST, J. (1990) Stryker dacron ligament: techniques and results. In *Proceedings of the Seventh Annual International Symposium on Advances in Cruciate ligament Reconstruction of the Knee: Autogenous vs Prosthetic.*, pp. 106-116.

GOOD, L., ODENSTEN, M., PETTERSSON, L., & GILLQUIST, J. (1989) Failure of a bovine xenograft for reconstruction of the anterior cruciate ligament. *Acta Orthopaedica Scandinavica, 60*, 8-12.

GOODFELLOW, J., & O'CONNOR, J. (1978) The mechanics of the knee and prosthesis design. *Journal of Bone and Joint Surgery., 60B*, 358-369.

GROOD, E. S., HEFZY, M. S., & LINDENFIELD, T. N. (1989) Factors affecting the region of most isometric femoral attachments Part I: The posterior cruciate ligament. *American Journal of Sports Medicine, 17*, 197-207.

GROOD, E. S., & SUNTAY, W. J. (1984) *Journal of Biomedical Engineering, 105*, 136-144.

GUPTA, B. N., & BRINKER, W. O. (1969) Anterior cruciate ligament prosthesis in the dog. *Journal of the American Veterinary Medical Association, 154*, 1057-1061.

HALLEN, L. G., & LINDAHL, O. (1966) The screw-home movement in the knee joint. *Acta Orthopaedica Scandinavica, 37(1)*, 97-106.

HART, A., MOTE, C. D. Jr., & SKINNER, H. B. (1991) A Finite Helical Axis as a Landmark for Kinematic Reference of the Knee. *Journal of Biomechanical Engineering, 113*, 215-222.

HEFZY, M. S., GROOD, E. S., & NOYES, F. R. (1989) Factors affecting the region of most isometric femoral attachments. Part II: The anterior cruciate ligament. *American Journal of Sports Medicine, 17*, 208-216.

HOLDEN, J. P., ORSINI J.A., & HOLDEN S.J. (1994) Estimates of skeletal motion: movement of surface-mounted targets relative to bone during gait. In *Proceedings of the Thirteenth Southern Biomedical Engineering Conference.*

HOLLISTER, A. M., KESTER, M. A., COOKS, S. D., BRUNET, M. E., & HADDAD, R. J. (1986) Knee axes of rotation: Determination and implication. *Trans. Orthop. Res. Soc., 11*, 383.

HUISKES, R., VAN DIJK, R., DE LANGE, A., WOLTRING, H. J., SELVIK, G., & VAN RENS, T. J. G. (1985) *Biomechanics: Current Interdisciplinary Research*, Perren S.M. and Schneider E. ed., Martinus Nijhoff Publishers, Dordrecht, The Netherlands.

HUNT, K. H. (1978) *Kinematic Geometry of Mechanisms*, Clarendon Press, Oxford.

ISACSON, J., GRANSBERG, L., & KNUTSSON, E. (1986) Three-dimensional electrogoniometric gait recording. *Journal of Biomechanics, 19*, 627-635.

JOHNSON, F. L. (1960) Use of braided Nylon® as a prosthetic anterior cruciate ligament of the dog. *J.A.V.M.A., 137*, 646-647.

KÄRRHOLM, J. (1989) Roentgen stereophotogrammetry: Review of orthopaedic applications. *Acta Orthopaedica Scandinavica, 60(4)*, 491-503.

KARLSSON, D., & LUNDBERG, A. (1994) Accuracy estimation of kinematic data derived from bone anchored external markers. In *Proceedings of the International Symposium on 3-D Analysis of Human Movement*, p. 27.

KETTELKAMP, D. B. (1976) Gait Characteristics of the Knee: Normal, Abnormal and Post-Reconstruction. *AAOS Symposium on recontructive Surgery of the Knee*, pp. 47-57.

KINZEL, G. L., HALL, A. S., & HILLBERRY, B. M. (1972) Measurement of the Total Motion Between Two Body Segments-i. Analytical Development. *Journal of Biomechanics, 5*, 93-105.

LABOUREAU, J. P., & BERCOVY, M. (1993) Indications actuelles des ligaments artificielles. In *3rd European congres of the orthopaedic traumatology society of the east of France.*

LADIN, Z., & WU, G. (1991) Combining position and acceleration measurements for joint force estimation. *Journal of Biomechanics, 24,* 1173-1187.

LAFORTUNE, M. A. (1984) *The use of intra-cortical pins to measure the motion of the knee during walking* Ph.D. Thesis, The Pennsylvania State University.

LAFORTUNE, M. A., & LAKE, M. J. (1991) Errors in 3D analysis of human movement. In *International conference on 3-D analysis of human movement,* pp. 55-56.

LAFORTUNE, M. A., LAMBERT, C., & LAKE, M. (1992) Skin marker displacement at the knee joint. In *Proceedings of the second north american congress on biomechanics,* p. 101.

LEVENS, A. S., INMAN, V. T., & BLOSSER, J. A. (1948) Transverse rotation of the segments of the lower extremity in locomotion. *Journal of Bone and Joint Surgery. American Volume, 30A,* 859-872.

LEWIS, J. L., & LEW, W. D. (1978) A Method for Locating an optimal "Fixed" Axis of Rotation for the Human Knee Joint. *Journal of Biomedical Engineering, 100,* 1978.

LEWIS, J. L., LEW, W. D., & SCHMIDT, J. (1988) Description and Error Evaluation of an In Vitro Joint Testing system. *Journal of Biomechanical Engineering, 110,* 238-247.

LIN, H. H., BUFORD, W. L., PATTERSON, R. M., & ELDER, K. (1995) A Real-Time, Interactive, 3-Dimensional, Computer Graphic System for the Study of One, Two, and Three degree of Freedom Joint Motion. In *Vth International Symposium on Computer Simulation in Biomechanics,* p. 84.

MACLEOD, A., & MORRIS, J. R. W. (1987)Investigation of inherent experimental noise in kinematic experiments using superficial markers In *Biomechanics X-B* (JOHNSON, B., editor) pp. 1035-1039, Human kinetics publishers, Champaign IL.

MARANS, H. J., JACKSON, R. W., GLOSSOP, N. D., & YOUNG, M. C. (1989) Anterior cruciate ligament insufficiency: a dynamic three-dimensional motion analysis. *American Journal of Sports Medicine, 17,* 325-332.

MCCLAY, I. S., CAVANAGH, P. R., SOMMER, H. J., WOLTRING, H. J., & KALENAK, A. (1991) Three-dimensional angular kinematics of the tibiofemoral joint during running. *International Conference on 3-D Analysis of Human Movement,* 189-192.

MILLS, O. S., & HULL, M. L. (1991) Rotational flexibility of the human knee dueto varus/valgus and axial moments in vivo. *Journal of Biomechanics, 24,* 673-690.

MORRISON, J. B. (1970) The mechanics of the knee joint in relation to normal walking. *Journal of Biomechanics, 3*, 51-61.

MURPHY, M. C. (1990) *Geometry and kinematics of the normal human knee Ph.D. Thesis, M.I.T.*

PAUL, J. P. (1995) One hundred years of measurement of human motion. In *3-D Reconstruction of Human Motion.*

PENNOCK, G. R., & CLARCK, K. J. (1990) An Anatomy-Based Coordinate System for the Description of the Kinematic displacements in the Human Knee. *Journal of Biomechanics, 23*, 1209-1218.

POULIOT, N., DE GUISE, J. A., & DROUIN G. (1989) *A three-dimensional interpolation algorithm* Thesis, Ecole Polytechnique.

QUINN, T. P., & MOTE JR., C. D. (1990) A six-degree-of-freedom acoustic transducer for rotation and translation measurements across the knee. *Journal of Biomechanical Engineering, 112*, 371-378.

RICHARD, A. (1995) *Recherche d'un axe fixe de rotation dans le genou* [Undergraduate Thesis], École Polytechnique.

RONSKY, J. L., VAN DEN BOGERT, A. J., NIGG, B. M., & WALLACE, C. (1995) Application of Magnetic Resonance Imaging for Non-Invasive Quantification of Joint Contact Surface Areas. In *IEEE Engineering in Medicine &Biology 17th Annual Conference,* p. 5.7.1.2.

SÖDERKVIST, I., & WEDIN, P. Å. (1993) Determining the movements of the skeleton using well-configured markers. *Journal of Biomechanics,* 1473-1477.

SATI, M., DE GUISE, J. A., & DROUIN, G. (1993) Design and realization of a non-invasive system for the generation of in vivo kinematic animations of knee movement. In *International conference on 3-D analysis of human movement.*

SATI, M., DE GUISE, J. A., & DROUIN, G. (submitted) Improving in vivo knee kinematic measurements: application to prosthetic ligament analysis. *The Knee.*

SATI, M., DE GUISE, J. A., LAROUCHE, S., & DROUIN, G. (in press) Quantitative assessment of skin-bone movement at the knee. *The Knee.*

SATI, M., DE GUISE, J. A., MARTEL, Y., MASSON, M., & DROUIN, G. (1991) An application of 3D medical imagery to the kinematic modelling of knee motion. In *International conference on 3-D analysis of human movement*, pp. 159-162.

SATI, M., & VAILLANCOURT, S. (1992) *Analyse d'un système de navigation et son utilisation dans le développement d'un outil d'assistance chirurgical*, Institute of Biomedical Engineering.

SEEDHOM, B. B. (1992) Reconstruction of the anterior cruciate ligament. In *Proceeding of the Association of Mechanical Engineers.*, pp. 15-27.

SHAW, J. A., & MURRAY, D. G. (1974) The longitudinal axis of the knee and the role of the cruciate ligaments in controlling transverse rotation. *Journal of Bone and Joint Surgery. 56A*, 1603-1609.

SHIAVI, R., LIMBIRD, T., FRAZERM., STIVERS, K., STRAUSS, A., & ABRAMOVITZ, J. (1987) Helical Motion Analysis of the Knee-I. Methodology for Studying Kinematics During Locomotion. *Journal of Biomechanics, 20*, 459-469.

SIEGLER, S., CHEN, J., & SCHNECK, C. D. (1988) The Three-Dimensional kinematics and Flexibility Characteristics of the Human Ankle and Subtalar Joint-partI: Kinematics. *Journal of Biomechanical Engineering, 110*, 364-374.

SMIDT, G. J. (1973) Biomechanical analysis of knee flexion and extension. *Journal of Biomechanics, 6*, 79-92.

SPOOR, C. W., & VELDPAUS, F. E. (1980) Technical Note: Rigid Body Motion Calculated From Spatial Co-Ordinates of makers. *Journal of Biomechanics, 13*, 391-393.

SUNTAY, W. J., GROOD, E. S., HEFZY, M. S., BUTLER, D. L., & NOYES, F. R. (1983) Error Analysis of a System for Measuring Three-Dimensional Joint Motion. *Journal of Biomechanical Engineering, 105*, 127-392.

TOWNSEND, M., ISAK, M., & JACKSON, R. (1977) Total Motion Knee Goniometry. *Journal of Biomechanics, 10*, 183-193.

ULLMAN, S. (1989) Aligning pictorial descriptions:an approach to object recognition. *Cognition: International Journal of Cognitive Science , 32*, 193-254.

ULLMAN, S. (1986) An approach to object recognition: aligning pictorial descriptions. *Artificial Intelligence Memo, M.I.T., No. 931*, 1-57.

VAN DEN BOGART, A. J., VAN WEEREN, P. R., & SCHAMHARDT, H. C. (1990) Correction for skin displacement errors in movement analysis of the horse. *Journal of Biomechanics, 23,* 97-101.

VAUGHN, L. C. (1963) A study of the replacement of the anterior cruciate ligament in a dog by Fascia, skin and Nylon®. *Veterinary Record, 75,* 537-541.

VELDPAUS, F., WOLTRING, H. J., & DORTMANS, L. (1988) A least squares algorithm for the equiform transformation from spatial marker co-ordinates. *Journal of Biomechanics, 21,* 45-54.

WALKER, P. S., SHOJI, H., & ERKMAN, M. J. (1972) The rotational axis of the knee and its significance to prosthesis design. *Clinical Orthopaedics, 89,* 160.

WANG, C. J., WALKER, P. S., & WOLF, B. (1973) The effects of flexion and rotation on the lengh patterns of the ligaments of the knee. *Journal of Biomechanics, 6,* 587-596.

WANG, X., REZGUI, M. A., & VERRIEST, J. P. (1993) Using the polar decomposition theorem to determine the rotation matrix from noisy landmark measurements in the study of human joint kinematics. In *Proceedings of the International Symposium on 3-D Analysis of Human Movement,* pp. 53-56.

WISMANS, J., VELDPAUS, F., & JANSSEN, J. (1980) A three-dimnsional mathematical model of the knee-joint. *Journal of Biomechanics, 13,* 677-685.

WU, G., & LADIN Z. (1993) The kinematometer- an integrated kinematic sensor for kinesiological measurements. *Journal of Biomechanical Engineering, 115,* 53-62.

YEN, E. H. K., POLLIT, D. J., WHYTE, W. A., & SUGA, D. M. (1990) Continuous stressing of mouse interparietal suture fibroblast in vitro. *J. Dent. Res., 69,* 26-30.